İSTANBUL TECHNICAL UNIVERSITY ★ INSTITUTE OF SCIENCE AND TECHNOLOGY

CHEMICAL AND ELECTROCHEMICAL POLYMERIZATION OF SUBSTITUTED CARBAZOLES IN THE PRESENCE OF ACRYLAMIDE

PhD Thesis by

Özlem YAVUZ, Msc.

(509950010012)

Date of submission : July 23, 1999

Date of defence examination: December 03, 1999

Supervisor (Chairman): Prof. Dr. A. Sezai SARAÇ

Members of the Examining Committee Prof. Dr. Yusuf YAĞCI (İ.T.U.)

Prof. Dr. Oğuz OKAY (İ.T.U.)

Prof. Dr. Ersin YURTSEVER (K.U.)

Dr. Léonard E. A. BERLOUIS (S.U.)

DECEMBER 1999

İSTANBUL TEKNİK ÜNİVERSİTESİ ★ FEN BİLİMLERİ ENSTİTÜSÜ

100697

SÜBSÜTİYE KARBAZOLLERİN AKRİLAMİD VARLIĞINDA KİMYASAL VE ELEKTROKİMYASAL POLİMERİZASYONU

DOKTORA TEZİ
Y. Kimyager Özlem YAVUZ
(509950010012)

Tezin Enstitüye Verildiği Tarih : 23 Temmuz 1999
Tezin Savunulduğu Tarih : 03 Aralık 1999

Tez Danışmanı :	Prof. Dr. A. Sezai SARAÇ
Diğer Jüri Üyeleri	Prof.Dr. Yusuf YAĞCI (İ.T.Ü.)
	Prof.Dr. Oğuz OKAY (İ.T.Ü.)
	Prof.Dr. Ersin YURTSEVER (K.Ü.)
	Dr. Léonard E. A. BERLOUIS (S.Ü.)

ARALIK 1999

PREFACE

I am grateful to my supervisor Prof. Sezai Saraç for his help and continuous encouragement and discussions during my Ph.D. thesis.

I would like to thank Prof. Michael Hitchman who gave me an opportunity to study at the University of Strathclyde during my Ph.D. thesis. I wish to thank him for useful discussion, his kind advice and financial support.

I wish to thank Dr. Len Berlouis for invaluable help, criticism and understanding.

I especially thank Ass. Prof. Esma Sezer for her criticism and advising at every stage my Ph.D. and sincerely thank my friends, Research Assistant Fevzi Çakmak Cebeci, Şerife Özkara and Chemical Engineer Gülay Uzelli, for their understanding and patience.

I am also grateful to my family, especially my mother and father for their understanding, patience and support both in my doctoral studies and at every stage in my life.

July 1999

Özlem YAVUZ

CONTENTS

LIST OF ABBREVIATIONS

NCz	: N-Carbazole
NVCz	: N-Vinylcarbazole
NECz	: N-Ethylcarbazole
AAm	: Acrylamide
Py	: Pyrrole
PCz	: Polycarbazole
PECz	: Polyethylcarbazole
PVCz	: Polyvinylcarbazole
PAAm	: Polyacrylamide
LNVCAm	: Low NVCz containing AAm
HNVCAm	: High NVCz containing AAm
PPy	: Polypyrrole
AIBN	: α,α'-Azoisobutrylonitrile
CAN	: Ceric Amonnium Nitrate
ACN	: Acetonitrile
DMF	: Dimethylformamide
THF	: Tetrahydofuran
TEAP	: Tetraethylamonniumperchlorate
OA	: Oxalic Acid
FT-IR	: Frouier Transform InfraRed
UV-Vis	: Ultra-Violet Visible Spectrophotometer
NMR	: Nuclear Magnetic Resonans
CV	: Cyclic Voltammogram
SEM	: Scanning Electron Microscope
TGA	: Thermogravimetric Analyses
DSC	: Differential Scanning Calorimetry
Tg	: Glass Transition Temperature

LIST OF TABLES

LIST OF FIGURES

CHEMICAL AND ELECTROCHEMICAL POLYMERIZATION OF SUBSTITUTED CARBAZOLES IN THE PRESENCE OF ACRYLAMIDE

SUMMARY

The copolymers and blends of heteroatomics have been of interest since the beginning of research on electrochemical polymerization to produce conducting polymers. The π-electron system along the polymer backbone and the crosslinking points between polymer chains, which confers rigidity, make conducting polymers insoluble, infusible and therefore poorly processable. Co-processing of conducting polymers may offer improvements in both mechanical properties and processing technology. Carbazole-based polymer systems have received considerable research attention because of their interesting thermal, electrical and photophysical properties. Therefore, in this work, the interaction of AAm and NCz derivatives is described. The aim of this study is to improve both the chemical and physical properties of the polymers formed from AAm and NCz derivatives and to investigate the mechanism of such reactions.

The homopolymerization of polyacrylamide was first investigated in order to understand the copolymerization mechanism. The polymerization yield, when the process was initiated with Ce (IV)-OA redox couple, was considerably increased by electrogenerated Ce (IV) in anodic compartment. The thermal stability of polymers increased with increasing Ce (IV) concentration, and was much greater than that of polymers obtained from AIBN media. NVCz containing AAm polymers were then synthesized in DMF and in DMF/water mixtures by using the Ce (IV)-OA redox pair (electrochemical synthesis) and by AIBN (chemical synthesis). NVCz was used since this is a speciality material of considerable academic and industrial interest due to its unusual electric, photoelectric and thermal properties. Low yield conversion was obtained when the Ce (IV)-OA redox pair was used due to solvent effect. Nucleophilic solvents such as H_2O can react with the radical cations or dications produced during the oxidation leading to degradation of the polymer. A much higher yield of polymer was obtained for NVCz polymerization in the presence of AAm in the DMF/water mixture, compared to polymerization in DMF medium alone.

The thermal properties of AAm polymers obtained by using the redox initiator was better compared to that obtained using the AIBN initiator. Furthermore, the thermal stability of PAAm appeared to increase with the amount of NVCz incorporated within the polymer. The solubility and fluorescence behavior was also studied for NVCz containing polymers. The copolymers were soluble in water and in water/acetonitrile mixture (50:50) in different amounts. Their solubility in dioxan, THF and chloroform increased with increasing NVCz content of the copolymer. They also exhibited fluorescence properties in water and in dioxane.

The polymerization of N-carbazole and N-ethylcarbazole was investigated in acrylamide medium. The polymer films were deposited onto platinum and indium tin oxide (ITO) by oxidative electropolymerization from ACN solution. The influence of the polymerization conditions such as electrode potential, monomer concentration, type of solvent and supporting electrolyte on the mechanical and electrochemical properties of copolymers have been studied. N-Ethylcarbazole and 3,3'-dibromethylcarbazole were used as model compounds for the *in-situ* spectro-electochemical measurements to understand the interaction between AAm and N-carbazoles. In the case of the unsubstituted NECz, reactions between monomers could occur and the formation of some oligomers took place. As a result, the peak intensities at 531 nm and 800 nm, corresponding to the radical cation (polaron) produced during the oxidation of the film, were increased. With the incorporation of AAm units into the structure, the peak at 531 nm disappeared (Figure 1). This data suggests that AAm monomers reacts with the radical cations of the oligomers. In the presence of bromine substituents in NECz, the absorbance values were halved and the data corrsponded more closely to those of NECz. This is due to reaction taking place at the –2 and/or 7 position of the carbazole ring, since the –3 and/or 6 position of carbazole ring are brominated. Accordingly, we can suggest a tentative mechanism as follows,

X : ClO_4^- (Et_4ClO_4, $HClO_4$), AAm **R:**

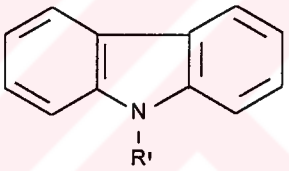

R' : H, $CH=CH_2$, C_2H_5

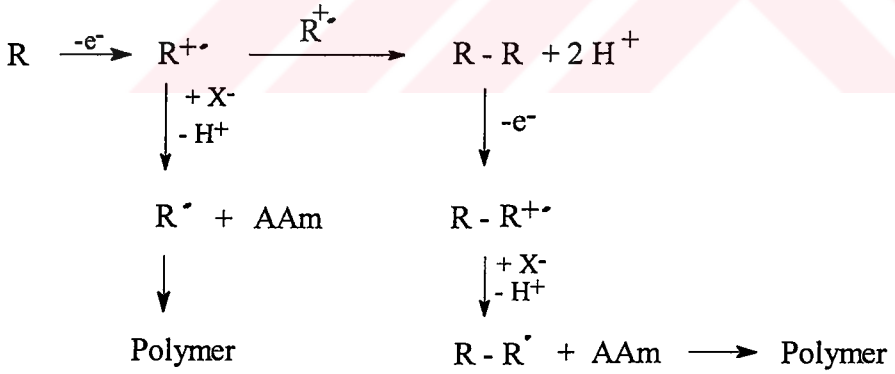

SCHEME 1

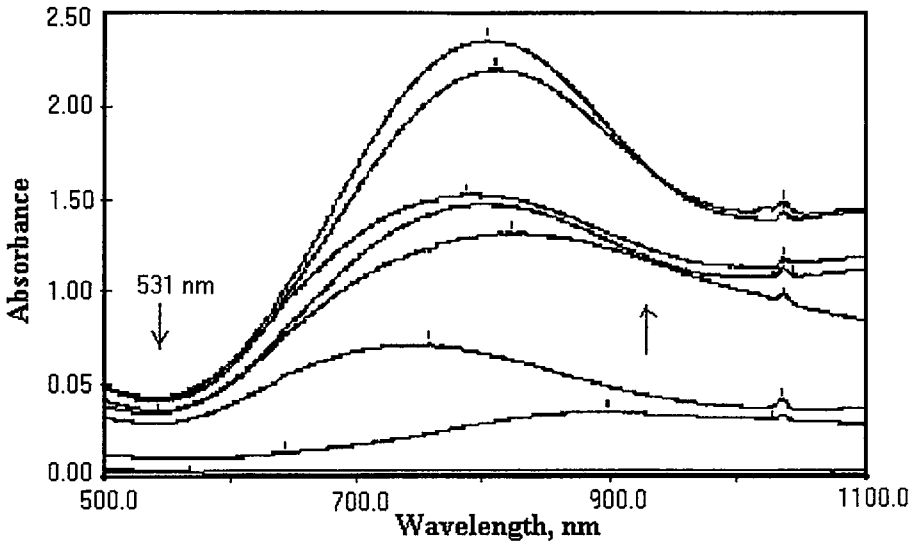

Figure 1 UV-Visible absorption spectra obtained *in-situ* over an 8 min period in a 20:1 (AAm: NECz) solution in ACN; supporting electrolyte: 0.1 mol dm^{-3} TEAP. Scan Rate: 0.5 V s^{-1}, Working and Counter electrode: Pt, Reference electrode: Ag/AgCI.

The formation and growth of PCz films and of its copolymer films in the presence of AAm on platinum electrodes have been followed *ex-situ* by gravimetric analysis. From the influence of monomer and electrolytic concentration on the polymerization rate, an empirical kinetics relationship can be obtained.

$$Rp = k\,[\text{N-Carbazole}]^{\alpha}\,[\text{Electrolyte}]^{\beta} \qquad (1.1)$$

In the presence of acrylamide, the empirical kinetic rearranges to the form;

$$Rp = k\,[\text{N-Carbazole}]^{\alpha}\,[\text{Electrolyte}]^{\beta}\,[\text{Acrylamide}]^{\gamma} \qquad (1.2)$$

From gravimetric analysis of the polymer generated on the electrode by changing the carbazole and electrolyte concentrations, the following relationship was derived,

$$Rp = k\,[\text{N-Carbazole}]^{0.50}\,[\text{TEAP}]^{0.625} \qquad (1.3)$$

and in the presence of AAm:

$$Rp = k\,[\text{N-Carbazole}]^{0.54}\,[\text{TEAP}]^{0.50}\,[\text{Acrylamide}]^{0.1} \qquad (1.4)$$

The thermal properties of the electrochemically deposited carbazole-acrylamide copolymers were studied by Differential Scanning Calorimetry (DSC) and Thermogravimetric Analysis (TGA). The thermal analysis data would lead us to conclude that the weight loss observed in the TGA analysis is linked to the stabilisation of the polymer matrix through crosslinking, with the observed weight loss

due to the leaving group. It is not possible at this stage to assign these individually but they may correspond to different leaving groups during the crosslinking process and hence to different levels of stability attained by the resulting polymer. There is an increase in the enthalpy associated with the crosslinking with increasing carbazole concentration suggesting that this component plays a dominant role in that process. For polycarbazole films grown in perchloric acid, the enthalpy associated with crosslinking is much reduced since the protonation of the amine group of the carbazole moiety prevents coupling at this position.

The optical technique of ellipsometry was employed *in-situ* to monitor the growth of the copolymer films and thus to verify, from the measured optical properties of the layer with film thickness, that the electrochemical growth did indeed lead to an effectively uniform film. The optical properties of NCz were also studied in the presence of AAm. The variation in the optical constants as a function of AAm:NCz ratio indicates a general increase in the value of the extinction coefficient *k* with increasing NCz content. This is corroborated by an examination of the UV-vis spectra of NCz and of the NCz copolymer with AAm since a broad peak centred at 800 nm can be observed in both spectra. This suggests that more carbazole is incorporated into the matrix as its monomer concentration increases and is as expected since the whole polymerization process is initiated by the formation of the NCz cation radical through electrooxidation. The ellipsometry measurements also revealed that incorparation of AAm into the structure caused a decrease in the rate of carbazole polymerization. The studies have concluded that whereas the optical properties of the layers appear to be independent of the growth medium and starting AAm:NCz ratio (in that similar values of refractive index are obtained) the rate of polymer film growth has a strong effect on the structure of the polymer layer. More compact and uniform films are produced at slow growth rates.

In the final part of this thesis, the redox behaviour of the polymer-coated electrodes was examined towards ferrocene and dopamine by cyclic voltammetry. Depending on the conditions, the electrode responded in a reversible manner and in some cases, in a quasi-reversible behaviour (Figure 2). PVCz/AAm electrodes synthesized using AIBN initiator and prepared by casting from DMF+THF+H_2O (45 %+ 45 % + 10 %) solution on Pt substrate were also examined for their response to dopamine and ferrocene. Cyclic voltammetric measurements for the NCz-AAm copolymer electrode showed reversible response to dopamine in phosphate buffer of pH 7. PVCz-AAm copolymer electrodes were also tested for their response to dopamine. The results suggest that depending on conditions (i.e scan rates, thickness of film) the electrode response was reversible or quasi-revesible.

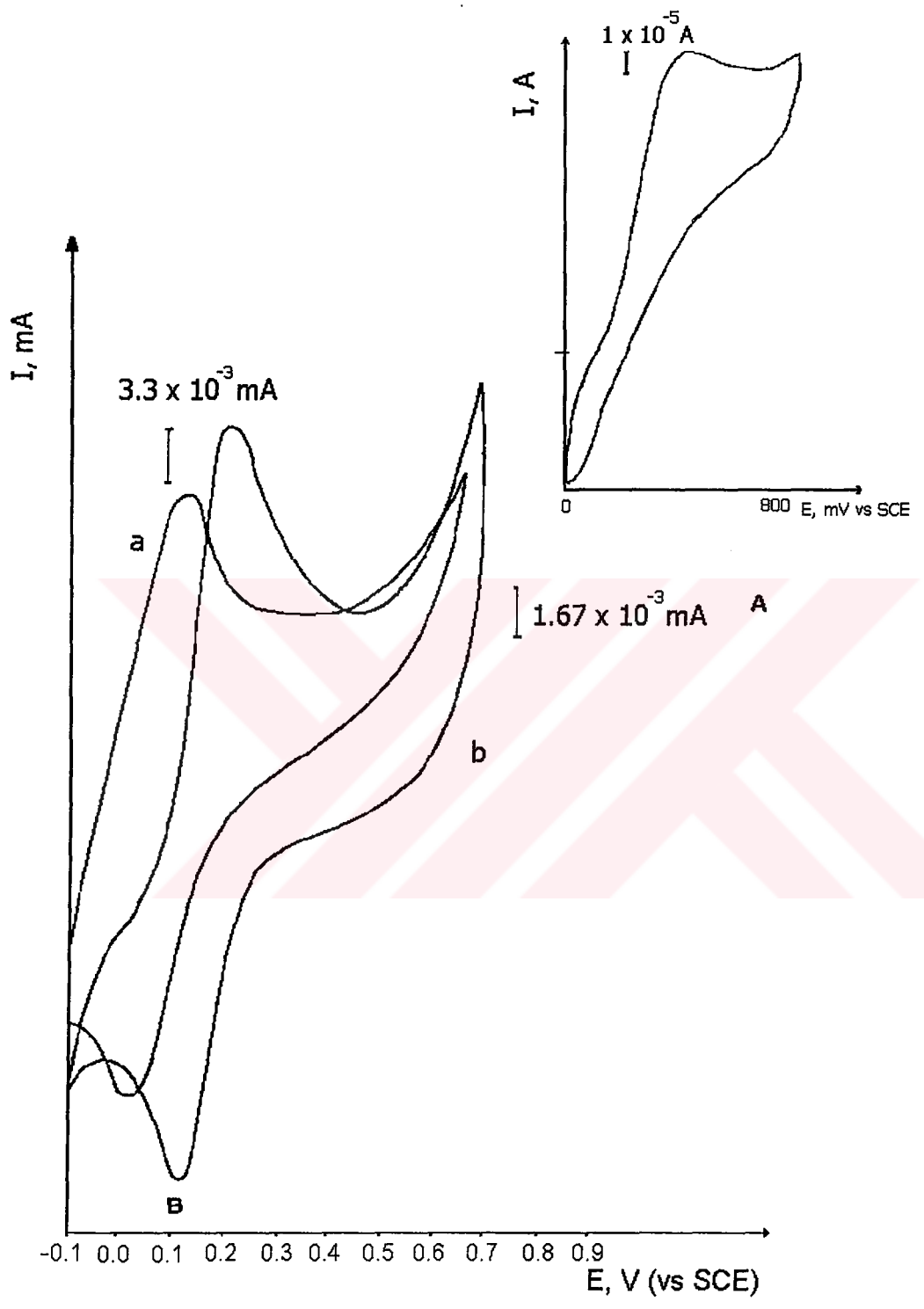

Figure 2 Cyclic voltammograms obtained for a 0.018 M dopamine in buffer solution (pH 7.4) at **(A)** a Pt electrode, **(B)** an AAm/NCz copolymer (n_{AAm}/n_{NCz}=50) electrode, a) newly prepared electrode, b) after three days. Scan Rate: 0.5 V s^{-1}.

SÜBSTİTÜYE KARBAZOLLERİN AKRİLAMİD VARLIĞINDA KİMYASAL VE ELEKTROKİMYASAL POLİMERİZASYONU

ÖZET

Karışımlar homojen yada heterojen olarak isimlendirilir. Polimer durumunda homojenler karışım yada kopolimer, heterojenler ise kompozit malzemeler olarak sınıflandırılabilir. Heterosiklik bileşiklerin kopolimerleri ve karışımları elektrokimyasal polimerizasyon sentezlerinin yapılmasından bu yana oldukça ilgi çekici bir hale gelmiştir. Bunun yanında polimer zincri boyunca polimere sertlik veren, polimer zincirleri arasında çapraz bağlanmaya sebep olan π-elektron sistemi iletken polimerlerin işlenebilirliğine, çözünebilirliliğine sınırlar getirmiş ve buna bağlı olarak endüstriyel kullanım açısından dezavantajlara neden olmuştur. İletken polimerlerin diğer monomer veya polimerlerle kullanımı bu polimerlerin mekanik özelliklerinden başka proses teknolojisinde gelişmelere neden olmuştur. Bu amaçla iletken bir polimer olan polikarbazol ve türevlerinin, bir yalıtkan polimer olan akrilamid ile etkileşmeleri incelenmiş, iletken ve fotoiletken polimerlere dezavantaj sağlayan çözünebilirlilik, kırılganlık gibi zayıf proses özelliklerinin iyileştirilmeye çalışılmış ayrıca, termal özellikleri zayıf olan poliakrilamid polimerlerinin iletken polimerler varlığında zayıf olan özelliklerinde iyileştirilmeler sağlanmış, ve reaksiyon mekanizması aydınlatılmaya çalışılmıştır.

Çalışmanın ilk bölümünde, N-vinilkarbazol (NVK) içeren suda çözünebilir polimerler radikal mekanizma ile AIBN başlatıcı varlığında dimetilformamid (DMF) ve Ce(IV)-oksalik asit (OA) redox çifti ile DMF yada DMF/su çözücü karışımında elektrokimyasal olarak sentezlenmeye çalışılmıştır. Bu çalışmaya ışık tutması amacıyla poliakrilamid (PAAm) her iki başlatıcı varlığında kiyasal ve elektrokimyasal olarak sentezlenmiştir. Elektrokimyasal olarak Ce(IV)-OA kullanılarak sulu çözeltiden sentez edilen poliakrilamid yüksek verimlere ulaşırken, aynı yöntemlerle organik bir çözücü (DMF ve DMF/su) varlığında verimde önemli bir azalma görülmüştür.

NVK' un tek başına ve AAm varlığında AIBN başlatıcılı kimyasal polimerizasyonundaki verimler, elektrokimyasal yöntemle Ce(IV)-OA redox çifti kullanılarak elde edilen AAm polimerlerinin verimlerine kıyasla düşmüştür.. NVK' un, DMF çözücü ortamında Ce(IV)-OA redox çifti kullanılarak yapılan elektrokimyasal polimerisazyonun da polimerizasyon verimi aynı şekilde düşük kalmıştır.

NVK monomerinin suda çözünme problemi ve diğer polimerler ile karşılaştırma nedeniyle, bazı reaksiyonlar DMF/su çözücü ortamında yapılmıştır. Bugüne kadar sulu ortamda yapılan vinilkarbazolun vinil grubundan elde edilen polimerinde literatürde de belirtildiği gibi beklenen polimerisazyon veriminin

düşmesi yerine polimerizasyon veriminde önemli bir artış gözlenmiştir. Bu verim artışının daha fazla NVK yapıya girmiş olabileceğinin yanında NMR sonuçlarına göre suyun varlığında DMF'in yapıya girmesinden kaynaklanmıştır.

Elde edilen yeni polimerlerin absorpsiyon ve emisyon spektral özellikleri incelenmiş aynı zamanda termal stabilitesi zayıf olan poliakrilamidin farklı başlatıcılar varlığında termal özellikleri ayrı ayrı incelenmiş, yüksek Ce(IV) konsantrasyonu kullanılarak elde edilen akrilamid polimerlerinin camsı geçiş sıcaklıkları (Tg), AIBN ortamında elde elde edilene göre daha yüksek bulunmuştur. Ayrıca, heterosiklik bir bileşik varlığında elde edilen poliakrilamidin stabilitesinin arttığı gözlenmiştir.

Suda çözünürlüğü bulunmayan polivinilkarbazolun, akrilamid varlığında elde edilen kopolimerinin NVKz' un belli bir oranına kadar suda çözündüğü bulunmuştur. Kopolimerdeki NVKz oranı arttıkça THF, dioxan ve kloroformdaki çözünürlükler artmıştır.

İkinci bölümde, N-karbazol (NKz) ve N-etilkarbazol (NEKz), akrilamid varlığında asetonitril (ACN) çözeltisinde tetraetilamonyumperklorat (TEAP) destek elektrolit kullanılarak polimerizasyonu gerçekleştirilmiştir. Elde edilen polimerler, Döngülü Voltamogram, UV-Visible, FT-IR spekrofotometre ile karakterize edilmiş, ayrıca 4 Nokta katı iletkenlik cihazı ile iletkenlikleri belirlenmiştir.

Reaksiyon çözücü ortamı değiştirilerek, polimerizasyona etkisi incelenmiştir. ACN:H_2O ($HClO_4$) karışımında halkada oluşan radikal katyonların asetonitril-su karışımının bu radikal katyonları deaktive etmesi beklenirken asit varlığı böyle bir etkiyi engellediği gözlenmiştir. Deaktivasyonun tersine akrilamid varlığında bu çözelti ortamı polimerizasyon hızını arttırmıştır ve yüzeyde oluşan polimerin elektroda daha iyi tutunmasını sağlamıştır.

3,6'-dibromoetilkarbazol (3,6'-dibrEKz) ve N-etilkarbazol (NEKz) *in-situ* spektro-elektrokimya ölçümleri için AAm varlığında karbazol halkasının AAm ile etkileşiminin aydınlatılabilmesi açısından model bileşik olarak kullanılmıştır. NEKz ve NKz arasındaki en önemli fark aynı koşullar altında NEKz elektrod yüzeyinde polimerik birikim elde edilmezken, çözeltide çözünebilir 3,3'-dimerler oluşturabilir. Karbazol de ise 3 ve 6 pozisyonunda halka reaksiyonları oluşur ve polimerizasyonun anot yüzeyinde devam etmesini sağlar. Buna karşılık 3 ve 6 pozisyonlarındaki Br' un varlığı polimerizasyonun anot yüzeyinde oluşumunu engellediği gözlenmiştir.

In-situ spektro-elektrokimyasal olarak gerçekleştirilen ölçümlerine göre, EKz' un radikal katyonlarına karşı gelen, 800 ve 531 nm' de absorpsiyon göstermiş ve reaksiyon ilerledikçe absorpsiyon şiddetleri artmış bununla birlikte, akrilamid varlığında ise 531 nm deki pikin kaybolduğu, 800 nm de elde edilen absorpsiyon pikinin şiddeti iki kat oranında arttığı gözlenmiştir (Şekil 1). Literatürde karbazol için katyon (polaron) radikaline ait pikin 410 nm de gözlendiği bulunmuştur. Bu durumda 531 nm deki pikin EKz oligomerlerinin bipolaronuna ait olduğu ve akrilamidin bipolaron ile reaksiyonu ile kaybolduğu söylenebilir. Br-sübstitüye etilkarbazol durumunda ise oligomer piklerinin 800 nm deki absorbans şiddetleri yarıya düşmüştür. Buda reaksiyonun 3-6 pozisyonunda brom olduğu için oligomer oluşunun 2-7 pozisyonundan gittiğini göstermektedir. Karbazol ve etilkarbazol absorpsiyon değerlerinin bromlanmış etil karbazole göre çok çok şiddetli olması,

reaksiyonun akrilamid varlığında yada yokluğunda 3-6 pozisyonunu tercih ettiği sonucunu vermektedir. In-situ olarak gerçekleştirilen UV-visible ölçümlerine göre, reaksiyon mekanizması aşağıdaki şekilde özetlenebilir:

X: ClO_4^- (Et_4ClO_4, $HClO_4$), AAm **R:**

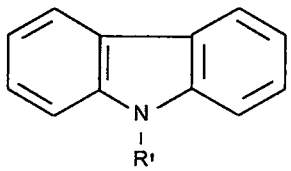

R' : H, $CH=CH_2$, C_2H_5

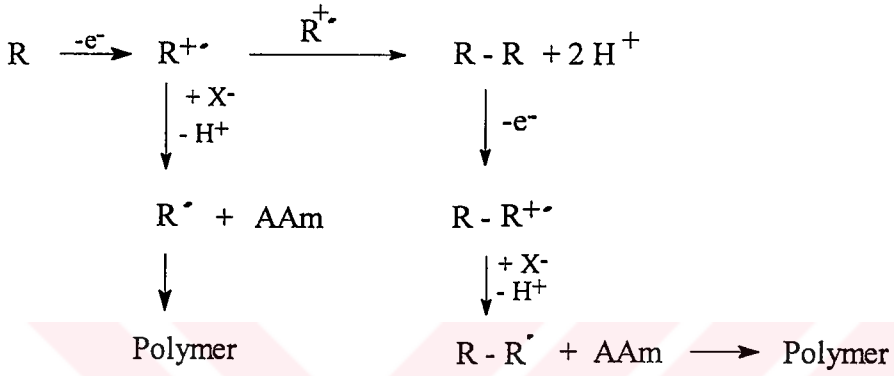

ŞEKİL 1

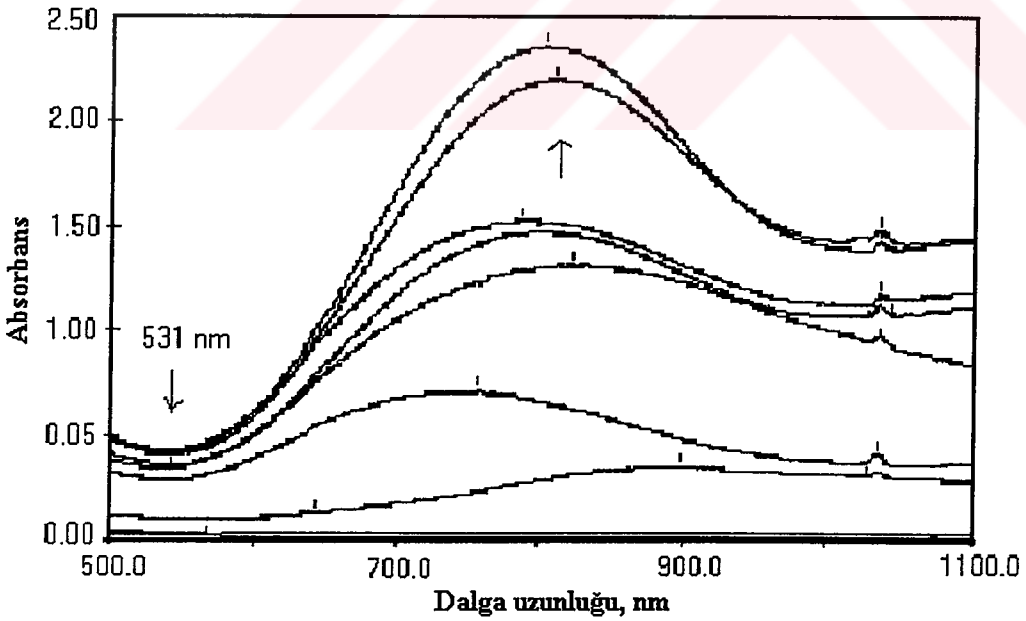

Şekil 1 Reaksiyon sırasında spektrokimyasal olarak elde edilen UV-Visible absorpsiyon spektra; 20:1 (AAm:NECz); Reaksiyon ortamı: Asetonitril, Destek elektrolit: 0.1 $moldm^{-3}$ TEAP, Tarama Hızı: 50 mV s^{-1}, Çalışan ve yardımcı elektrot: Pt, Referans elektrot: Ag/AgCI (8 dakika).

Elektrod yüzeyinde oluşturulan polimerlerin gravimetrik olarak yapılan kinetik ölçümlerine göre reaksiyon mertebeleri hesaplanmaya çalışılmışrır. Karbazol ve kullanılan elektrolitin konsantrasyonlarının degişimi ile elde edilen kinetik ölçümlerine göre:

$$Rp = k\,[\text{N-Karbazol}]^{0.50}\,[\text{TEAP}]^{0.63} \qquad (1.1)$$

bulunmuştur.

Akrilamid varlığında ise Rp:

$$Rp = k\,[\text{N-Karbazol}]^{0.54}\,[\text{Akrilamid}]^{0.1}\,[\text{TEAP}]^{0.50} \qquad (1.2)$$

olduğu saptanmıştır.

25 °C-400 °C arasında relatif kütle kayıpları elektrokimyasal olarak elde edilen AAm:NKz karışımları için termogravimetrik analiz ile belirlenmiştir. Aynı sıcaklık aralığında DSC ölçüm değerleri alınmıştır. Polimerin parçalanma prosesisinin açıklanmasıyla ilgili olan endotermik prosesden çok ekzotermik reaksiyon olduğu gözlenmiştir. Görsel kütle kaybı genelikle polimerin bileşimine bağlı olduğu için, TGA ölçümleri, çapraz bağlanan polimer matriksinin stabilizasyonuna bağlı olarak matriksden ayrılan grupların kütle kaybını verir. Literatürde, H_2SO_4 varlığında sadece bağlanmanın 3,3'-dikarbazyl boyunca olduğunun bulunması, karbazolun amin gruplarının protonasyonu 9,9'-karbazyl' in oluşumu engellediği için çapraz bağlanma ile ilişkili olan entalpinin düştüğü görülmüştür.

Elektrod yüzeyindeki filmlerin karekterize edilmesi elektrokimyasal çalışmalar açısından güçlükler içermektedir. Fakat son spektroskopik teknikler bunları çalışılmaya uygun hale getirmiştir. Elipsometri ise film kalınlıklarının ve kompozisyonlarının ölçülmelerinin sağlamasıyla bu konuda önemli bir ilerleme elde etmiştir. Bu metod ile elektrokimyasal büyüme devam ederken ışığın polarizasyonunu ölçülür. Böylece bu çalışmada üçüncü adım olarak, elipsometrik yöntem yardımıyla, karbazol ve akrilamid monomer karışımlarından oluşan asetonitril ve asetonitril-protik asit varlığındaki çözeltiden oluşarak büyüyen polimer filmlerinin optik özellikleri saptanmıştır.

AAm:NKz oranının fonksiyonu olarak optik sabitlerin değişimleri incelenmiş, karbazol miktarı arttıkça absorpsiyon katsayısının arttığı gözlenmiştir. Bu daha fazla karbazolun, matriks yapısının içine girdiğini göstermektedir. Bu yüzden karbazol monomer konsantrasyon oranı akrilamide göre düşük olduğunda, örnek olarak 50:1 AAm:NKz oranında, ölçülen absorpsiyon katsayısı akrilamid polimerizasyonunu başlatan karbazol katyon radikallerin azalması ile düşmektedir. Asetonitril-perklorik asit ortamında, asit grubunun etkisi ile daha stabil katyon radikallller oluşması ile, polimerizasyon hızında artışa neden olmuş ve böylece absorpsiyon katsayısı artmıştır. Ayrıca, film kalınlıkları akrilamid oranına göre incelenmiş, artan akrilamid oranıyla yüzeyin yapısının düzelmesi nedeniyle, kalınlğın arttığı saptanırken, perklorik asit ortamında aynı şarlarda elde edilen film kalınlıklarının artan reaksıyon hızı nedeniyle azaldığı gözlenmiştir.

En son aşamada, AAm varlığında polimerleştirilen karbazolün redox davranışları, ferrosen ve dopamin içeren çözeltilerde döngülü voltamogram yardımıyla test edilmiştir. Ferrosen için oldukça tersinir davranış gösterirken, dopamin varlığında şartlara bağlı olarak literatüre göre, tersinir ve tersinere yakın sonuçlar vermiştir (Şekil 2). Ayrıca, kimyasal olarak sentez edilen akrilamid-vinilkarbazole kopolimeri toluen-siklohekzan çözücü ortamında çözüldükten sonra Pt üzerine kaplanarak, elde edilen bu yeni elektrodun da ferrosen ve dopamine karşı redoks davranışları incelendi. Koşullara bağlı olarak (tarama hızı ve kalınlık) tersinere yakın sonuçlar elde edildi.

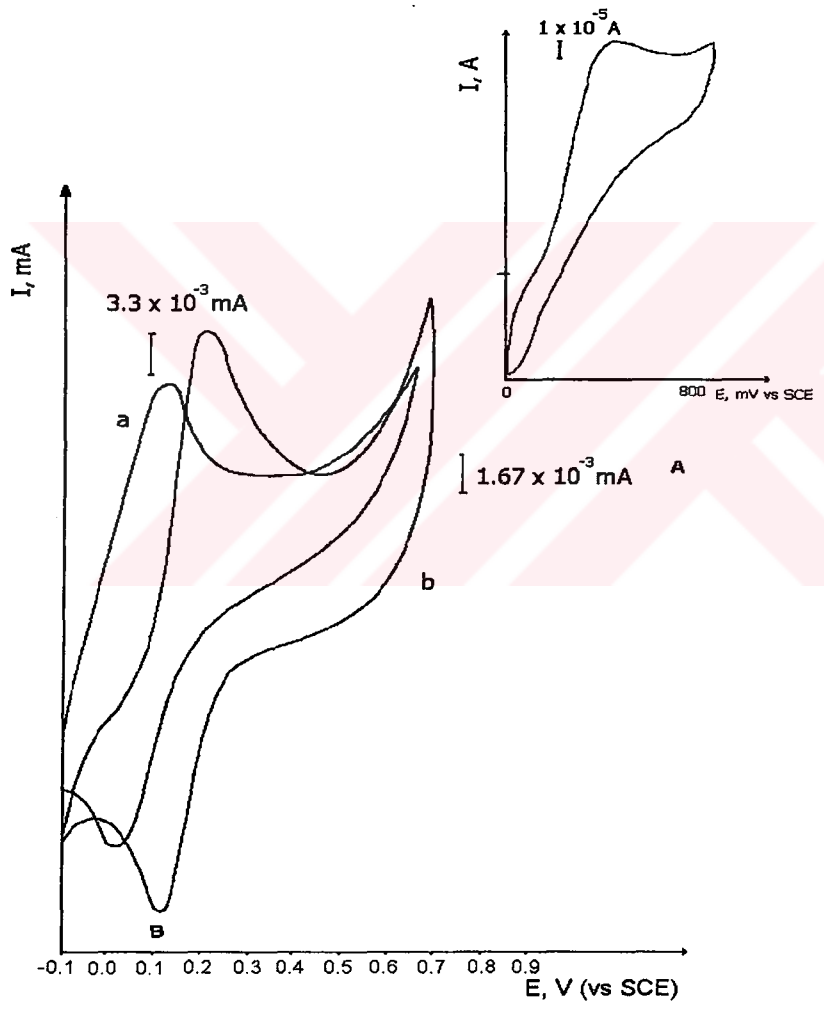

Şekil 2 Tampon çözeltide ki (pH 7.4) 0.018 mol dm^{-3} Dopaminin döngülü voltamogramı; **(A)** Pt elektrot, **(B)** akrilamid/karbazol kopolymer (n_{AAm}/n_{NKz}=50) elektrot, a) yeni hazırlanan elektrod, b) üç gün sonra elektrodun davranışı, Tarama Hızı: 50 mV s^{-1}.

1. INTRODUCTION

The mixtures of materials can be homogenous or heterogenous. In the case of polymers the homogenous mixtures are classified by plastic technologists as blends or copolymers and the heterogenous are defined as composites depending on the type of interaction. The objectives are the preparation of polymeric materials with good surface properties and processability associated with electronic conductivity or electrochromism.

Composites are generally defined as the mixture of two immiscible materials. Conductive polymer blends and composites are prepared by combining an insulating polymer or copolymer with an intrinsically conductive polymer [1]. The most commonly used conductive polymers are polypyrrole, polythiophene, polyaniline and polycarbazole and derivatives.

The copolymers and blends of heteroatomics were of interest since the beginning of the research on electrochemical polymerization to conducting polymers. The π-electron system along the polymer backbone, which confers rigidity, and the crosslinking points between polymer chains make conducting polymers insoluble, infusible and therefore poorly processable. Co-processing of conducting polymers may offer improvements in their mechanical properties and processing. Carbazole-based polymer systems have received the research attention because of their interesting thermal, electrical and photophysical properties [2].

Polyacrylamide (PAAm), and copolymers of acrylamide (AAm) with other monomers are shown a number of properties leading to a variety of industrial applications. Of growing importance are those related to their use as water-soluble viscosifiers and displacement fluids in enhanced oil recovery [3]. PAAm as such has a variety of applications due to its ability to flocculate solids in aqueous suspension [4]. Therefore, the advantage of copolymers are their gradually changeable physical

properties, and copolymerization of AAm and N-carbazole (NCz) derivatives which have also not been reported previously.

Poly (N-Vinylcarbazole) (PVCz) is a specialty material of considerable academic and industrial interest, because of its unusual fluorescence, electric and photoelectric properties [5-7]. It has been used as high temperature dielectric material in the electric industry [6]. The PVCz has a glass transition temperature of 227 °C, which is among the highest known for vinyl polymers. In our work, using of acrylamide as a comonomer is of interest because the homopolymer of AAm has a low glass transition temperature (T_g=85 °C) [8] and is soluble in water. The aim was to obtain both parts of the copolymers in which PAAm inclusion will allow high glass transition temperature and PVCz to be water.

Due to its solubility and other physical properties, initiation and polymerization mechanism of AAm by metal ion-organic reducing system were established and some studies in our group were reported previously [9-16]. Electroinduced polymerization of NVCz were also studied alone [17]. In this study radical polymerization of AAm by using both α,α'- Azoisobutrylonitrile (AIBN) as initiator and redox initiator was investigated. As PVCz is polymerized not only through carbazole units but also through vinyl groups, it was also tried to polymerize electrochemically and chemically in the presence of AAm by radical mechanism through the vinyl groups. Redox initiator was chosen to understand the effect of reducing agent to the vinylcarbazole polymerization in the presence of AAm

As NCz is a prototypical organic molecule, polymers based on this molecule have good electro- and photo- active properties due to their high hole transporting mobility. Strong absorption in the ultraviolet spectral region and the formation of a conducting polymer is of interest in understanding the charge transport as this polymer is highly π-conjugated as compared to other known polymers [18-20]. Due to the fact that, *in-situ* and *ex-situ* spectro-electrochemistry of NCz were studied in detail in the presence of AAm. The mechanism between NCz and AAm was proposed. N-ethylcarbazole (NECz) and 3,6'-dibrethylcarbazole (3,6'-dibrECz) was selected since it enables to build up model system in the presence of acrylamide.

While the organic synthetic metals have prospective usage as electrodes in fuel cells, in rechargeable batteries [21-22] or biological active molecules [23-24], a key problem in their development has been associated with their stability. The pinholes (nonsmooth deposits) and weakly adhering nature of the deposits cause one factor, which is responsible for this instability, especially with PCz type electrodes. Therefore, to prevent this negativeness of the PCz electrode, new electrode which consist of polymer of AAm and NCz was prepared and the redox behaviour was checked on ferrocene and dopamine containing solution by cyclic voltammetry. Depending on the experimental conditions, the electrode response may be reversible or quasi reversible behaviour.

The optical, and electrochemical properties of polymer films grown, from acrylamide and carbazole monomer mixtures have been studied. Ellipsometry, which is an optical technique, was employed *in-situ* to monitor the formation of Co-polymer films. The optical properties of the layers appear to be independent of the growth medium and starting AAm:NCz ratio, in that similar values of refractive index *n* are obtained.

The thermal and fluorescence properties of NCz or NVCz containing polymers were also studied. Thermal stability of acrylamide appears to increase with the amount of carbazole incorporated to the polymer. Glass Transition Temperature (Tg) of AAm polymers obtained by using redox initiator show higher value than polymer obtained by using AIBN initiator. Soluble NVCz containing polymers also show fluorescence properties in water or in dioxane.

2. THEORY

2.1. Electrochemical Initiation

The use of electrochemical methods to initiate polymerization reactions goes back to 1918 [25], but the use of electrodes to initiate polymerization was a dormant field until around 1950, when the method was applied by several workers, such as Parravano [26] and Yang et al. [27].

Faraday's law is the fundamental principle governing electropolymerization. A comparison of product yield charge transferred is a reliable criterion for judging whether a simple a reaction path is followed or a complex set of reactions takes place. The occurrence of chain propagation reactions is immediately evident when large numbers of monomer units are polymerised per electron transferred [28-29].

An electrode reaction, by definition, takes place by a transfer charge between two phases. Often this is associated with the change of charge carrier (e.g. electrons in a metal and ions in an electrolyte). All electrode reactions are interfacial in nature, which means reacting species must be transported to and from the interface [30]:

$$R\,(s) \xrightarrow[\text{(oxidized)}]{} O + e^- \qquad \text{s: substrate} \qquad (2.1.1)$$

The particular characteristic of electrode reaction is that depends on the potential applied to the electrode surface. The rate of the electrode reaction is conveniently measured as a current because each elementary reaction is accompanied by the transfer of a unit charge across the interface.

In electro-organic reactions, the active species is generated on the electrode surface through electron transfer between a substrate molecule and the electrode in which the substrate molecule is transformed to a cation radical or anion radical,

depending on the direction of electron transfer. Thus the active species is generated through electron transfer between a substrate and an electrode, as this always involves inversion of the polarity of the substrate, this type of inversion is not always easy in organic synthesis.

The electrochemical synthesis of conducting polymer is an electro-organic process rather than an organic electrochemical one, because the emphasis is on electrochemistry and the electrochemical process rather than organic synthesis.

Electrochemical polymerization is a radical combination reaction and is diffusion controlled. The radicals generated thus diffuse together and react faster than they can diffuse away from the electrode vicinity. Hence at lower potential the generation of radicals can be controlled in such way that diffusion away from the electrode surface is minimised to avoid a disproportionate reaction of these free radicals. Electropolymerization appears to be a very straightforward synthesis, but for a proper understanding of the phenomenon, attention should be paid to the metal electrode/solution interface.

2.2. Electropolymerization of N-Carbazole Derivatives

2.2.1 Electrocopolymerization of N-Carbazole

NCz, a relatively unimportant molecule in the past, is of considerable interest at present due to the uses of substituted carbazoles in the polymerization studies [31]. Since the carcinogenic activity of carbazole molecules may be associated with their redox properties, and considering that present and future studies may verify the presence of other substituted carbazoles, it was deemed desirable to carry out a broad survey of the anodic oxidation pathways of a number of variously substituted carbazoles. Due to solubility problems, these studies were limited to nonaqueous media, namely acetonitrile.

NCz is a prototypical organic molecule that has shown potential for technological applications. Polymers based on this molecule have good electro- and photo- active properties due to their high hole-transporting mobility, strong absorption in the ultraviolet spectral region and blue-light emission as well. Already,

within the xerographic industry, such as polymers have been considered for use as photoconductive charge-transport layers [32].

. Previous work had established that carbazole, upon anodic oxidation, forms a very unstable cation radical reacts via coupling-deprotonation to 9,9'-and 3,3'-bicarbazyls [33], higher polymers were thought to form upon prolonged electrolysis [34]. When alkyl and phenyl groups were placed on the carbazole nitrogen only the corresponding 3,3'-bicarbazyls formed, in quantative yields, and they appeared to be quite stable under electrolytic conditions.

The electrochemistry of these molecules has been presented in detail previously [35].

When NCz is oxidized in ACN (TEAP) at platinum, the initial step is a (proposed) removel of one electron to form a very unstable cation radical. This cation radical reacts by deprotonation-coupling to form the 9,9'-and 3,3'- bicarbazyl is more easily oxidized than carbazole itself and so the former losses two electrons in two reversible one electron steps to yield a moderately stable dication with extensive conjugation. The 9,9'- bicarbazly is only formed initially under cyclic voltammetric conditions and could not be isolated from controlled-potential electrolyses in unbuffered ACN. The 9,9'- bicarbazyl is only formed initially under cyclic voltammetric conditions and could not be isolated from controlled-potential electrolyses in ACN; the 3,3'-bicarbzyl was isolated in moderate yields. The 9,9'-bicarbazyl was found to form quantatively, however, when electrolyses were carried out in the presence of an organic base such as pyridine. This fact led to the conclusion that the carbazole cation radical forms the 9,9'- bicarbazyl by diffusing out into solution, followed by deprotonation of the central nitrogen and subsequent coupling of the resultant free radicals in solution before they can diffuse back to the electrode to be further oxidized.

Ambrose and Nelson [35] have shown that the electrochemical oxidation of carbazole displays all the characteristics of a classical Electrochemical-Chemical-Electrochemical (ECE) mechanism, and proposed the following reaction scheme:

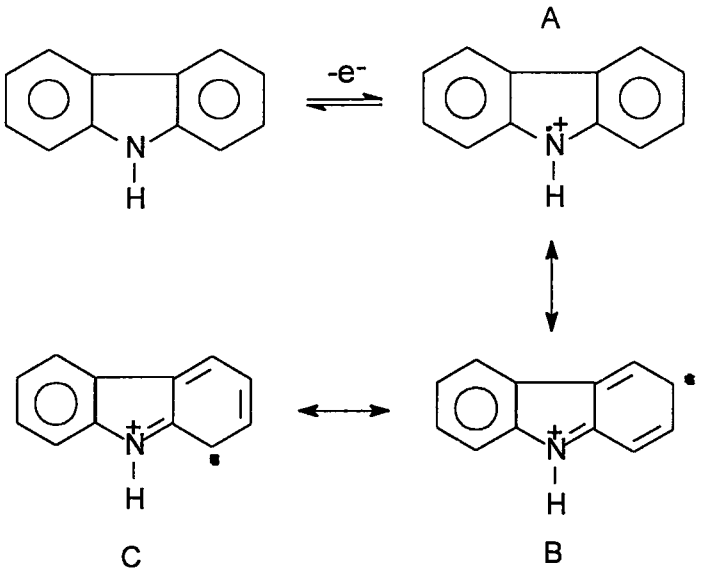

(2.2.1.1)

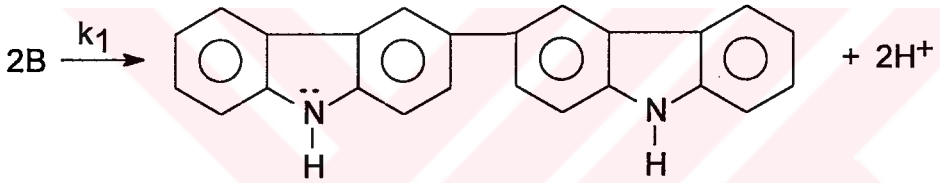

(2.2.1.2)

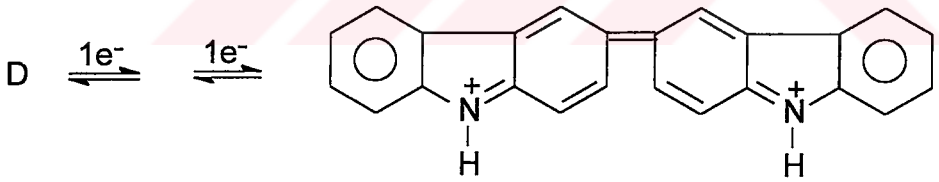

(2.2.1.3)

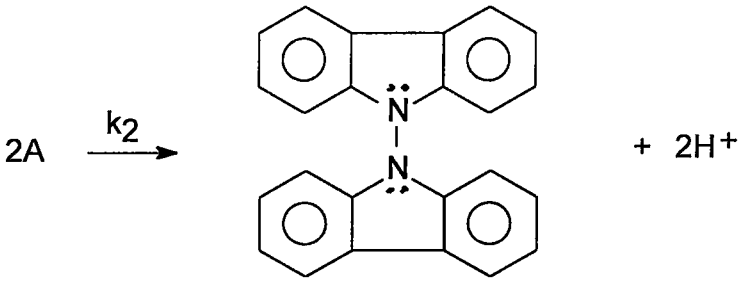

E (2.2.1.4)

Structures A, B and C in the above scheme are the most important resonance forms for the carbazole cation radical. According to these outhors, when there is no proton scanvenger such as pyridine the dimerization of cation radicals (A) occurs at the 3 position and leads to the formation of 3,3'-dicarbazyl (C); this compound, which oxidizes more easily than carbazole, then gives the quinoidal dication (E) which precipitates in the electrolysis cell.

Although the films could be reduced chemically , neither the redox properties nor the film stabilty was tested by Bargon et al. [36].

Electrochemical oxidation of NCz in ACN containing TEAP versus Standart Calomel Electrode (SCE) yields an amorphous conducting film which adheres to the Pt anode. Unlike polypyrrole, polythiophene or polyazulene, these films are very brittle and crack easily. The films have low electrical conductivities of $10^{-4}<\sigma<10^{-1}$ Ω^{-1} cm^{-1} at 300 °K, and the elemental analysis data, $(C_{12}H_{13}N)$ $(ClO_4)_{0.14}$, reveal that they are very rich in hydrogen and contain a high level of perchlorate anions. The films are more likely a mixture of low molecular weight oligomers, but certainly different from the crystalline radical cation salt.

A better morpholgy and adhesion of the coating to the substrate were achieved by pulse galvanostatic oxidation of carbazole in DMF [37], although the electrochemical properties of the deposits were not described in this case either. And, the oxidation of carbazole in protic acid medium provides an easy, straight route for synthesizing films bound to an inert electrode substrate which, in a suitable acid electrolyte, exhibit fair conductivity and stable redox behaviour. The films obtained are similar to those deposited from aprotic media, as both behave in the same way when they are tested under the same conditions.

According to Maitland and Tucker [38], the reaction medium affects the isomer distrubution drastically: In the presence of sulfuric acid, using dichromate as the oxidant, only the 3,3'-dicarbazyl is obtained, whereas in the absence of sulfuric acid the 9,9'- carbazyl is also formed. Electrochemical oxidation studies of Ambrose et al. [39] revealed that the 3,3'- dicarbazyl is typically the dominating electro-oxidation product. The 9,9'- dimer was only formed very early during electrolysis, before the proton concentration build up. Addition of H_2SO_4 suppressed the

formation of the 9,9'- dimer altogether, whereas addition of base as a proton scavenger (pyridine) increased its yield significantly.

2.2.2. Electropolymerization of N-Ethylcarbazole

The achievement of N-substituted carbazoles as coherent films bound to the anode substrate (i.e. modified electrodes) depends strongly on the nature of the substituent.

Dubois and co-workers [28] found that the anodic oxidation of NECz in ACN does not produce filming: the green colour, ascribed to oxidized 3,3' – dicarbazyl units, was seen to diffuse into solution.

Following the findings, NECz produced by anodic oxidation of the relevant monomer in acidic aqueous solutions. The analytical data indicated that the material is a C-C coupled NECz oligomer: voltammetric and coulometric runs suggest that at least tetramers are the basic constituents. This may be totally oxidized to iminum salts by two separate stages involving similar charge amount: however, only the first system, engaging the oxidation of one nitrogen out of two, represents a stable form of the material.

The best defined electrochemical activity is shown by PECz which, however, has the lowest solid state dc conductivity in the homologue series explored. Therefore, other properties such as permeability to the electrolyte, morphology and overall ionic conductivity appear more important for characterizing modified electrodes. In agreement with this point, ac investigation revealed that the close similarity of the PECz film with a redox polymer film, in which electroactive species are dispersed inside a non(electrically) conducting matrix.

Further, it was assessed that the second oxidation state of PECz is more stable than the corresponding state of PCz. These thermodynamic stability conditions require high energy to be distrupted and PCz does show the further oxidation stage at a definitely more positive potential than PECz: at this potential other oxidative degradation reactions probabaly occur [40]. In agreement with this explanation, the second oxidation of PECz, though showing better reversibilty than PCz, occurs at approximately the same potential and thus leads to the degradation.

2.2.3. Electropolymerization of N-Vinylcarbazole

It should be noted that up till 1982 the electrochemical polymerization of NVCz has only been undertaken for preparative purposes [41-42], and that only products obtained in solution have attracted attention. Ambrose and Nelson [35], who are the first to have studied the mechanism involved in the electrochemical oxidation of a certain number of carbazoles, reported a complex behaviour for NVCz which they did not attempt to elucidate.

Electrochemical polymerization of NVCz is different from that of pyrrole (Py), thiophene etc. [43-44]. In comparison with the rather simple molecules of these five membered heterocycles, NVCz represents a more developed π-electron system with more mesomeric forms of the cation radical and with polymerization centres on both the benzene ring and the vinyl group [45]. It should be emphasized that PVCz is polymerized not only through carbazole units but also through vinylene groups. Consequently polymers with different structure and composition can be prepared by electrochemically [46].

Furthermore, it is possible to regulate the extent of polymerization through carbazole units and vinylene groups. It was found previously that the main role in this process is played by water present in acetonitrile solution of the monomer.

The electrochemical oxidation of NVCz is a complex process which depending on experimental conditions, involves several reaction pathways.

When NVCz is subjected to controlled-potential electrolysis, since oxidation of the solvent or of the supporting electrolyte salt is hindered, it seems likely that the first step in the electrochemical oxidation of NVCz involves a monoelectron transfer which yields the cation radical $(NVCz)^{\bullet+}$.

Several authors have reported that polypyrrole, polythiophene and Poly (N-vinylcarbazole) films obtained in solutions containing added water are uniform and adherent, although they exhibit lower conductivity than films prepared in dry acetonitrile [45, 47-50]. The substantial differences in polymer resistance have been

ascribed to structural transformations during polymerization. The modification of the conducting and mechanical properties of the film may also result from changes in chain length, and there is evidence that shorter chains are produced in the presence of water [47]. During redox cycling of the polymers, ion and solvent exchange occur and nucleophilic solvents such as H_2O can react with the cation radical cations or dications produced during oxidation leading to degradation of the polymer [45, 51-52].

The redox behaviour of PVCz films depends strongly on the water content of the acetonitrile solution. In dry acetonitrile, the redox process is relatively fast and reversible. In a mixture containing 10% H_2O + 90% CH_3CN , irreversible changes of the polymer occur during oxidation, and these are attributed to nucleophilic reaction of water molecules with the radical cations of PVCz. In a solution containing 90% H_2O + 10% CH_3CN, oxidation of the polymer is inhibited, probably because of a strong contraction of the polymer film in contact with the aqueous phase.

2.3. Electropolymerization of Acrylamide

There have been many reports on the electroinitiated polymerization of AAm using water as a solvent [53-56]. Some work has also been done on the polymerization of AAm in organic solvent media. DMF [57], ACN [58] have also been studied as a solvent.

The anodic and cathodic polymerizations of AAm which occur together were also studied [55]. In electrolytic polymerization initiating species are produced either by the direct activation of the monomer or by electrode reaction of supporting electrolyte or solvent. The active species may be free radicals or ions thus, it is feasible by electrochemical means to obtain simulteneous free radical, anionic and cathodic polymerization of the same monomer. It is suggested that the direct reduction of AAm at the cathode leads to the anionic polymerization. It is also suggested that an indirect type of initiaiton through the supporting electrolyte leads to the free radical polymerization of AAm with a C-C chain structure of polymers obtained by radical and anionic polymerization were different.

The experimental findings reveal that the cathodic and anodic polymerizations have the following markedly different characters [55]:

1) The cathodic polymerization initially furnishes a homegeneous medium which becomes heteregeneous with the increase of polymer conversion. The continued electrolysis resulted in excessive polymer coating of the cathode which hindered the passage of a constant current. The anodic polymerization proceeds in heteregeneous phase because the resulting polymers precipitate in a finely divided form and no polymer coating on the anode occurs. Relatively more initial monomer concentration is required in order to obtain successful anodic polymerization.

2) The anodic polymerization continues slowly even after the cessation of electrolysis and increases the polymer yields.

3) The anodic polymerization is completely inhibited by a free-radical scavenger such as p-benzoquinone indicating the likelihood of a free-radical mechanism. However, the cathodic polymerization takes place also in the presence of p-benzoquinone, but reduced yield.

4) The anodic polymer yield is comparatively lower than the cathodic one under the same experimental conditions.

5) Anodic polymers are readily soluble in water, whereas the cathodic ones are only partly soluble in water, the water insoluble parts being highly soluble in formic acid.

The findings suggest that the anodic and cathodic polymerizations which occur in DMF solutions of sodium nitrate as supporting electrolyte, the species being oxidised first is either DMF or the nitrate ion. Ross et all. [59] concluded that since DMF is oxidised relatively at a more positive potential, it is the nitrate ion which is discharged as a primary anodic reaction to form a nitrate radical.

$$NO_3^- \longrightarrow e^- + NO_3. \qquad (2.3.1)$$

If two electron transfer occurs at the anode, then NO_3^+ will be generated as follows:

$$NO_3^- \longrightarrow 2e^- + NO_3^+ \qquad (2.3.2)$$

The anodic polymerization of AAm proceeds through free-radical species, NO_3, formed as stated earlier, and/or HNO_3 generated in situ presuambly according to the following reaction scheme as suggested by Ross et all.;

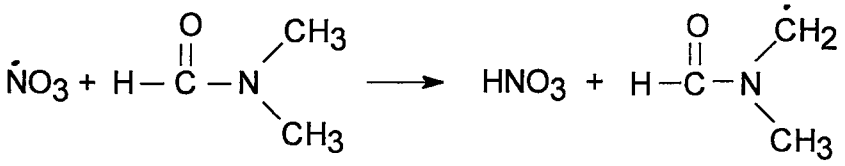

or (2.3.3)

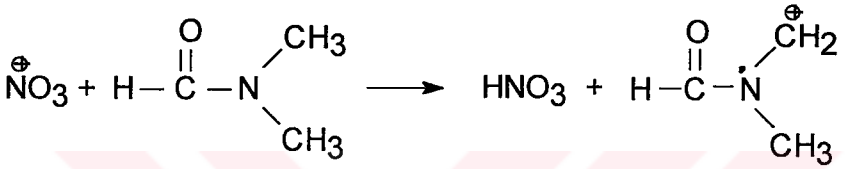

Nitric acid and/or the nitrate radical may interact with AAm to produce monomeric free radicals which give rise to PAAm with C-C chains, -CH2-CH(CONH2)-....., similar to its free-radical polymers formed with azodisobutyronitrile or peroxide [60].

The cathodic polymerization does not seem to be proceeding through a radical mechanism [61-62]. Experimental data show that the cathodic polymerization occurs by direct electron transfer from cathode to AA resulting in the formation of primary radical ions· The radical ions may dimerism and form dimeric dicarbanions, which may continue their growth by a mechanism similar to the anionic polymerization. An anionic mechanism may be suggested in the present case, which may be outlined as follows:

CH_2=CH-CO-NH_2 + Cath. Surf. → CH_2=CH-CO-NH_2 + (adsorb. on the cath.)

(2.3.4)

CH_2=CH-CO-NH_2 (ads) + e^- → CH_2=CH-CO-NH + H^+ , **A** (2.3.5)

$2H^\bullet \rightarrow H_2$ (2.3.6)

CH_2=CH-CO-NH + CH_2=CH-CO-NH_2 → CH_2=CH-CO-$NHCH_2$-$CHCONH_2$

B (2.3.7)

B + CH_2=CH-CO-NH_2 → CH_2=CH-CO-$NHCH_2CH_2CONH_2$ + **A** (2.3.8)

C

A+**C**→ CH_2=CH-C-NH-CH_2-$CHCONHCH_2CH_2CONH_2$ (2.3.9)

In order to explore the view that the anodic polymerization may also be initiated by $HClO_4$, generated electrochemically in situ, the chemical polymerization of AAm was carried out with perchloric acid [63]. It has been found that the acid is quite capable of initiating the polymerization of AAm, which is analogous to its anodic polymerization. The result indicates that the specie being oxidized first is either DMF or the perchlorate ion. As DMF is oxidized at a more positive potential [59], it is the perchlorate ion, ClO_4^-, which is discharged as a primary anodic reaction to form a perchlorate radical, $ClO_4^\bullet$. Consequently, two possibilities of the initiation reaction in the anode compartment are then open: first, the direct interaction between $ClO_4^\bullet$ and AAm may cause a free radical polymerization; second, $ClO_4^\bullet$ may pick up an $H^\bullet$ atom and $HClO_4$ (generated in situ) may react with the monomer to form polyacrylamide with C-C chains, -CH_2-$CH(CONH_2)$- [60].

AAm has also been polymerized electrochemically in aqueous medium in the presence of tartaric acid. The use of dibasic acid in particular is quite interesting from the mechanistic point of view as these systems might involve the formation of diradical or radical ions. To clarify this point the tartaric acid was chosen as the electrolyte[64].

2.4. Electrocopolymerization of N-Carbazole Derivatives, Conductive Polymers and Acrylamide Polymers

In conventional polymer synthesis, copolymerization is a common strategy for modifying polymer properties. Because of the problems associated with copolymerization of monomers of very different reactivates, many authors have looked at an alternative approach which is to synthesise appropriate sections of the desired polymer chain, then couple them electrochemically to get the final polymer.

The copolymerization of hetero-aromatics was of interest since the beginning of the research on electrochemical polymerization to conducting polymers. The advantage of copolymers is their gradually changeable physical properties.

The copolymerization of NVCz monomers with conventional comonomers has been extensively studied [65]; however, some interesting copolymerizations between NVCz and some spesific comonomers (Table 1) afford materials with distinctive photoconductive, electrical and thermal properties relative to those of the conventional copolymers and homopolymers based on pendant carbazole units. In general, these materials have been obtained through free-radical (AIBN) copolymerization in dry benzene at ambient temperature. In a few cases, cationic copolymerization techniques have been employed (Table 2.4.1) using aprotic acid initiators, e.g. $AlCl_3$, $SnCl_2$, $SnCl_4$.

The copolymerization of Py and N-methylpyrrole with NVCz and NECz was investigated [66]. The grafting of Py onto PVCz was examined.

PVCz and poly(pyridylvinylene phenylene vinylene copolymer derivatives was also studied for photoluminescene and electroluminescene purposes. The blends of the two polymers show a similar new photoluminescene emission for a large of concentrations [67].

Table 2.4.1 Copolymerization involving N-vinylcarbazole

Comonomers	Copolymerization Process
NVCz/p-nitrostyrene	(a) Photoirradiation (b) Thermal/AIBN
3-Vinyl-N-ethylcarbazole/styrene	Free Radical
3-Vinyl-N-methylcarbazole/styrene	
3-Methyl-NVCz/styrene	Free-radical
NVCz/N-vinylphthalimide	Free-radical
NVCz/vinylferrocene	Free-radical
NVCz/4-vinylpyridine	Free-radical
NVCz/5-nitroacenapthene	Free-radical
NVCz/m-nitrostyrene	Free-radical
NVCz/styrene	Free–radical
NVCz/N-vinylpyrrolidone	Cationic
NVCz/N-propenylcarbazole	Cationic
NVCz/1-vinylnaphthalane	Free-radical
β-N-Carbazolylethyl vinyl ether/maleic anhydride	Free-radical
β-N-Carbazolylethyl vinyl ether/N-substituted maleimide	Free-radical
NVCz/divinylbenzene	Cationic

Conductive polymer composites and copolymers of Py and NVCz was investigated as well [68]. Both insulating and conducting polymers of NVCz are utilized in the electroinitiated polymerization of Py. These study showed that, a sufficient homogeneity of the films can also be achieved by blending/grafting a conducting with a nonconducting polymer which has an electroactive group.

Although some studies have been conducted on the copolymerization of AAm with vinyl monomers, there is not much studies about copolymer of AAm with conjugated polymers [69]. In spite of many studies about conductive polymer blends and composites are prepared by combining an insulating polymer with an intrinsically conductive polymer. Polyamide/polypyrrole composite film was obtained by the electrode coating method [69]. The polyamide film was obtained in situ by coating a stainless steel electrode with a polyamic acid film followed by imidization with pyridine and acetic anhydride. The coated electrode was submitted

to a constant current in a Py/$LiClO_4$ solution in acetonitrile. Combination of polypyrrole with this polyamide was shown to increase markedly its thermal and enviromental stability.

Electrochemical polymerization of Py in an excess of AAm was studied whose oxidation potentials are significantly different, from a mixture of each monomer by our groups [70]. Eventhough conductivity decreases by the introduction of AAm into PPy as expected, the increase in flexibility of resulting polymer film might be an advantage in most of the application of conductive polymer.

2.5. Other Polymerization Type of N-Carbazole Derivatives

A great deal of attention has been given to PVCz over the years because of its unusual electrical and photoelectrical properties. Earlier work on PVCz focused on its dielectric characteristics while more recently its electrophotographic properties have been utilized in commercial photoreceptors. Its unusual electrical behaviour, high glass-transition temperarture (227°C) and brittleness, ease of polymerization by a variety of techniques, and intriguing morphological features and solution properties combine to make PVCz a polymer of considerable current interest.

NVCz is a reactive monomer towards radical and cationic polymerization because of its ability to stabilize electron-deficient centers by resonance involving the nonbonding electron pair on the nitrogen atom in the carbazole ring.

Free- Radical Polymerization: Free-radical polymerizations carried out in dispersion and suspension. Like many free-radical polymerizations, that of NVCz is inhibited by oxygen. Perhaps more important is the effect of certain impurities (anthracene, phenanthrene and sulfur) inherent in carbazole derived from coal-tar sources.

Bevington and Dyball have carried out end group studies on PVCz prepared by polymerization at 60 °C in benzene using either AIBN or BPO as initiator [71]. AIBN gave polymers having an average of 1.35 initiator fragments per molecule. BPO gave polymers of unexpectedly low molecular weight, having close to two initiator fragments per molecule at concentrations of monomer greater than 0.08 mol

dm^{-3}. That a competitive process is operative, in which simple free-radical polymerization may also be occurring to a small extent, is indicated by the presence of a small amount of high molecular weight polymer.

Cationic Polymerization: In its free-radical polymerization, NVCz is typical of many other vinyl monomers (methylvinyl ether, N-vinylpyrrolidone, etc.). However, unlike other electron rich monomers, NVCz can be polymerized cationically even by the weakest initiators. Indeed, it has been polymerized with protonic acid [72]. Even the generally accepted concept that basic solvents preclude cationic polymerization can not be applied to NVCz .

Boweyer et al. [73] have studied the cationic polymerization of NVCz by tropylium hexacholoroantimonate and tropylium perchlorate. Polymerization initiated by both catalysts showed identical features. Molecular weights of PVCz from the perchlorate initiation were slightly lower than those from the hexachloroantimonate catalysis and did not show the same temperature variation. From both catalysts, however, the molecular weight data showed clear evidence of a transfer reaction characteristic of homogeneous cationic systems [74].

Ledwith and Sherrington [75] have also reported the only example of a propagating dication by reaction of NVCz with the stable cation-radical tris-(p-bromophenyl) aminium hexacholoroantimonate. Although this system with the propagating dication is extremely interesting and important, a question remains as to why relatively large amunts of catalyst must be used and why a molecular weight of ≈10.000 can be achieved. Ledwith [76] has suggested that this may be caused by competitive cyclodimerization.

There are numerous other reports of the cationic polymerization of NVCz, utilizing a variety of acidic reagents [77]. Among the most recent studies are those by Pielichowski [78] who described the polymerization of NVCz initiated by hydrogen halides, HF, HCI, HBr and HI [79].

2.6. Degradation and Stability of N-Carbazole Derivatives

Although there is a very wide spectrum of conductive materials with extremely different behaviour, we can still identify certain fundamental processes involved in the degradation and stability behaviour of conductive polymers.

Since PVCz is a vinyl derivative with a high Tg, requires high processing temperatures (> 230 °C),and sees enviroments in photoelectric applications such as UV light, oxygen and corona discharge, the molecule is expected to degrade. Very little work has been done in the past on the thermal and radiative degradation, oxidation and ozonization of PVCz.

Decomposition of polymers can occur via a direct or indirect process. Direct decomposition occurs when chromophores or irregular bonds are contained in the main chain [80]. Indirect decomposition includes energy-transfer processes and radical reactions following absorption by impurities. Whether by direct or indirect decomposition, the formation of a free radical can lead to one or more reactions [80]. The first step is associated with the initiation reaction and is influenced by the presence of radical initiators, oxidation products and sensitizers. The second step is associated with propagation and is influenced by the presence and diffusion of oxygen. The third step is causes of branching and crosslinking in the polymer.

Oxidation of pendant group is also possible. In vinyl polymers it is initiated by an attack on the tertiary hydrogen and, in some cases, by an attack directly on the pendant group [76]. Generally, the aromatic groups oxidized to form quinones, which can then undergo further reactions to form alcohols [81].

Thermal, oxidative and enviromental degradation tests have been performed on several commercial and fractionated PVCz materials as a function of ambience, temperature and time [82]. Low molecular weight samples were the most resistive to degradation in air and argon at 180, 280 and 330°C. High molecular weight PVCz performed better than an '' as receieved '' commercial material which contained approximately 5% impurities. The impurities evidently initiate and help propagate

degradative reactions leading to a discolored cross-linked matrix. The differences observed in air and argon are due to the presence of oxygen which, according to the suggested reactions, increases the propagation reaction and leads to branching and crosslinking.

There are quite studies about thermal properties of modified or copolymers of PVCz. Polymerization way also effect thermal characteristic. For insantance, thermogravimetric analysis reveals that PVCz prepared with $FeClO_3$:NVCz mole ratio of 9:1 exhibits higher stability than that obtained with a ratio of 6:1. The temperatures for initial 20%, 40% and 60% for these two polymers are respectively, 230, 190; 310, 280; 420, 370 and 460, 420 °C. In either case, the polymers undergo 95% decomposition at >550 °C. The higher stability of the 9:1 PVCz is evidently due to a higher molecular weight than the 6:1. The $FeClO_3$ initiated PVCz, on the other hand, exhibits a somewhat higher initial decomposition temperature, about 260 °C, but beyond 20% decomposition becomes progressively less stable (40% at 350 °C and 50% at 390 °C) than the suspension-polymerized PVCz. The trend is again consistent with the lower molecular weight for this polymer. Differential thermal analysis reveals a sharp exotherm around 450 °C, signifying oxidative degration of the polymer network [83].

Copolymers of methyl and ethyl methacrylate with NVCz were synthesized by free radical bulk polymerization using benzoyl peroxide as an initiator. It has been found that with an increase of NVCz content in the copolymers, their thermal stability increases [84].

The thermal degradation of phosphorylated PVCz also was studied by thermogravimetry. The onset degradation temperature decraeses with respect to that of unmodified PVCz indicating a lower thermal stability for the phosphorylated sample [85].

Hydrogen halides were studied to understand effecting this group of thermal properties of PVCz. It was found that the polyvinylcarbazole-hydrogen halide molecular complexes undergo thermal decomposition with release of hydrogen halides in the temperature range of 80-180 °C. Thermal stability of PVCz, after removal of hydrogen halides, is higher by approx. 10°C in comparison with PVCz

itself. This can be explained by a more streoregular structure of PVCz obtained upon polymerization in the presence of hydrogen halides [86].

Ferric Chloride-initiated polymerization of pyrrole in the presence of N-Vinylcarbazole was studied.The initial decomposition temperature, is PPy (210°C)<P(Py-NVCz) (225 °C)<PVCz(255 °C) has been found.The DSC scan for PPy is similar but the peaks are less sharp. It is obvious from the DSC scan the major structural degradation occurs in the range 250-520 °C in these systems [87].

2.7. Ellipsometric Studies of Electrochemically Growth of Polymer Films

Characterizing films on the electrode surfaces have always been a challenging problem in electrochemistry. Recent developments have lent new impetus to efforts to adapt classical spectroscopic techniques to make them suitable for studies of these films. Such studies have found considerable contemporary importance in the chemical modification of electrodes [88] and in the discovery of electonically conducting heterocyclic polymers [89]. Ellipsometry have especially played key role in this area that providing a measure film thickness and overall composition. This method can be used to study films *in situ* during electrochemical growth, cycling and degradation, thus providing information of direct relevance to that obtained by other electrochemical techniques.

Ellipsometry was originally developed specifically for the optical characterization of thin films. In principal therefore it is an ideal technique for characterizing the optical properties of electroactive polymer-modified electrodes. Because it is a reflectance technique, it is straight forward to perform the experiment *in situ* in the electrochemical cell, allowing measurements to be performed as a function of potential. Additionally ellipsometry is very sensitive, so submonolayer amounts of materials can be detected. A related further advantage is its high degree of surface selectivity. This is important since, in an *in situ* experiment, where it is often diffucult to distinguish between a given species (for example, solvent or ions) in the surface film and the huge excess of the same species in solution.

An ellipsometer measures the polarization state of light. Applied to electrode surfaces, monochromatic plane-polarized light is incident on the working electrode.

The state of polarization of the reflected light is different: it is in general elliptically polarized, and the change in polarization depends on the optical properties (that is, the refractive index) of the surface. The ellipse is characterized by two parameters: the azimuthal angel between its major axis and the plane of incidence, and the ratio of the minor to major axes. If our electrode is covered with a film, the state of polarization of the reflected beam also depends on the refractive index and thickness of the film.

In principle ellipsometric measurements are a way of determining film thickness *in situ*, as a function of redox state, and this was an early driving force behind attempts to apply ellipsometry to eletroactive polymers [90]. The thickness of an electroactive polymer film is a highly significant parameter. As a function of the redox state of the material, thickness can be expected to vary with, among other parameters, polymer tertiary structure and solvent and ion populations. Nonoptical methods of determining film thickness are rather unsatisfactory, since they are invariably made *ex situ.*

Because both electrode and electroactive polymer materials are nearly always optically absorbing over the usual wavelength range used for ellipsometry (400-900 nm), their refractive indices are complex quantities $N_J = n_J - ik_J$, where n_J is the real and k_J the imaginary component of the refractive index. The quantity k is also known as the extinction coefficient. Ellipsometry measures two parameters, the two angles that characterize the ellipse of polarization.

So far there have been no studies for the ellipsometric analysis of the carbazole, carbazole derivatives and copolymers. But there is a great deal of studies about the other electroactive polymers such as, polyaniline, polythiophene, polypyrrole.

The story of ellipsometric studies of polyaniline (PA) shows that increasing sophistication in the technique has led to successively more valuble information from experimental data. Conclusions from these studies are remarkably consistent: Ellipsometric data collected both for the oxidized and reduced forms of the film could be fitted to a model involving a single homegenous film of constant n and k and increasing thickness, up to a thickness of ca. 150-200 nm.

Results show that in fact the film growth by a mechanism so that nucleation at limited points on the elctrode occurs, producing a thick film with refractive index close to that of the electrolyte. Subsequently as the film grows, it also increases in density, as the initial nucleation sites grow laterally and begin to overlap. This observation is consistent with results from investigations by other workers on the growth of heterocyclic-conducting polymers. Clearly whatever electrochemical method is used to grow the film, the necessity for nucleation to occur cannot be obviated, so this mechanism probably aplies to all films previously described [91].

Like PA, PPy has been the subject of several studies using different types of ellipsometer [92]. Using three-parameter ellipsometry, extensive work has been done on the growth and subsequent electrochemistry of PPy films. Films were produced under conditions most commonly encountered in the literature (neutral aqeous or acidic aqeous solutions, acetonitrile containing varying amounts of water) and effects of monomer concentration and growth potential were also tested. The most striking fact is that the magnitude of n for the film as grown is directly related to growth conditions. The more optimal these are (as assessed from literature relating to film conductivity and mechanical properties), the lower is n at 633 nm. For example in ACN solution, employing low concentrations of monomer and high growth potentials, film with high values of k were made, but n was higher than for films made using high monomer concentrations and less extreme potentials, which are known to produce better, more conductive films. In aqueous solution acidic conditions are known to produce better films than neutral conditions, and this, too reflected in n values in this study. Interestingly if more concentrated pyrrole solutions (0.1 mol dm^{-3}) are employed in neutral media, the film's optical properties approach values seen for growth in acid media [93]. This is because protons are produced during polymerization, which leads to a suitably acidic pH near the electrode. The growth mechanism for all films made, assessed by examining the evolution of n, k and L as before, was similar to that expounded in the preliminary communication.

2.8. Polymer Modified Electrodes

Electroactive polymers can be divided into three broad classes: electronically conducting polymers, such as PPy in which conduction is associated with motion of charge carriers along the chains; redox polymers, such as poly (vinylferrocene) in which conduction is associated with cross-exchange reactions between discrete redox sites; and polymer electolytes, such as nafion, in which conduction is associated with ion motions within the film.

Films of these polymers can be deposited on the electrode surface by a variety of methods, including electropolymerization and dip or drop, coating from solutions of the performed polymer. The former technique has two advantages: Deposition can be controlled by adjusting the electrode potential, and the process is localized at the electrode surface. This has led many groups to study electropolymerised films as method for immobilizing enzymes and other biological components. However to use this technique, the polymer must be soluble in the elctrolyte solution ultimately used for electrochemical studies.

Modified electrodes are used for detecting and measuring the concentration of various chemical species in liquid or gas phase. An ideal chemical sensor should exhibit high sensivity, selectivity, high operation speed, reversibilty and stability under operating conditions. Morever, it should not be sensitive to temperature changes of various kind.

For over ten years extensive investigations of various metals, oxides, inorganic semiconductors, solid electrolytes, carbon- and silicon like materials have been carried out and changes in the electrochemical potential, electrical, optical, magnetic, thermic and other properties taking place in these materials as a result of their interaction with particular gases have been studied [94].

Electronically conducting polymers with conjugated π bands, e.g. polyacetylene, polyparaphenylene, polypyrrole, polythiophene, polyaniline, polycarbazole are likely to show properties meeting the requirements mentioned above, because their conductivity depends on the electronic structure which can undergo changes under the influence of a chemical species adsorbed on the surface

of the polymer layer. These changes may result e.g. from redox or acid-base interactions between polymer and the chemical species.

For instance, polyacetylene may be used for determining the concentration of nitrate ions in acid solutions because, as the result of the process involving the intercalation oxidation. The conductivity of this polymer changes which is probably due to disturbances occurring in the band structure of π electrons [95].

Interestingly with our studies, polycarbazole has been investigated earlier [96-97, 37] for its catalytic activity. It was not known at the time whether this polymer would be selective enough for the oxidation of biologically active molecules. And then it is established that this electrodeis selective some biolgical active molecules. For this purpose, it was used to determine dopamine [23-24].

3. EXPERIMENTAL WORK

Table 3.1 Structures and abbreviations of monomers and polymers

Monomer	Structure	Abbreviation	
		Monomer	Polymer
N-Carbazole	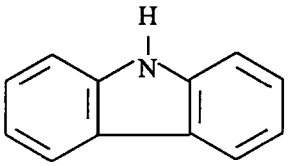	NCz	PCz
N-Vinylcarbazole	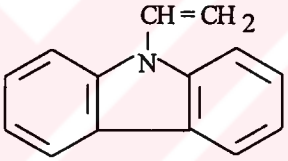	NVCz	PVCz
N-Ethylcarbazole	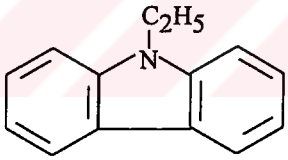	NECz	PECz
3,6-dibromoethylcarbazole	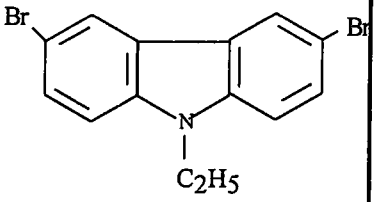	3,6-dibrECz	
Acrylamide	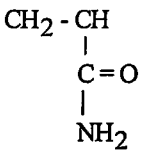	AAm	PAAm

3.1 Materials

N-Carbazole (NCz, BDH), N-ethylcarbazole (NECz, Aldrich), N-vinylcarbazole (NVCz, Aldrich), Acrylamide (AAm, Merck), Ferrocene (Aldrich), Dopamine (Aldrich), Cericamonnium nitrate (CAN, GPR), Cericsulphate (Fluka), Oxalic acid (Merck), Acetonitrile (ACN, Carlo Erba HPLC grade), Dimethylformamide (DMF, Carlo Erba, Spectroscopic grade), Dioxan (Carlo Erba), Tetraethylammonium perchlorate (TEAP, Fluka), Perchloric acid ($HClO_4$, Aldrich). α,α'-Azobisisobutyronitrile (AIBN) provided by Fluka was recrystallized from methanol.

3,6'-dibromethylcarbazole (3,6'-dibrECz) was synthesized according to the literature [98].

3.2 Instrumentations

The electrochemical measurements were carried out using an EG & G Princeton Applied Research Model 362 scanning potentiostat in conjunction with LLOYD instruments PL3 X-Y recorder for data display and Wenking POS 73 Model Potentiostat connected with a Kipp and Zonen X - Y recorder. FT-IR spectra were recorded using Mattson 1000 Spectrophotometer by in KBr pelet. UV-Visible spectra were obtained from filmed tin oxide glass and in solution by Shimadzu 160 A Recording Spectrophotometer. The SEM experiments were made on a Jeol JSM 840 Scanning Electrode Microscope. ^{1}H-NMR analyses were recorded on a Bruker 250 MHz NMR electrospin.

For *in-situ* measurement of the optical properties of the resulting polymers, a computer-controlled Gaertner L116B rotating analyser ellipsometer was used with a He-Ne laser of wavelength $\lambda = 632.8$ nm (1.96 eV) incident onto the sample surface at an angle of 70°. A diagram of ellipsometer are used for these experiments is shown in Figure 3.2.1.

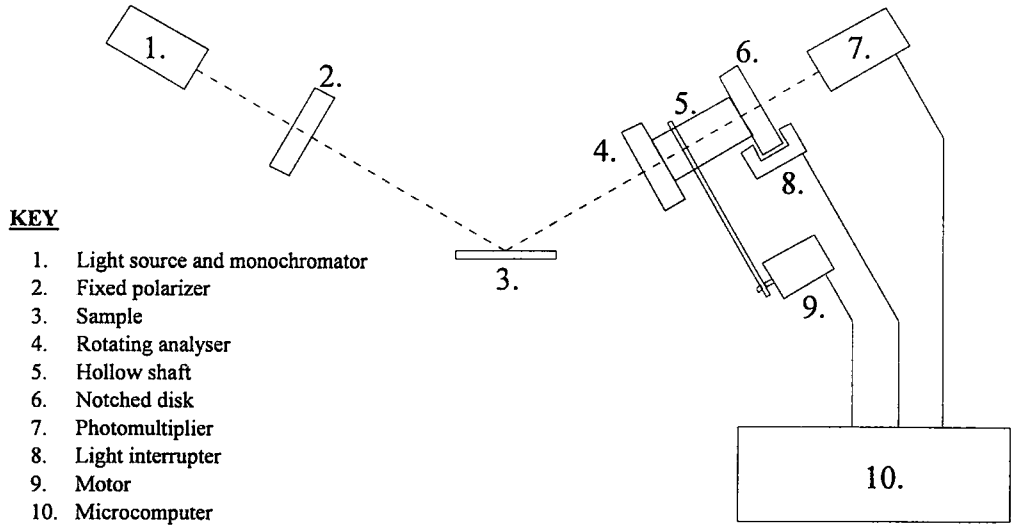

Figure 3.2.1. A diagram for ellipsometer

The electrode substrate was mounted in a special electrochemical cell constructed of polytetrafluoroethylene (PTFE) and fitted with quartz windows for the incident and reflected beams.

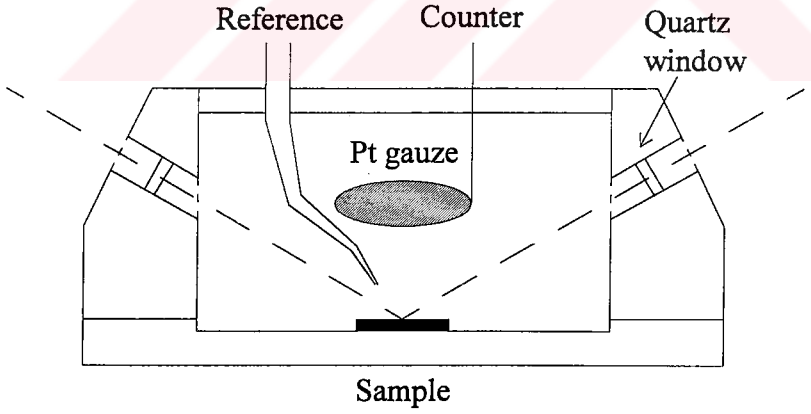

Figure 3.2.2 Schematic representation of the ellipsometry experiment prior to film growth polarized light is reflected from the solution.

The ellipsometry angles of Δ and Ψ, representing the phase difference and amplitude ratios respectively between the *P*- and *S*-polarised lights, are defined by:

$$\tan\Psi \cdot \exp(i\Delta) = \frac{\tilde{r}_P}{\tilde{r}_S} \qquad (3.2.1)$$

where $\tilde{r}$ represents the complex reflection coefficient for the *P*- and *S*-polarised light after reflection from the surface of interest. The ellipsometry measurements were carried out simultaneously with the measurement of the charge consumed during the growth of the polymer film using an EG&G PAR 279 digital coulometer so ass to allow independent verifcation of the film thickness. DSC experiments were performed with a Mettler-Toledo DSC30 controlled by a TC11 processor, and interfaced to a personal computer. Aluminium pans were used for both the loading of the samples and as the reference pan. The system was sealed and flushed with nitrogen gas at a flow rate of ~10 ml min^{-1} for 10 min before any measurements were carried out. The flow of N_2 was also maintained during the measurements to minimise convection effects as well as to ensure that the system remained free of oxygen. The heating rate normally employed was 10 K min^{-1} over the temperature range 25°C to 500°C. Thermogravimetry analysis (TGA) was performed with a Perkin-Elmer TGA 7 with a TAC7/DX controller, again linked to a personal computer for data logging and control. Helium gas at 10 ml min^{-1} flow rate was used as the inert purge gas and the heating rate was 10 K min^{-1} from 25°C to 500°C.

Conductivity was measured on the pressed discs at room temperature on a Keithley 617 Electrometer connected to a four probe head with gold tips and calculated from following equation [99].

$$\sigma = I \times V^{-1} (\ln 2 / \pi d) \qquad (3.2.2)$$

Where, V is applied potential, I is current, d is thickness in cm.

3.3 Preparation of N-Vinylcarbazole Containing Acrylamide Polymers with Using AIBN initiator

Polymerization of acrylamide and their copolymers, in two feed ratios, was carried out by the free radical solution polymerization technique [100] as described below:

Copolymer of NVCz with AAm were prepared by the radical polymerization with an initiator (AIBN), in degassed DMF in a three-necked reaction flask. The reaction mixture was heated at 80 °C for a period of 1 hour under nitrogen atmosphere. The starting concentration of the NVCz were and 0.01 mol dm^{-3} and concentration of acylamide were 0.99 and 0.90 mol dm^{-3}, respectively and that of the initiator (AIBN), 0.05 mol dm^{-3}. The first copolymer was called as LNVCAm (low NVCz containing AAm) and the second one was called as HNVCAm (high NVCz containing AAm). The precipitate was filtered and unreacted monomers were removed by washing the product with DMF and acetonitrile, respectively. The product obtained was repeatedly washed with diethyl ether and finally dried vacuum before charecterisation.

Since the LNVCAm behaves like its homopolymer, its molecular weight measurement was performed with the help of Ubbelohde viscometer and the same constant for used with its homopolymer [102]. The molecular weight was obtained as 21000 for LNVCAm.

3.4 Preparation of Electrochemically Induced Redox Polymers of Acrylamide

Electrochemical polymerization of acrylamide has been studied in aqueous solution in the presence of Ce(IV)-OA redox initiator systems in the temperature range of 20-70 °C. A two compartment electrochemical cell was employed and the compartment were divided by sintered glass disc to avoid polymer diffusion. Constant magnetic stirring was maintained during current flow the cell placed, in a thermostatic bath kept at constant temperature. A 2 cm^2 platinum was employed as working electrode and placed into the anolyte. 2 cm^2 Pt electrode was used as a counter electrode. In order to determine the amount of polymer formed a constant potential was passed through the reaction mixture for the desired time period. At the end of experiment, the anolyte was poured into excess of acetone, the solution was filtered, dissolved in water again and reprecipated wih acetone in order to remove monomer and electrolyte contamination from the polymer.The polymer was dried at vacuum to constant weight.

3.5 Preparation of N-Vinylcarbazole Containing Acrylamide Polymers with Using Redox Initiator

Electrochemical redox polymerization of NVCz with AAm has been studied in DMF and DMF:water mixture in the presence of Ce(IV)-OA redox initiator system at the room temperature. The controlled potential electrolysis system was applied in a electrolysis cell. The reference electrode was Ag/AgCI electrode, 0.1 mol dm^{-3} H_2SO_4 was used. Cathode and anode were 0.4 cm^2 platinum.

A two compartment electrochemical cell was also employed for this system. Acetone was used as the polymerization medium in the precipation method. The samples withdrawn periodically were precipated in acetone, filtered and dried in vacuum oven.

3.6 Electropolymerization of N-Carbazole in the Presence of Acrylamide

Co-polymerization of AAm:NCz has been grown electrochemically from solution consisting 0.1 mol dm^{-3} TEAP as a supporting electrolyte in CH_3CN. The working electrode was a Pt (A=0.4 cm^2) and placed in a cell with a three electrode configuration using saturated calomel electrode (SCE) as a reference and Pt coils as a counter electrode. In comparison, PCz:PAAm composite was also prepared electrochemically by polymerization of acrylamide onto precoated PCz.

Polarising the electrode performed electrodepositing of polymeric films by CV techniques between 0.0-1.2 V or 0.0-2.0 V (vs. SCE). Net electrodepositing charge was recorded about $7.2x10^{-2}$ C. Polymerization was occurred at the anode surface. The films obtained on the electrode surface were washed with ACN and water several times to remove unreacted monomers and homopolymers.

The reaction media chosen was also mixed solvent consisting of 50% ACN and 50% $HClO_4$ which could dissolve 0.008 mol dm^{-3} NCz (which is poorly water soluble) and 0.4 mol dm^{-3} AAm.

3.7. Electropolymerization of N-Ethylcarbazole in the Presence of Acrylamide

The reaction media chosen were ACN and a mixed solvent of consisting 50% ACN and 50% $HClO_4$ (from 0.1 to 2 mol dm^{-3} $HClO_4$). The co-polymer films were deposited potentiostatically, using the technique of cyclic voltammetry between the potential limits of 0.0 V and 1.8 V at a scan rate of 0.1 V s^{-1}. The working electrode was a Pt foil and indium tin oxide (ITO) placed in a three electrode cell with SCE as the reference electrode. A coiled Pt wire used as the counter electrode.

3.8 Thermogravimetric Measurements

Thermogravimetric Analysis (TGA) was performed on a number of the co-polymer samples prepared by the electrochemical oxidation and chemical polymerization method. The technique was used in order to establish the thermal properties of the material as well as to asses the amount of solvent incorporated within the film. The same samples were also analysed for their thermal response by Differential Scanning Calorimetry (DSC) over the same temperature under an inert N_2 atmosphere. The enthalpy recorded for the major enthalpy event as well as the peak temperature.

3.9 Preparation of Polymers as Electrodes

After polymer deposited onto Pt, it was left to the vacuum for 48 hours. The response of coated electrodes to Dopamine (0.018 mol dm^{-3}) and Ferrocene (0.004 mol dm^{-3}) were tested in buffer solution (pH= 7.10) and 0.1 mol dm^{-3} TEAP containing ACN respectively, at different scan rate. The stability of electrodes was tested by leaving them in 0.1 mol dm^{-3} H_2SO_4 and acetonitrile solution for different time intervals. The filmed electrodes were tested by CV in a cell of the same configuration.

The response of VCz/AAm electrodes to dopamine and ferocene which were synthesized by using AIBN initiator prepared by casting from DMF+ THF+ H_2O

(45%+ 45%+ 10%) solution on Pt. To remove the solvent, they were heated at 383°K in vacuum of 10^{-3} Pa for 5 hour.

Phosphate buffer solution of pH=7 was prepared by mixing approximately 60 ml of a 1/15 mol dm^{-3} solution of $Na_2HPO_4.2\ H_2O$ with 40 ml of a 1/15 mol dm^{-3} solution KH_2PO_4 and adjusting the pH to 7 by adding either KH_2PO_4 or Na_2HPO_4 [96].

4. RESULTS AND DISCUSSION

4.1 Polymerization of Acrylamide with Redox Couple

Polymerization of AAm was studied in an aqueous solution in the presence of a Ce (IV)-OA initiator system in an electrochemical cell with and without separation of anolyte and catholyte. For reactions, which required the cathode and anode sections to be analysed individually, a cell, whose compartments were divided by a sintered glass disk of medium porosity, was employed. Polymerization is initiated by the free radical formed by the fast reaction of Ce (IV) and OA. The electrolysis of the reaction solution results in the regeneration of Ce (IV), which oxidize oxalic acid to produce radicals. The reaction was also followed by cyclic voltammetric measurements. Results indicated that the electrolysis method with a divided cell (85% conversion) shows advantages, compared with non-electrolytic (5% conversion) and with undivided electrochemical cell (25% conversion) methods where high concentrations of initiator were used.

4.1.1 Characterisation of Polymers

The reaction between Ce (IV) and OA was obtained by UV-visible absorption measurements. The absorption spectrums of the fresh solution of Ce (IV) and OA alone are given in Figure 4.1.1.1 a and b. While Ce (IV) shows a maximum absorbance at 300 nm and OA has two maximums at 208 and 251 nm in an aqueous 0.5 mol dm^{-3} acidic solution. When they are reacted, the yellow colour disappears to yield at 253 and 241 nm (Figure 4.1.1.1 c). Cyclic voltammetric measurements also show that the reaction occurs between OA and Ce(IV). Furthermore, the absorption spectrum of polymers obtained both from anode and cathode compartments were also taken by dissolving in water (Figure 4.1.1.2 a, b, c). The same maximums, which were observed for OA and Ce (IV), were also seen for polymers obtained at 0.03 mol dm^{-3} Ce (IV) concentration (Figure 4.1.1.2. a, b). The intensity of these absorption peaks decreased with the decrease in polymer obtained at a low

concentration of Ce (IV) (Figure 4.1.1.2 a, c). These results suggest that radical species produced from the reaction between OA and Ce (IV) to initiate the polymerization and inclusion of Ce (IV) into the resulting polymer occurs. The interesting point is that increase in the Ce (IV) concentration about two times for polymerization experiments about two times increase in the absorbance value of redox polymerization of alone. The increase in the yield of anode compartment as the Ce(IV) concentration increases and having higher values than in the cathodic section as well as an undivided cell, show the regeneration of Ce (IV) which reacts again with OA to produce more radicals initiating polymers.

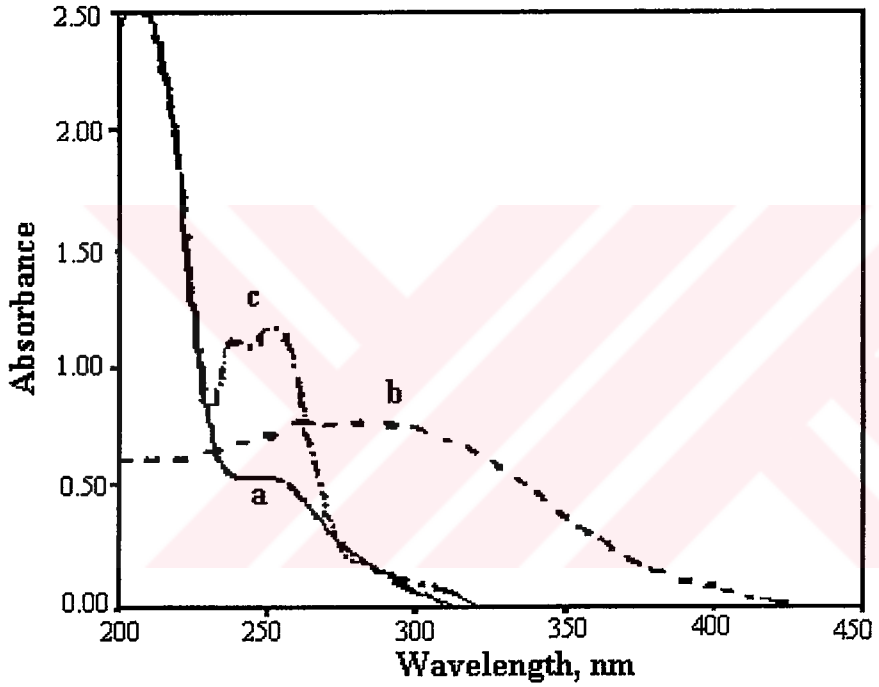

Figure 4.1.1.1 UV-Visible spectra of [Ce (IV)], [OA]; a) [OA]= $2x10^{-2}$ mol dm^{-3}, b) [Ce(IV)]= $5x10^{-4}$mol dm^{-3} , c) Ce(IV)-OA.

In addition to the UV-visible measurements showing the reaction between Ce (IV)-OA, CV of OA and CAN are shown in Figures 4.1.1.3 and 4.1.1.4 a, respectively. Although CAN shows reversible behaviour, OA has only one anodic peak. Under these experimental conditions, on the other hand, AAm has no peak in anodic sweeps, showing that there is no direct electron transfer reaction in this scale. When the OA is added to CAN solution, the oxidation at about 1.35 V is greatly decreased, indicating the reaction between CAN and OA (Figure 4.1.1.4 curve a, b and c). In the presence of AAm, decrease in anodic current is higher, since radical

species produced from the reaction between OA and CAN is rapidly used to initiate the polymerization of AAm.

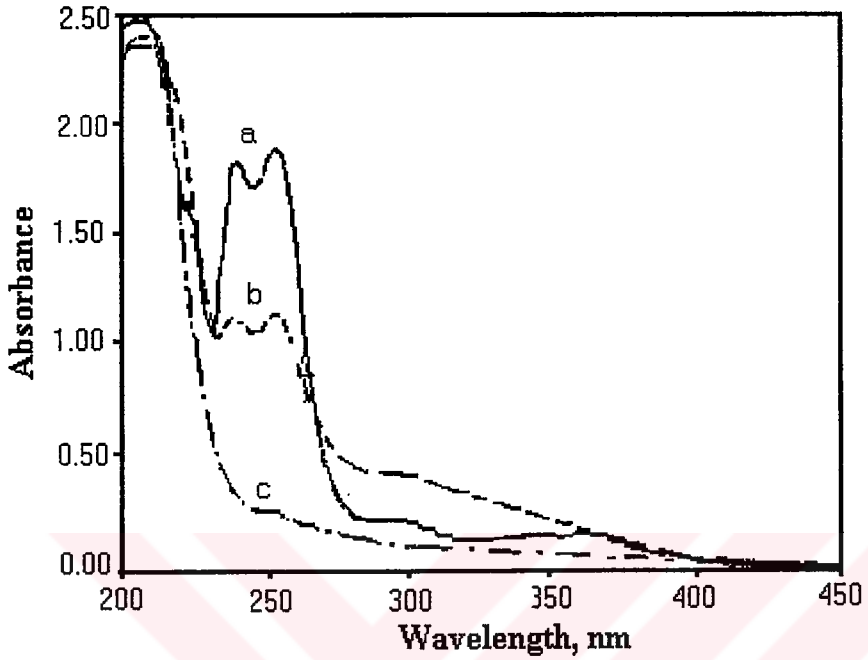

Figure 4.1.1.2 UV-Visible absorption spectra of polymers according to Ce (IV) concentration and differences between anode and cathode compartments; a) [Ce (IV)]= $5x10^{-2}$ mol dm^{-3} at anode, b) [Ce (IV)]= $5x10^{-2}$ mol dm^{-3} at cathode, c) [Ce (IV)]= $5x10^{-4}$ mol dm^{-3} at anode; [AAm]= $5x10^{-1}$ mol dm^{-3}, [OA]= $2x10^{-2}$ mol dm^{-3} $[H_2SO_4]$= $2x10^{-2}$ mol dm^{-3}, ($C_{polymesr}$= $2x10^{-2}$ g dm^{-1}).

The FT-IR spectra of polymers, formed at the anode and cathode are seen from the curves of Appendix A.1 a and b. This spectrum quite resembles the spectrum of PAAm reported by earlier workers [102-103]. Because of having the same polymer structure obtained from anode and cathode compartments, it is also proposed that polymerization goes through the same mechanism and agrees with literature findings.

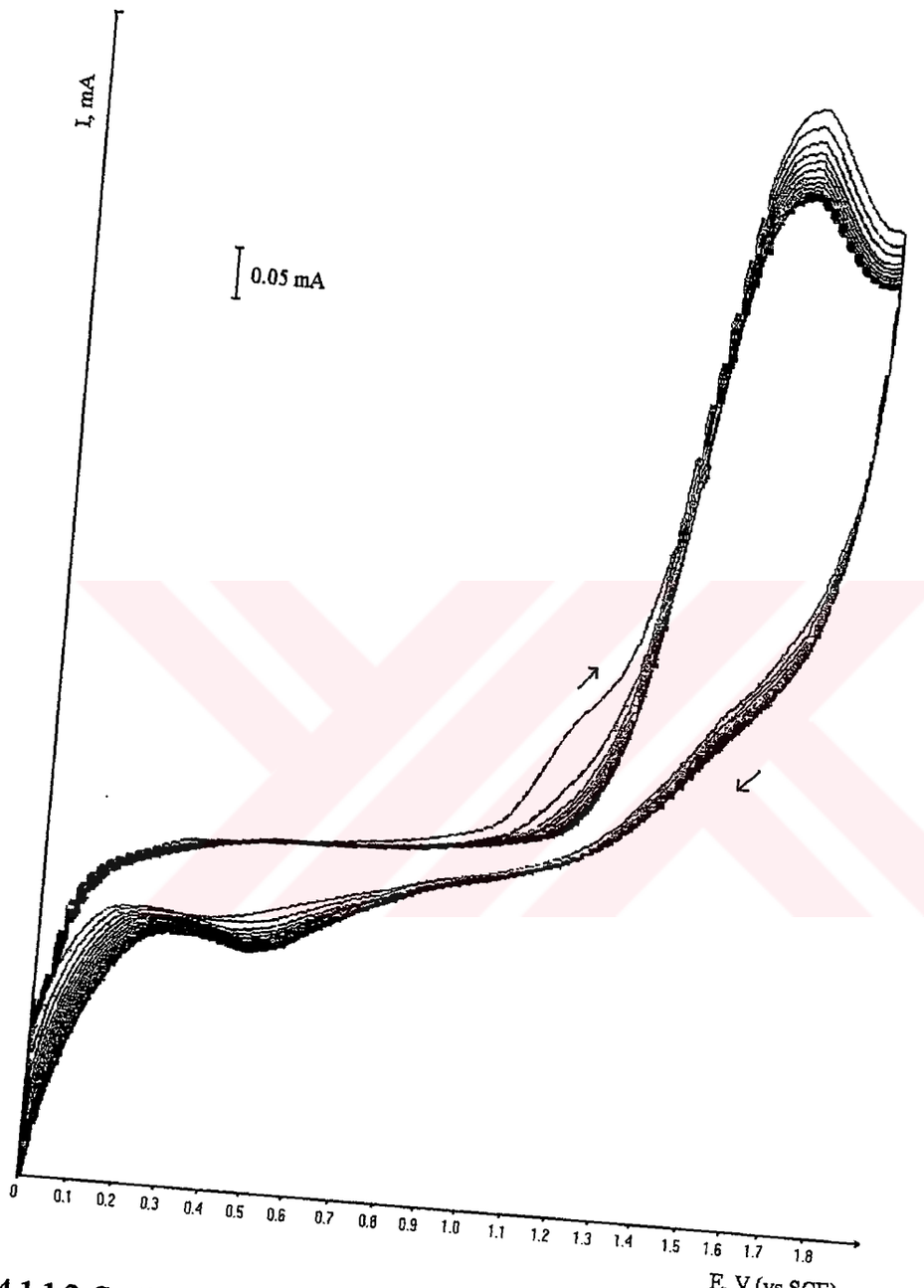

Figure 4.1.1.3 Cyclic Voltammogram of, $2x10^{-2}$ mol dm^{-3} OA in $1x10^{-1}$ mol dm^{-3} containing $NaClO_4$ in ACN. Scan Rate= 0.05 V s^{-1}, Working Electrode: Pt.

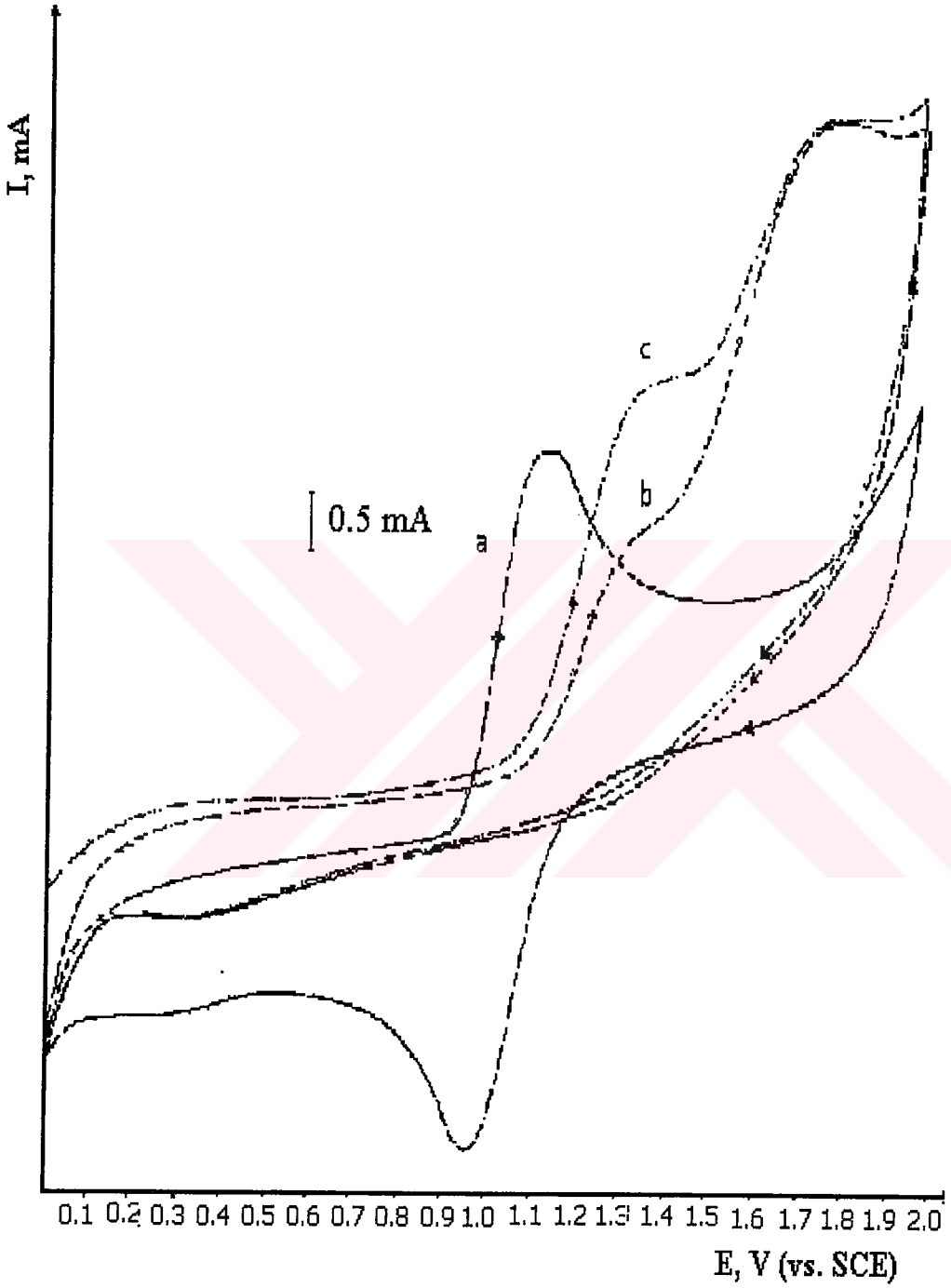

Figure 4.1.1.4 Cyclic Voltammogram of CAN in $1x10^{-1}$ mol dm^{-3} containing $1x10^{-1}$ mol dm^{-3} $NaClO_4$ in ACN, a) CAN+OA first cycle b), second cycle c), [Ce (IV)]= $5x10^{-4}$ mol dm^{-3}, [OA]= $2x10^{-2}$ mol dm^{-3}. Scan Rate= 0.05 $V.s^{-1}$, Working Electrode: Pt.

4.1.2 Thermal Analysis Studies

Thermogravimetric Analysis (TGA) was obtained for different kind of redox polymers. They showed a three-staged decomposition as observed before [104]. A typical TGA curve was obtained on heating the sample at 10 K min^{-1} from 25 °C to 400 °C in an inert He atmosphere (Figure 4.1.2.1). First was the loss of water. This was followed by subsequent loss of ammonia and other gaseous products from the polyacrylonitrile structure formed during decomposition of PAAm and partly from the remaining PAAm in the course of heating up high temperatures. The relative weight loss generally depended on the concentration of the Ce (IV) concentration and the results obtained are tabulated in 4.1.2.1. The table also includes data showing the effect of the polymerization type. It can be seen from the Table when Ce (IV) concentration was increased, weight loss during thermal decomposition decreased and decomposition weight was not effected by polymerization type, due to inclusion of Cerium into the polymer, which thermally stabilizes the polymer. However, AAm polymers initiated with AIBN show low decomposition temperature and Tg in comparison to the redox polymers.

Table 4.1.2.1 TGA results of the redox polymers; [AAm]= $5x10^{-1}$ mol dm^{-3}, [OA]= $2x10^{-2}$ mol dm^{-3}, [H_2SO_4]= $5x10^{-1}$ mol dm^{-3}. Voltage: 1.9 V, 22 °C; [a] [H_2SO_4]= $138x10^{-2}$ mol dm^{-3}, [b] Temperature: 50 °C. Polymerization Time: 1 hour.

Polymerization Medium		**Weight loss %**		
[Ce (IV)] x 10^{-2} mol dm^{-3}	**Type**	**100-260 °C**	**260-340 °C**	**340-400 °C**
0.05	Anodic	7	19	23
0.05 [a]	Anodic	8	20	20
0.05 [b]	Anodic	9	17	21
0.01	Anodic	9	14	38
3	Chemical	7	12	20
3	Cathodic	5	11	19
3	Undivided	7	5	19

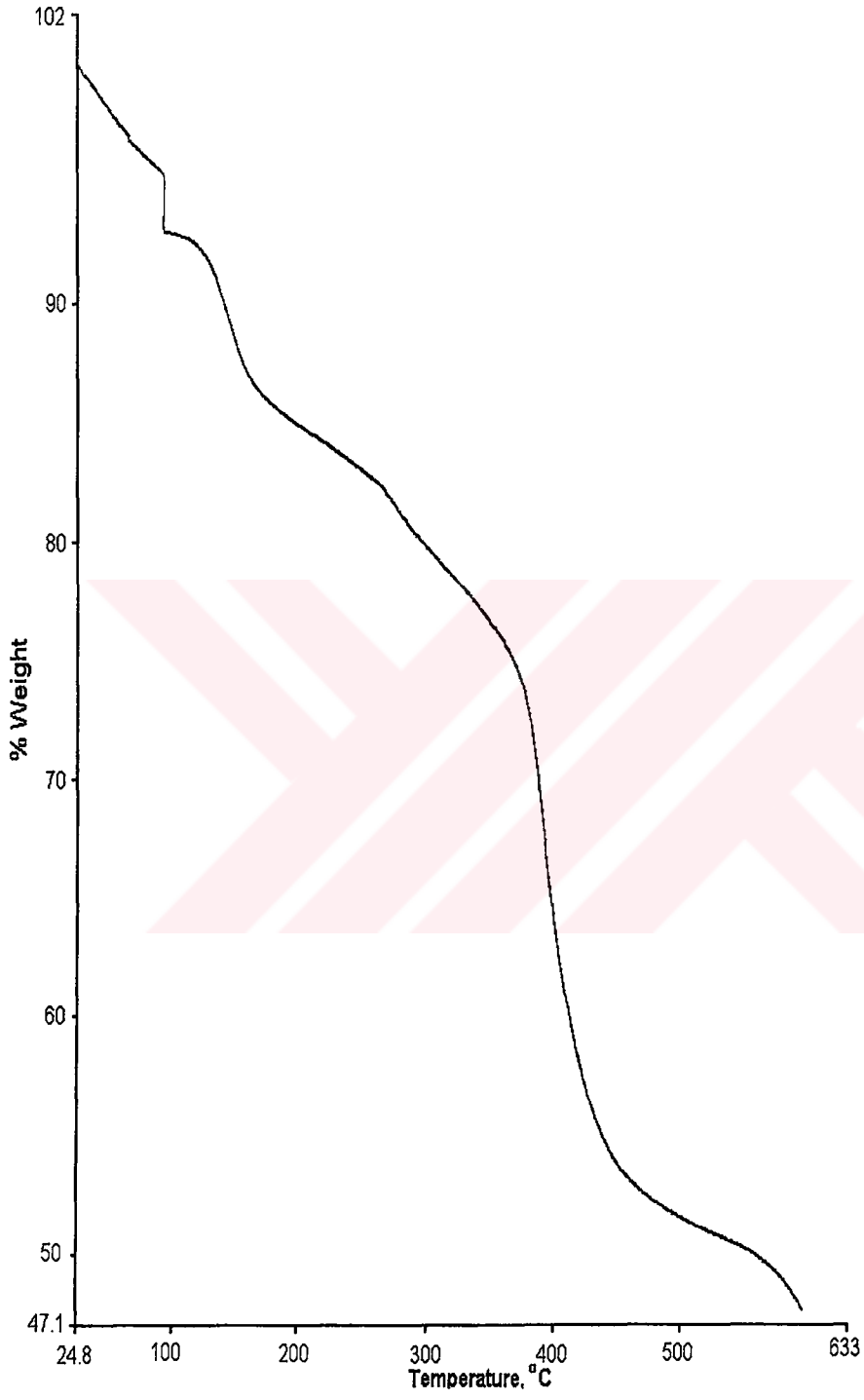

Figure 4.1.2.1 TGA thermogram of chemically obtained PAAm with using Ce (IV)-OA initiator; [AAm]= $5x10^{-1}$ mol dm^{-3}, [OA]= $2x10^{-2}$ mol dm^{-3}, [Ce (IV)]= $3x10^{-3}$ mol dm^{-3}, $[H_2SO_4]$= $5x10^{-2}$ mol dm^{-3}, 50 °C. Polymerization Time: 1 hour.

The same samples were also analysed for their thermal response by Differential Scanning Calorimetry (DSC) under the same temperature shown in Table 4.1.2.2. Tg of PAAm was observed at different temperatures depending on the concentration of Ce (IV) and method of polymerization. Different temperatures were also observed according to the literature. Reported Tg values of PAAm were 84.5 °C [105], 165 °C [106].

Table 4.1.2.2 Tg temperatures of redox polymers of AAm obtained electrochemically at 1.9 V; [AAm]= $5x10^{-1}$ mol dm^{-3}, [OA]= $2x10^{-2}$ mol dm^{-3}. Polymerization Time: 1 hour, 22 °C.

Medium			Tg °C
[Ce (IV)] x 10^{-2} mol dm^{-3}	[H_2SO_4] mol dm^{-3}	Method	
3.00	0.05	Anodic	229
3.00	0.05	Cathodic	227
0.05	1.40	Anodic	153
0.05	0.50	Cathodic	154

4.2 Copolymerization of Acrylamide and N-Vinylcarbazole Initiated with Ce (IV)-Oxalic Acid Reducing Agent

The increasing amount of industrial applications of water-soluble polymers with fluorescence groups, their characteristics and synthesis (with economically feasible monomers) makes it necessary to investigate and characterise such systems. In this respect, this section reports some results on the copolymerization of industrially important vinyl monomer, with an aim of obtaining water soluble carbazole containing PAAm, which has enough amounts of conductive and fluorescing groups, allowing both detailed characterisation and application in different directions.

AAm is one of the most industrially important monomers, which can be polymerized in water. A thorough review of the literature reveals that limited work

has been done on the electropolymerization of AAm in organic solvent media due to inactive behaviour during electrochemical polymerization and coating on the surface of electrode without allowing the procession of polymerization. Water in combination with ethylene glycol [107], dimethylformamide [102], and acetone [108], were employed as solvents for this purpose. In our study, either in view of the insolubility of NVCz in water or high yield polymers obtained in DMF for NVCz and AAm, and as the high yield polymers were obtained for AAm in water, this reaction mixture was chosen.

NVC:AAm copolymerization was initiated by the free radical method which was formed by the reaction of OA and Ce (IV) in DMF and DMF:Water system chemically and electrochemically with divided and undivided cells and results given. Reaction conditions were chosen as described in section 3.4. NVCz polymers were also obtained using a Ce (IV)-OA redox initiator in the same conditions to understand if high yield PVCz occurred and DMF was a suitable media or not.

4.2.1 Characterisation of Acrylamide-N-Vinylcarbazole Copolymers

The polymerization of NVCz initiated with Ce(IV)-OA redox agent in DMF:Water mixture was failed under experimental conditions. There is also no work published about this system in literature. In the presence of AAm, low yield polymers were obtained. When the reaction media, DMF was chosen, yield decreased to a very low quantity; if the reaction was a DMF:Water mixture, the yield increased compared to that obtained in DMF media.

The polymerization of NVCz and AAm was carried out in different percentage of DMF:Water solvent mixtures (100, 75:25, 40:30 (%vol.)). The reaction mixture was poured into the acetone to precipitate the resulting polymer. The product was obtained on reprecipitation was washed with ACN.

Elemental analyses of the polymers obtained in DMF and in DMF:Water media were carried out to understand the effect of water in the reaction. The calculated structure ($C_{3.38}H_{5.84}N_{1.0}$) for DMF media fits the assumption of 29 AAm units combined with 1 NVCz, and ($C_{4.08}H_{9.8}N_{1.0}$) for DMF:Water mixture fits the assumption of 9 AAm units combined with 1 NVCz.

UV-Visible absorption spectra of the resulting product of PVCz, which is carried in DMF:Water mixture, dissolved in water (Figure 4.2.1.1 and Table 4.2.1.1.) and showed two absorptions. These peaks as 253 and 240 nm were observed to arise from the reaction between Ce (IV)-OA which the condition of reactions were given Chapter 3. As it was seen Figure 4.2.1.1 there is no NVCz peak in the spectra, as Ce (IV)-OA complexation reaction occurred and this complexation might prevent initiation of the polymerization. No product was obtained when the polymerization media was chosen, as DMF for the NVCz, due to the fact that the reaction between Ceric nitrate and DMF (Ceric nitrate was chosen, as there is no solubility Ceric sulphate in DMF itself) is so much faster than the reaction between DMF:Water and Ceric sulphate.

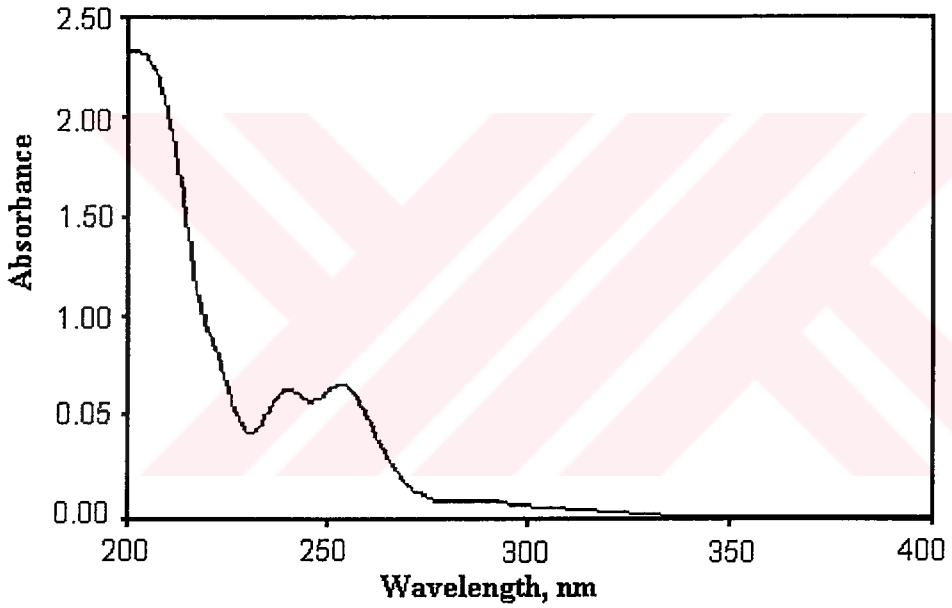

Figure 4.2.1.1 UV-Visible absorption spectra of PVCz at 1.6 V; [Ce (IV)]= $5x10^{-3}$ mol dm^{-3}, [NVCz]= $3x10^{-2}$ mol dm^{-3}, [OA]= $2x10^{-2}$ mol dm^{-3} $[H_2SO_4]$= $1x10^{-1}$ mol dm^{-3}. Time: 1 hour, Polymerization Media: DMF:Water (75%:25%), ($C_{polymers}$= $2x10^{-2}$ g dm^{-1}).

NVCz containing polymers were obtained only when AAm was used. The UV-visible absorption spectra of copolymerized AAm with NVCz (by electrochemically in divided and undivided cells) were obtained in DMF and DMF:Water (75%:25%) mixture given, in Figure 4.2.1.2. It is known that PVCz is not water soluble [109] and no absorption peak was observed when it was dissolved in water. In the case of copolymer, the intensity of the characteristic peaks of NVCz

(λ = 260, 292, 327, 341 nm), changed depending on the polymerization method applied such as anodic (in the anode compartment), cathodic or in undivided cells (Figure 4.2.1.2 a and b).

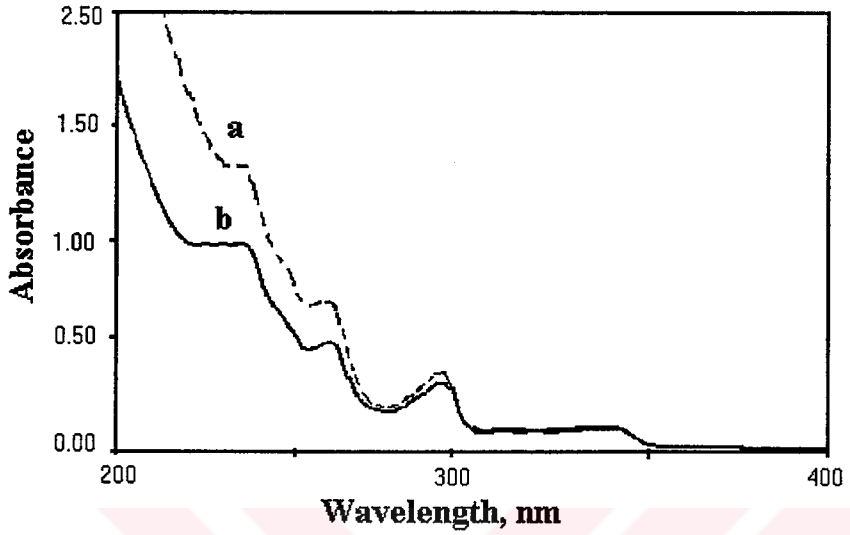

Figure 4.2.1.2 UV-Visible absorption spectra of NVCz copolymerized with AAm at 1.6 V; a) in undivided cell, b) in the anode compartment; [Ce(IV)]= $5x10^{-3}$ mol dm^{-3}, [NVCz]= $3x10^{-2}$ mol dm^{-3}, [AAm]= $5x10^{-1}$ mol dm^{-3}, [OA]= $2x10^{-2}$ mol dm^{-3} [H_2SO_4]= $1x10^{-1}$ moldm^{-3}. Time: 1 hour, Polymerization Media: DMF:Water (75%:25%), ($C_{polymers}$= $2x10^{-2}$ g dm^{-1}).

The FT-IR spectrum of NVCz containing PAAm shows generally the characteristic peaks of AAm. But in the high ratio of NVCz the 2930 cm^{-1} asymmetric stretching of NVCz corresponds to the – CH of the aromatic ring arising from NVCz moiety. 1625 cm^{-1} doublet of PVCz is due to the C=C str. vibration of the vinyl group which merges at 1650 cm^{-1}. This peak can be seen with –C=O peak of AAm. A shoulder at 1600 cm^{-1} and two peaks at 1478 and 1446 cm^{-1} arise from the ring vibration of the NVCz and from –C-N peaks of AAm. The characteristic absorption bands show bands at 938 and 860 cm^{-1} due to the vinyl group of NVCz. Also the peaks at 746, 721 cm^{-1} are owing to aromatic out of plane C-H bending and ring deformation of substituted aromatic structure (Figure 4.2.1.3 a, b, c).

According to our results, which are also mentioned in the next section, yields increase with the polymerisation method and reaction media. Although our yields for these copolymers are low, an electro-induced polymerisation system is better such as that obtained for AAm polymers.

Table 4.2.1.1 UV-Visible spectra results of obtaining PVCz in the presence and absence of AAm electrochemically at 1.6 V; [Ce (IV)]= $5x10^{-3}$ mol dm^{-3}, [NVCz]= $3x10^{-2}$ mol dm^{-3}, [AAm]= 0.5 mol dm^{-3}, [OA]= $2x10^{-2}$ mol dm^{-3} $[H_2SO_4]$= $1x10^{-1}$ mol dm^{-3}. Time: 1 hour, Polymerization Media: DMF:Water (75%:%25), [a] absence of AAm, [b] absence of NVCz.

Polymerization Type	**Absorbance Values at , nm**				
	240	253-260	292	327	341
Undivided[a]	0.630	0.657	-	-	-
Undivided[b]	0.721	0.551	-	-	-
Undivided	-	-	0.934	0.268	0.275
Anode	-	-	0.354	0.348	1.264
Cathode	-	0.810	0.539	0.158	0.161
Chemical	0.739	0.697	0.162	-	-

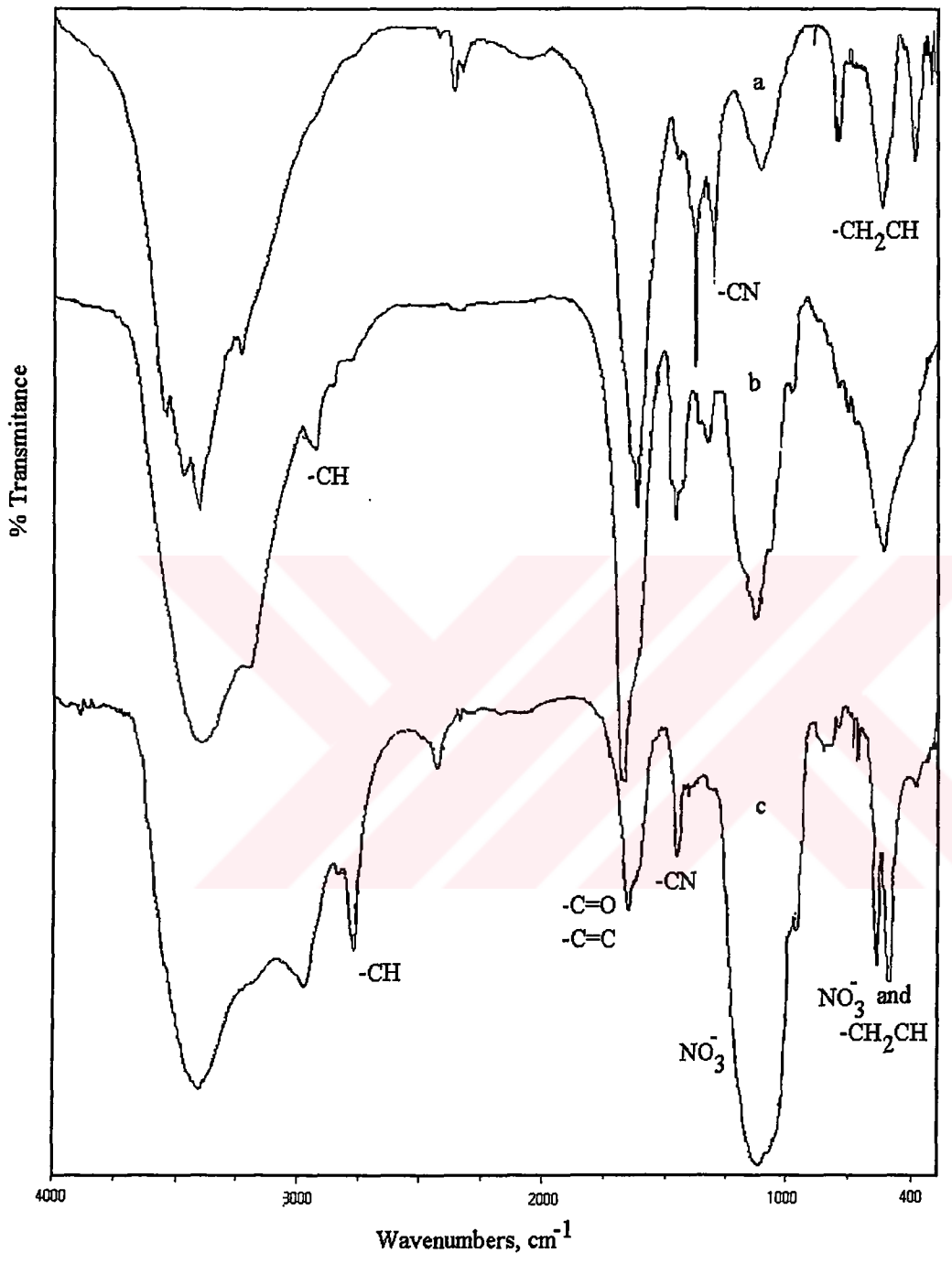

Figure 4.2.1.3 The FT-IR spectrum of NVCz:AAm copolymers; a) [NVCz]= 0.03 mol dm^{-3} (in anode compartment), b) [NVCz]= $3x10^{-2}$ mol dm^{-3} (in undivided), c) [NVCz]= $1x10^{-1}$ mol dm^{-3} (in undivided); [AAm]= $5x10^{-1}$ mol dm^{-3}, [Ce(IV)]=$5x10^{-3}$ mol dm^{-3}, [OA]= $2x10^{-2}$ mol dm^{-3} , [H_2SO_4]= $1x10^{-1}$ mol dm^{-3}. Oxidation Potential: 1.6 V, Time: 1 hour, Polymerization Medium: DMF.

4.2.2 Steady-State Fluorescence Spectra of Polymers

The fluorescence excitation spectra of dilute solutions of various copolymers dissolved in water, dioxan or dioxan/water mixture consists of two maxima centred at 350 and 326 nm excitation wavelength. The fluorescence emission spectra of dilute solutions of polymers exhibit emission characteristics of that carbazole [110] with two maxima centred at (λ ~347 nm) and (λ ~362 nm). Electrochemical polymerization in the presence of 25% and 40% water shows considerable decrease in the fluorescence behaviour, as polymerization shows a trend go through the carbazole ring, and this causes self-quenching of the carbazole chromophore, and molecular motion of NVCz is restricted when it is bound to a polymer chain. Figure 4.2.2.1 a might be attributed to the NVCz containing polymer which was not dissolved enough in the case of water, because the intensity of NVCz group is low, but when the solvent mixture of water/dioxane was used, fluorescence behaviour increased.

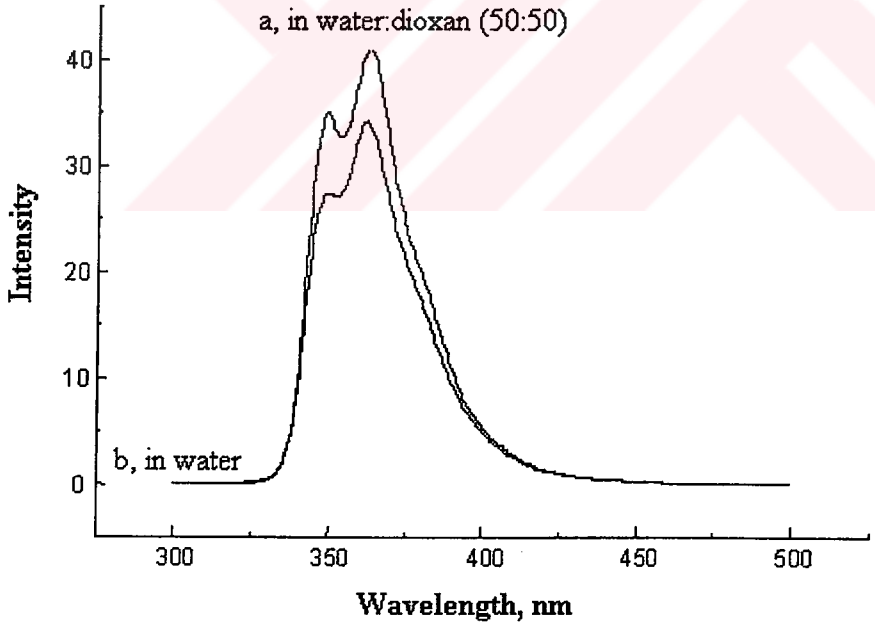

Figure 4.2.2.1 Steady-State fluorescence spectra of NVCz:AAm copolymers in, a) 40% water, b) 25% water; [AAm]= $5x10^{-1}$ mol dm^{-3}, [NVCz]= $3x10^{-2}$ mol dm^{-3}, [Ce(IV)]= $5x10^{-3}$ mol dm^{-3}, [OA]= $2x10^{-2}$ mol dm^{-3} , [H_2SO_4]= 0.1 mol dm^{-3}, ($C_{polymers}$=$3x10^{-2}$ g dm^{-1}). Oxidation Potential: 1.6 V, Time: 1 hour, Excitation Wavelength is λ= 326 nm.

4.3 Copolymerization of Acrylamide and N-Vinylcarbazole Initiated with AIBN

The increasing amounts of practical applications of water-soluble polymers with fluorescing groups, their characterisation and synthesis with economically feasible monomers make it necessary to investigate such systems. In these respects this study reports some results on the copolymerization of some industrially important vinyl monomers, with the aim of obtaining water soluble, carbazole containing polyacrylamides which have enough amounts of conductive and fluorescence groups allowing both detailed characterisation and application in different directions.

In literature, copolymer composition of NVCz was determined by UV-visible spectroscopy. The determination was based on the characteristic absorption band of carbazole chromophore of copolymer observed at 342,5 nm in dioxane. The validity of this method was confirmed first by Tada et al. [110] and then by Chiellini [108, 111] through the excellent correlation of the results obtained by UV-vis spectroscopy with those taken by elemental analysis. The copolymer composition was calculated from the extinction coefficient value $\varepsilon = (2.861 \pm 0.189)\ 10^3$ lt.mol cm^{-1}. Of the carbazolyl group in the NVCz homopolymer prepared under the same experimental conditions were as the copolymers.

Copolymer of NVCz with AAm was not dissolved in dioxane and same comparison could not be done. However, their composition was determined by elemental analysis. Calculated structure $[-(C_{4.0}H_{5.4}N_{1.0}O_{0.9})_n-]$ for HNVCAAm fits the assumption of 13 AAm units combined with 1 NVCz and $[-(C_{3.1}H_{5.1}N_{1.0}O_{0.9})_m-]$ for LNVCAAm fits the assumption of 99 AAm units combined with 1 NVCz.

The UV-visible absorption spectra of copolymerized NVCz with AAm (at mol ratios $n_T/ n_{NVCz} = 100$ and $n_T/ n_{NVCz} = 10$) were obtained in water and given in Figure 4.3.1 As it was mentioned before, PVCz is not water-soluble. PAAm homopolymer shows a maximum absorbance at $\lambda = 208$ nm. In the case of the copolymer, the intensity of the characteristic peaks of NVCz ($\lambda = 259, 292, 327, 340$ nm), increase with increasing mol content of NVCz (Figure 4.3.1 a and b). The same results were also obtained in the case of polyacrylic acid [112].

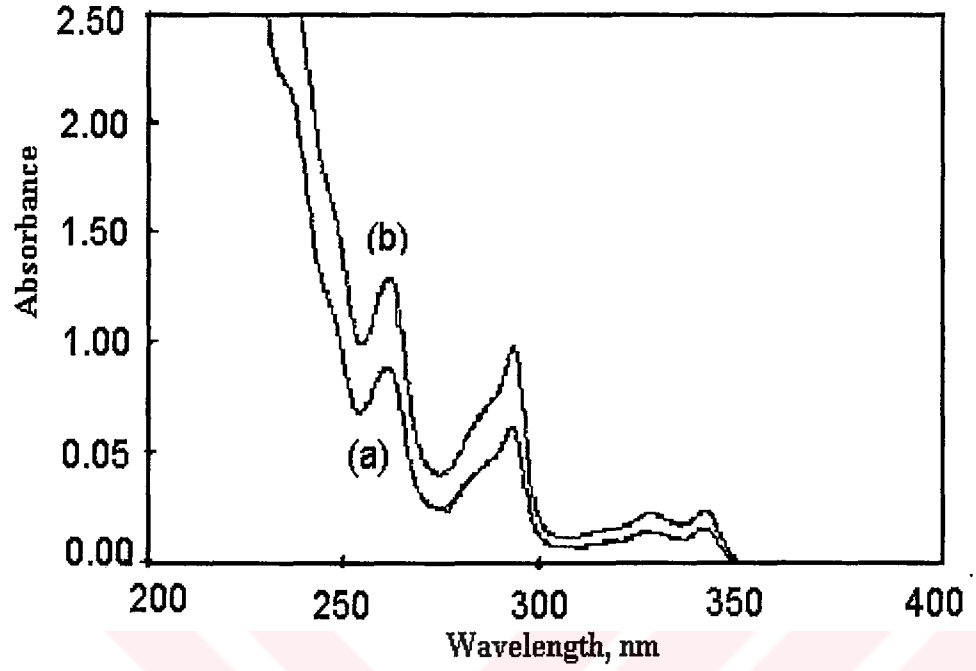

Figure 4.3.1 UV-Visible absorption spectra of NVCz:AAm copolymers, dissolved in water for different mole ratios; (a) n_T/ n_{NVCz} =100; [NVCz]= $1x10^{-2}$mol dm^{-3}, [AAm]= $9.9x10^{-1}$ mol dm^{-3} and (b) n_T/ n_{NVCz} = 10; [NVCz]= $1x10^{-2}$ mol dm^{-3}, [AAm]= $9x10^{-1}$ mol dm^{-3}, ($C_{polymers}$=$2x10^{-2}$ g dm^{-1}).

These results suggest that, although the co-polymers contain NVCz group, they are as water-soluble as PAAm, which shows its characteristic absorption behaviour.

In the FT-IR spectra of PAAm obtained in the presence of NVCz, only the characteristic bands of PAAm, at 1667, 1450, 1415, 1367, 1330, 1130 and 616 cm^{-1} were observed. The C=O band of the carbonamide group absorbs at 1650 cm^{-1}. The C-N stretching band of primary amide was observed near 1400 cm^{-1}. PAAm showed characteristic absorptions, which agreed very well with those reported in literature, [114]. The bands, which correspond to PVCz were not detected, as the amount of NVCz contents in the copolymer is low. The same findings were found for the methylmethacrylate copolymer containing NVCz [115].

4.3.1 Steady-State Fluorescence Spectra of Polymers

Steady-state fluorescence spectra of copolymerized NVCz with AAm in water having the same the concentration of carbazole chromophore were measured to examine the fluorescence behaviour of the prepared copolymer (Figure 4.3.1.1 a and b). As it was seen from the Figure, fluorescence intensities increased by the increase of NVCz in the copolymer. The long wavelenght was assigned (λ ~420 nm) to an intra-chain eximer formation between two pendant nearest neighbour carbazole groups. The emission at shorter wavelength (λ ~380 nm) was attributed the normal carbazole emission [109]. The same results were also obtained for NVCz copolymerized with acrylic acid [112].

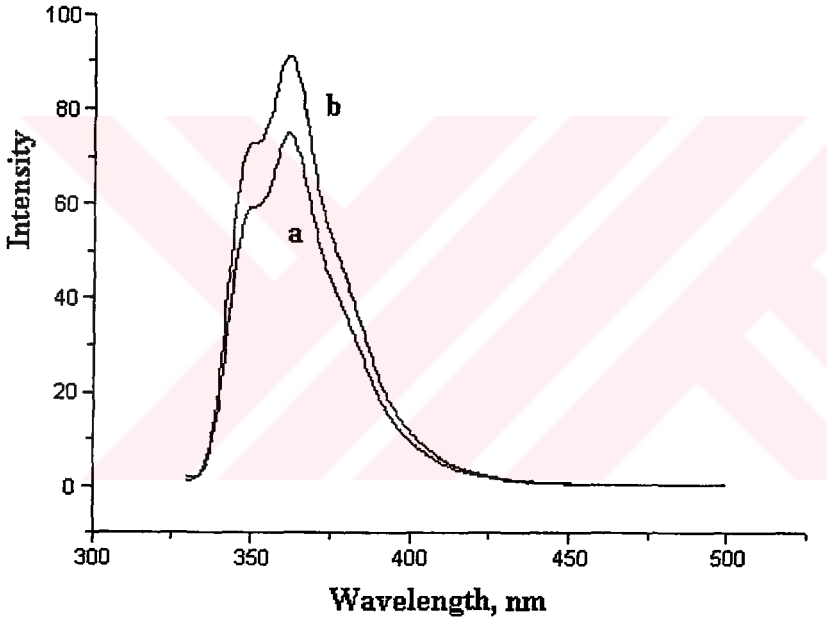

Figure 4.3.1.1 Flourescence spectra of NVCz:AAm copolymers in DMF solution for different mole ratios; a) $n_T/ n_{NVCz} = 100$; [NVCz]= $1x10^{-2}$ mol dm^{-3}, [AAm]=$9.9x10^{-1}$ mol dm^{-3} and b) $n_T/ n_{NVCz} =10$; [NVCz]= $1x10^{-2}$ mol dm^{-3}, [AAm]= $9x10^{-1}$ mol dm^{-3} in water, ($C_{polymers}=3x10^{-2}$ g dm^{-1}). Excitation wavelength is λ = 326 nm.

The solvent effect was also observed. When the solvent was ACN:Water mixture, the intensity of the copolymerised NVCz with AAm increased compared to the case when solvent was used as water (4.3.1.2).

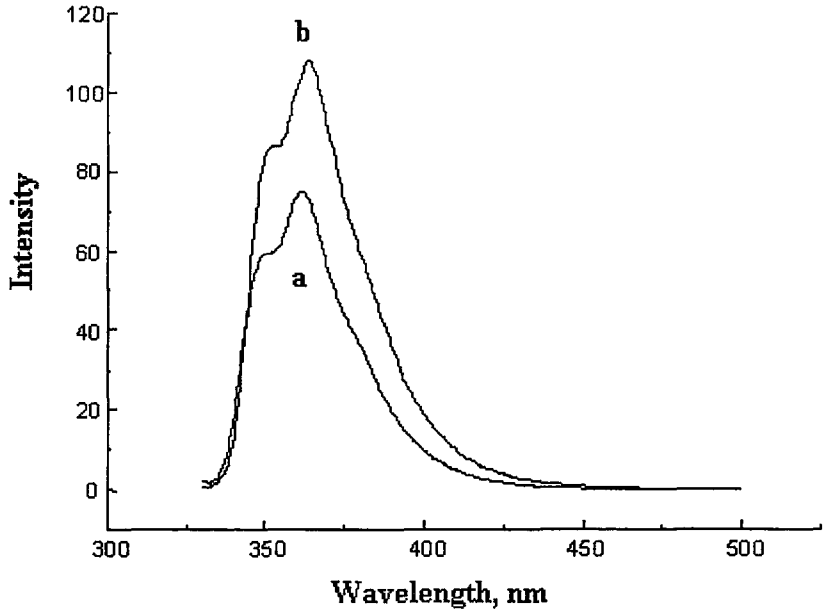

Figure 4.3.1.2 Fluorescence spectra of NVCz:AAm copolymers for different mole ratios $n_T/ n_{NVCz} = 100$; [NVCz]= $1x10^{-2}$ mol dm^{-3}, [AAm]= $9.9x10^{-1}$ mol dm^{-3}; in a) water, b) ACN:Water (%50:%50) mixture, ($C_{polymers}$=$3x10^{-2}$ g dm^{-1}). Excitation Wavelength is λ = 326 nm.

4.3.2 Thermal Analysis Studies

A typical TGA curve obtained on heating the sample at 10 K min^{-1} from 25° C to 400°C in inert He atmosphere is shown in Figure 4.3.2.1. The same samples were also analysed for their thermal response by DSC over the same temperature range under an inert N_2 atmosphere. In the case of PVCz alone, there are two weight losses at 90 °C and 400 °C, and these data are quite compatible with literature [116]. The major weight loss after 90 °C is attributed to the evaporation of solvent. The main decomposition of PVCz begins at 350 °C and it shows a weight loss of 10% at 400 °C. This polymer proves to be the most thermostable, perhaps due to its chain rigidity imposed by the great volume of the lateral group. As it was mentioned before, PAAm shows three stages of decomposition (Figure 4.1.2.1). In the presence of AAm, there are three major stages of weight loss at around 90, 250 and 350 °C as shown in Figure 4.3.2.1 a, b and c for the copolymers obtained at mol ratios n_T/n_{NVCz}= 100 and 10. As a comparison to the PVCz, the thermal processes at the lower temperatures could be associated with the elimination of volatile and

decomposition of AAm groups, because weight loss in the PAAm case takes place at lower temperatures. These results suggest that introducing NVCz group in to structure and this increase can increase thermal stability of PAAm highly in the case high content of NVCz moiety.

The glass transition temperature (Tg) was also examined. Normally a glass transition appears as a sudden change in the slope of the DSC curve but sometimes it appears as an endothermic peak [117]. In our case, the DSC curve clearly shows a normal glass transition, and exothermic peaks were noted at one endothermic process for PNVCz temperature between 400-500 °C, and three endothermic processes for PAAm between 100-500 °C (Appendix C.1).

A glass transition of a polymer is marked by drastic changes in its physical properties. The cooperative motion of a large chain segment takes place in the glass transition region, which includes Tg. At the temperatures above Tg, the polymer is in a rubbery state while at temperatures below Tg, it behaves as a glass. For the NVCz-containing PAAm, the glass transition takes place in the temperature 100-200 °C. A glass transition appears as a sudden change in the slope. (Figure 4.3.2.2). The Tg increase with increasing the mole ratio of NVCz because the PVCz has very high glass transition temperature (230 °C) [118] in comparison to PAAm which shows low Tg (84.5 °C), as mentioned before.

4.3.3 Solubility of Copolymers

PVCz is soluble in solvents, which are not friendly to the environment, such as toluene, dioxan, and THF. In contrast, PAAm is soluble in water, ethylene glycol and formamide. Different concentrations copolymers are soluble in water and in Water:ACN mixture (50:50). Their solubility increases with an increase of NVCz content of the copolymer in dioxan, THF and chloroform.

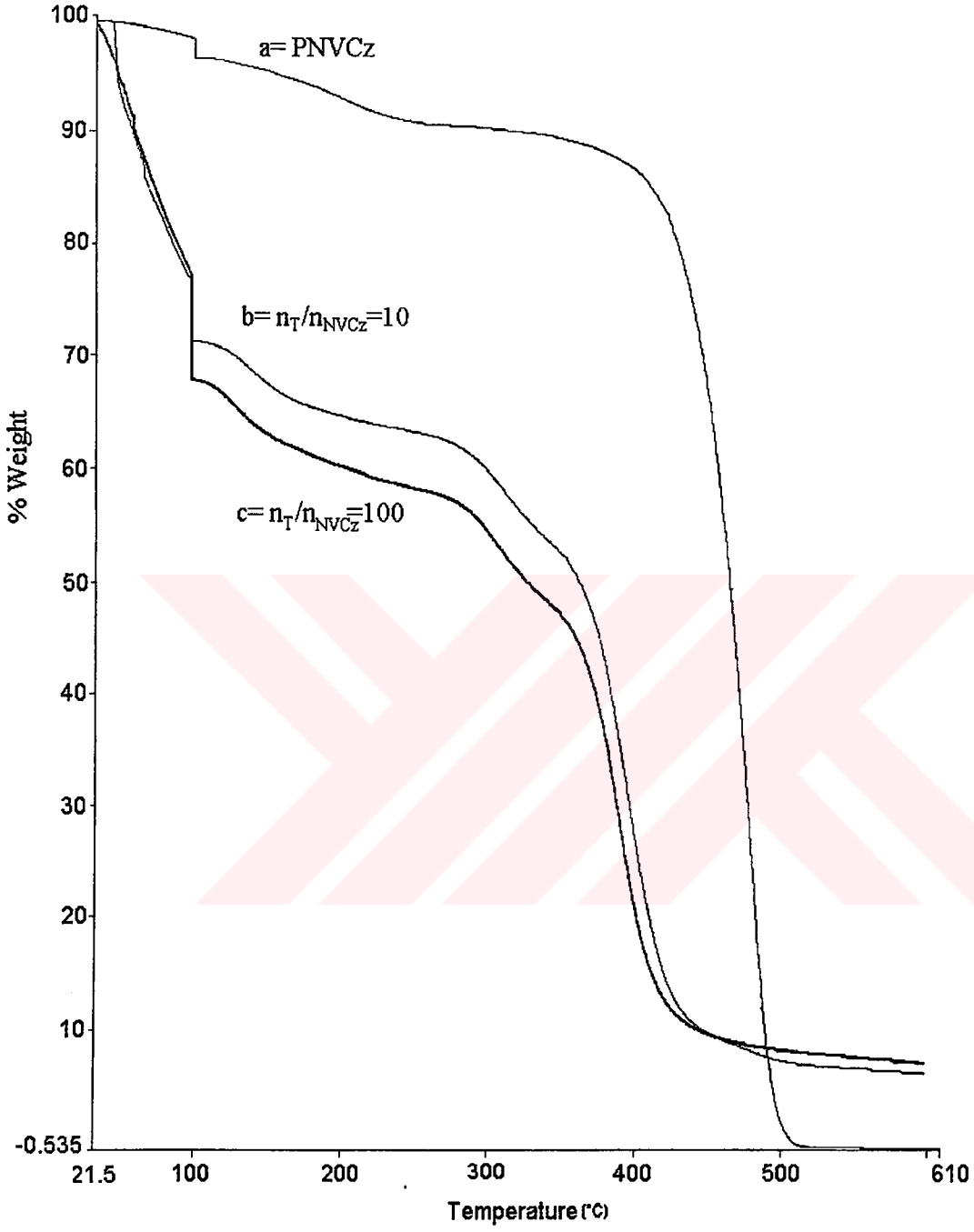

Figure 4.3.2.1 TGA thermogram of (a) PNVCz, (b) AAm:NVCz copolymers for different mole ratios n_T/ n_{NVCz} =10; [NVCz]= $1x10^{-2}$ mol dm^{-3}, [AAm]= $0.9x10^{-1}$ mol dm^{-3} and (c) n_T/ n_{NVCz} = 100; [NVCz]= $1x10^{-2}$ mol dm^{-3}, [AAm]= $9.9x10^{-1}$ mol dm^{-3}.

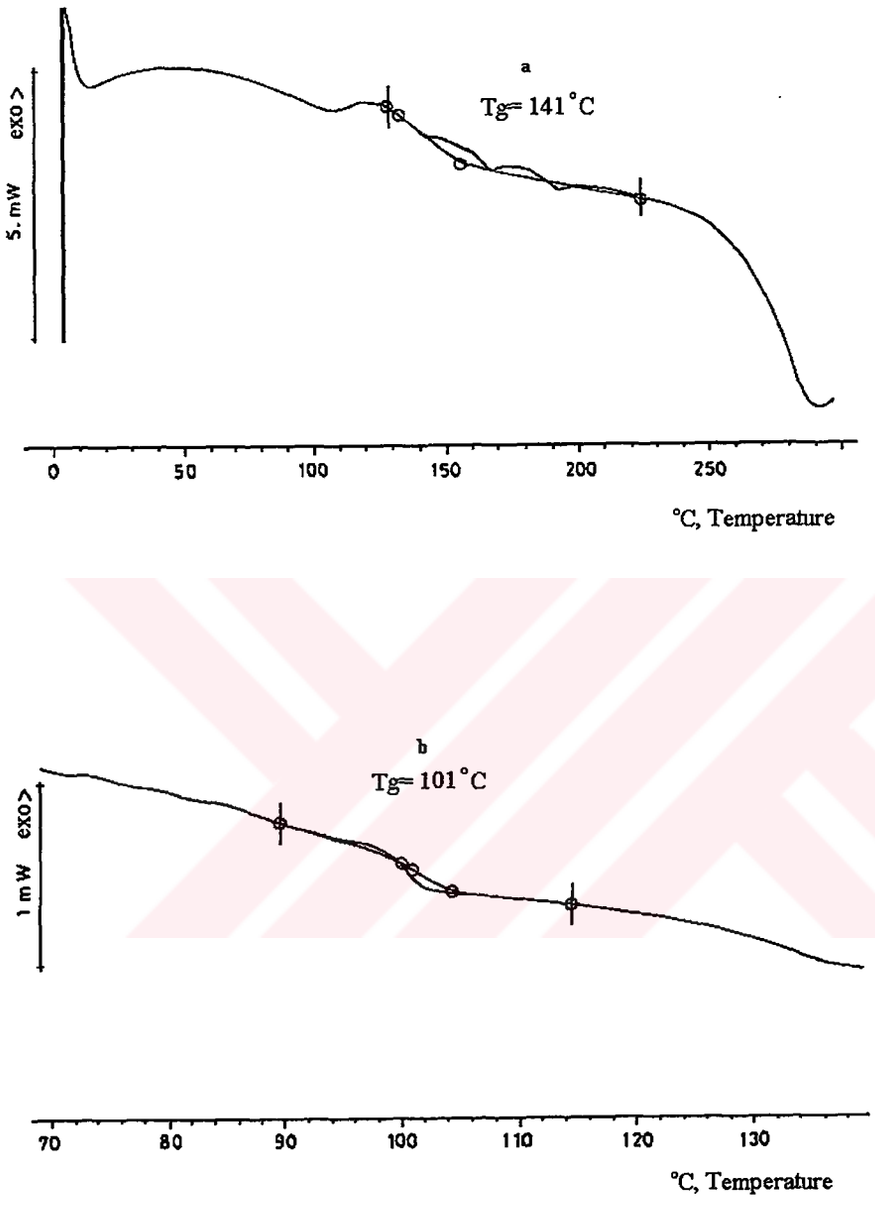

Figure 4.3.2.2 The DSC curves to show Tg of AAm:NVCz copolymers for different mole ratios; a) n_T/ n_{NVCz} =10; [NVCz]= $1x10^{-2}$ mol dm^{-3}, [AAm]= $0.9x10^{-1}$ mol dm^{-3} and b) n_T/ n_{NVCz} = 100; [NVCz]= $1x10^{-2}$ mol dm^{-3}, [AAm]= $9.9x10^{-1}$ mol dm^{-3}.

4.3.4 Yield of Polyacrylamide and N-Vinylcarbazole Containing Acrylamide Polymers

The effect of Ce (IV) concentration in the polymer obtained electrochemically and chemically by using AIBN for AAm is summarized in Table 4.3.4.1. The increase in the yield of anode compartment as the Ce (IV) concentration increases and having higher values than in cathodic section as well as undivided cells, show the regeneration of Ce (IV) which reacts again with OA to produce more radicals initiating polymerization. Electrochemical polymerization shows an advantage over the chemical polymerization obtained both in the presence of a reducing agent and AIBN.

In comparison to AAm polymerization the same experiments were done in the presence of NVCz. In view of the insolubility of NVCz in water, the electrochemical polymerization of this monomer was performed in DMF and DMF/water system. As it was seen in Table 4.3.4.2, regeneration of Ce (IV), which can oxidise oxalic acid to produce radicals, did not result polymerization in the presence of DMF medium. Low conversion was obtained both with the copolymer of AAm with NVCz and PAAm itself by electropolymerization. But, there is a slight increase in the conversion of AAm:NVCz copolymers performed in the Water:DMF mixture.

Table 4.3.4.1 Effect of Ce (IV) concentration on the yield with different method and AAm polymerization using AIBN initiator; [AAm]= $5x10^{-1}$ mol dm^{-3}, [OA]= $2x10^{-2}$ $moldm^{-3}$, [H_2SO_4]= $5x10^{-2}$ mol dm^{-3}, [a] Higher than 100% conversion is due to inclusion of initiators namely, Ce (IV) and OA into the polymer, [b] [H_2SO_4]= $5x10^{-1}$ mol dm^{-3}, [c][AAm]= $5x10^{-1}$ mol dm^{-3}.

Initiator (mol dm^{-3})	Polymerization Type (Conversion %)				Medium
	Anode	Cathode	Undivided	Chem.	
Ce (IV)= $3x10^{-2}$	121 [a]	98	63	66	Water
Ce (IV)= $5x10^{-4}$	68	43	33	52	Water
Ce(IV)= $1x10^{-4}$ [b]	16	9	2	8	Water
Ce (IV)= $5x10^{-3}$			9		Water:DMF
Ce (NO_3)= $5x10^{-3}$			5		DMF
AIBN= 0.05 [c]				70	DMF, 70°C

Table 4.3.4.2 Conversion changes of electrochemical redox NVCz/AAm cpolymers; [AAm]= $5x10^{-1}$ mol dm^{-3}, [NVCz]= $3x10^{-2}$ mol dm^{-3}, [OA]= $2x10^{-2}$ mol dm^{-3} , [H_2SO_4]= $1x10^{-2}$ mol dm^{-3}. Temperature= 22 °C.

Initiator (mol dm^{-3})	Polymerization Type (Conversion %)				Medium
	Anode	Cathode	Undivided	Chem.	
Ce (NO_3)= $5x10^{-3}$	5	4	3		DMF
Ce (IV)= $5x10^{-3}$	9	8	5	9	Water:DMF

In contrast to high yield obtained for chemical polymerization of copolymers initiated with AIBN, in the case of DMF:Water mixture causes an increase in the yield (Figure 4.3.4.3). According to literature, water prevents the precipitation in the solution corresponding to the vinyl polymerization of NVCz polymerization in ACN [43]. The same phenomenon was also explained for PPy. From the experimental results of PPy, three regions of behaviour was defined as a function of the water content added to the organic electrolytic solution:

Region A: Very low water contents (< 0.1% in vol.)

Region B: 0.1-2.5% and 50-100% of water content

Region C: 2.5-50% of water content

Interaction of water in ACN effects the mechanism of polymerisation in two ways. The coupling of the water molecule (acetonitrile) facilitates the approximation of water to the organic (polymeric) electrode. On the other hand, the water discharge is helped by the formation of these hydrogen bonds with acetonitrile, due to the increment in the nucleophilic character of the hydroxylic oxygen [119-120] Scheme 1. This kind of interaction was not seen in DMF:Water mixture, due to the fact that water mixed with organic solvents on polymerization of monomer would combine the advantages of solution in a number of ways to change polymerization conditions and improve product properties.

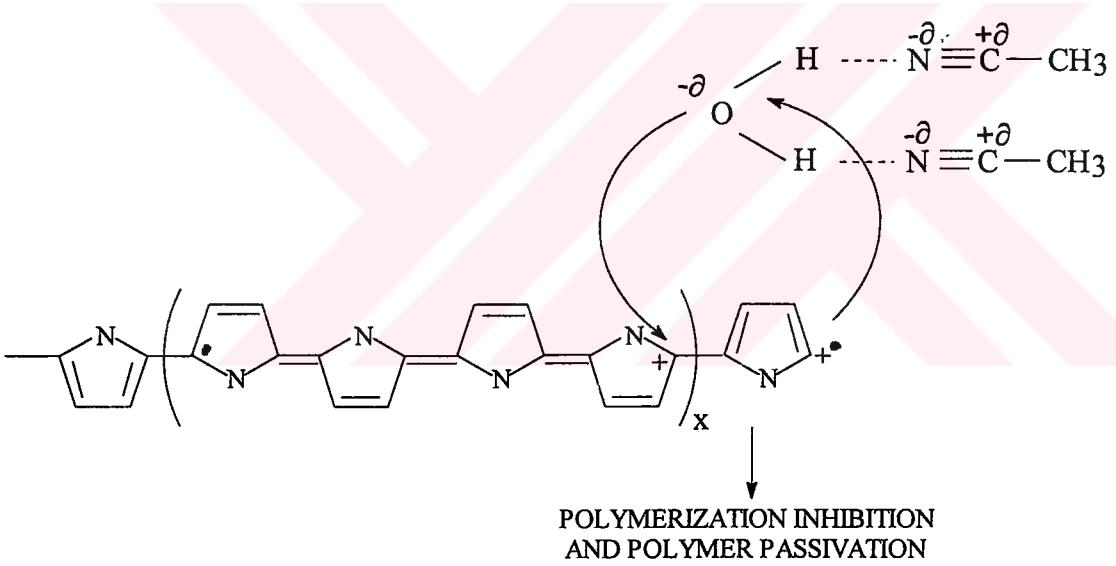

SCHEME 1 Proposed mechanism for the effect of ACN:Water interactions on the mechanism.

Therefore, the yield of copolymer obtained in DMF:Water mixture was also increased compared to copolymer obtained in DMF media where the presence of water favours the radical formation of NVCz resulting in a vinyl polymerization with AAm and corporation with DMF into the structure in the water-organic solution system. NMR measurements support this idea mentioned above (Figure 4.3.4.1). It was seen from Figure 4.3.4.1 that there are two sharp peaks owing to DMF protons at 3 ppm. DMF goes into the monomer layer and is found to increase with an increase

in the DMF content in the medium. If the polymerization proceeded without water, no DMF protons were obtained (Figure 4.3.4.2). NVCz protons were also not observed, as the NVCz ratio of polymer was so low as in the FT-IR spectrum in comparison to the UV-visible and Fluorescence measurements (4.3.4.2). AAm protons were seen such as in obtaining radical mechanism as described in literature [61]. For the spectra in D_2O, we can readily assign the peaks at 1.50 and 2.50 ppm to the hydrogens on the α and β carbons of the monomer units in the interior of the chain. For the spectra taken in D_2O, we did not observe amide hydrogens because of the interchange reactions between the hydrogen and deuterium.

It is concluded from these results that the properties of the polymers can be varied by varying the medium in which the polymerization is conducted. The water-solvent systems are a good polymerization media because they combine advantages of solution and polymerization.

Table 4.3.4.3 Chemical polymerization conversion for AAm:NVCz copolymers; [a] [NVCz]= $2x10^{-2}$ mol dm^{-3}, [AAm]= $8x10^{-1}$ mol dm^{-3}, [b] [NVCz]= $1x10^{-1}$ mol dm^{-3}, [AAm]= $9x10^{-1}$ mol dm^{-3}, [c] [NVCz]= $1x10^{-2}$ mol dm^{-3}, [AAm]= $9.9x10^{-1}$ mol dm^{-3}.

Initiator (mol dm^{-3})	**Conversion (%)**	**Medium**
AIBN= 0.05 [a]	42	DMF,80°C
AIBN= 0.05 [b]	45	DMF,80°C
AIBN= 0.05 [c]	50	DMF,80°C
AIBN= 0.05 [a]	77	Water:DMF, 80°C

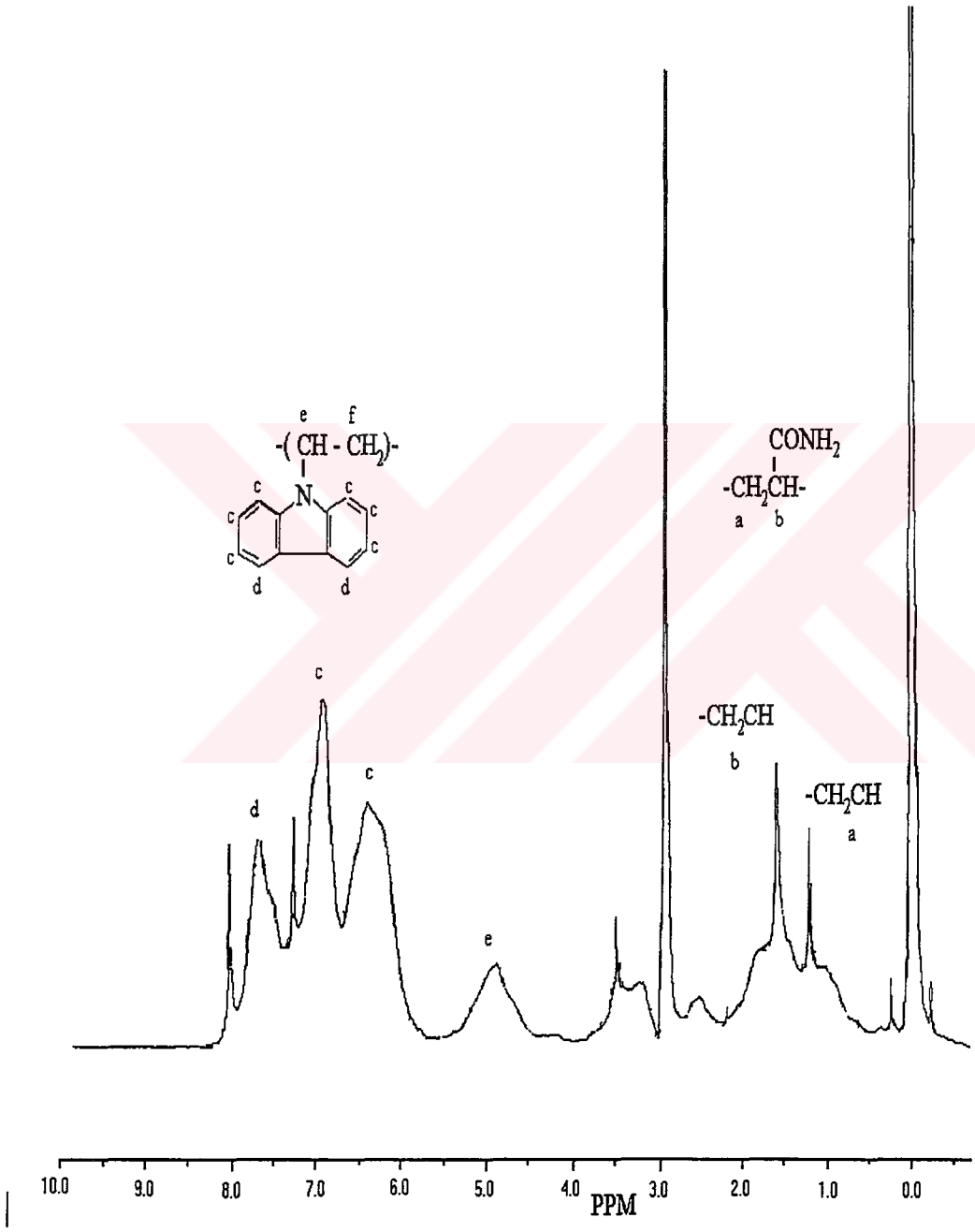

Figure 4.3.4.1 ^{1}H-NMR spectra in $CDCl_3$ solution of obtained by chemically using AIBN initiator at mole ratio n_T/n_{NVCz}= 10; ([AAm]= $9x10^{-1}$ mol dm^{-3}, [NVCz]= $1x10^{-1}$ mol dm^{-3}, [AIBN]= $5x10^{-2}$ mol dm^{-3} in DMF:Water mixture.

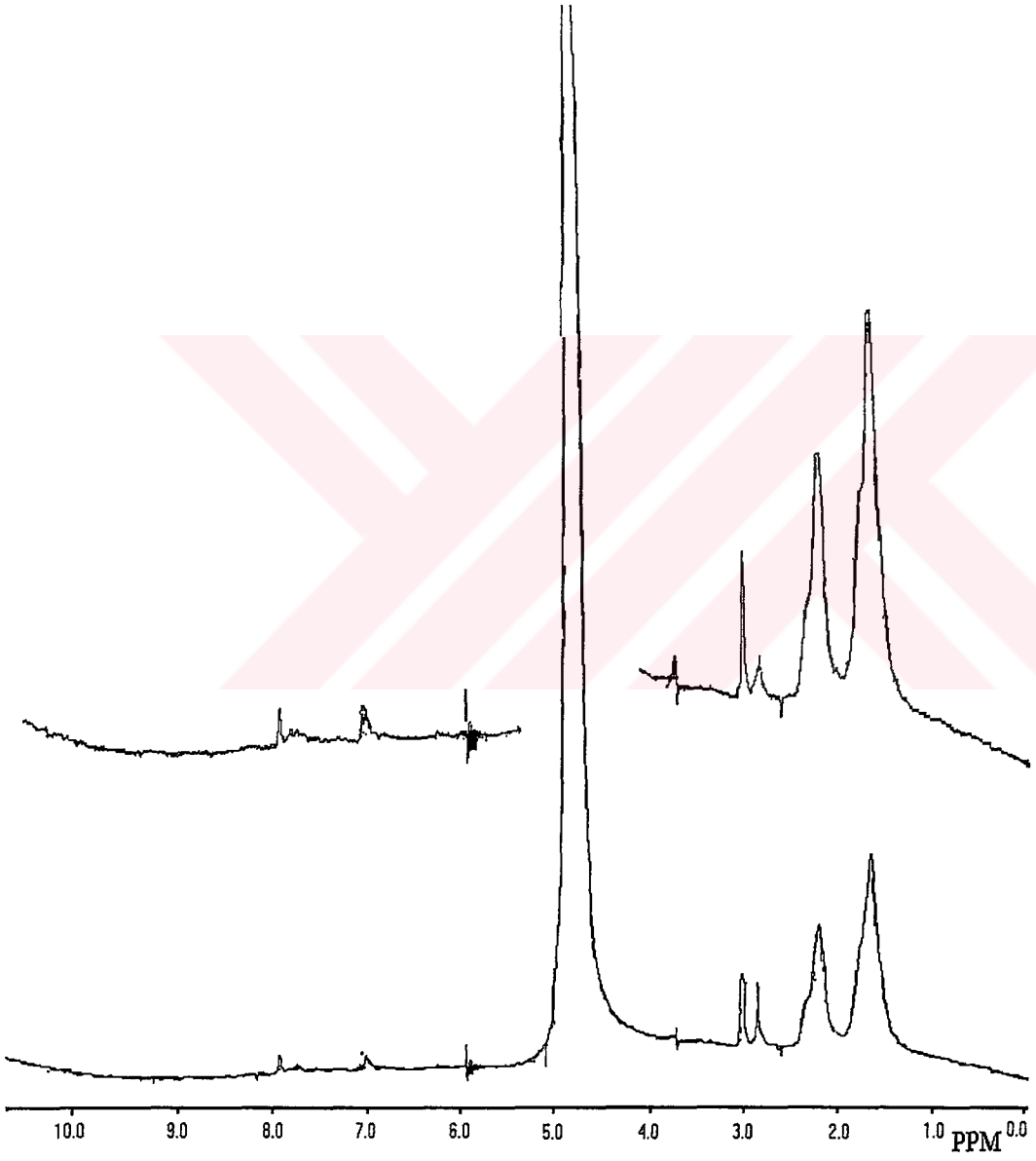

Figure 4.3.4.2 ^{1}H-NMR spectra in D_2O solution of copolymer obtained by chemically using AIBN initiator at mole ratio n_T/n_{NVCz}= 100 in DMF ([AAm]= $9.9x10^{-1}$ mol dm^{-3}, [NVCz]= $1x10^{-2}$ mol dm^{-3}, [AIBN]= $5x10^{-2}$ mol dm^{-3}.

4.3.5 Mechanism of Copolymerization Acrylamide and N-Vinylcarbazole Initiated with AIBN and Ce(IV)-OA Reducing Agent

A classical reaction occurs beetween N-vinylcarbazole and acrylamide initiated with AIBN.

I:

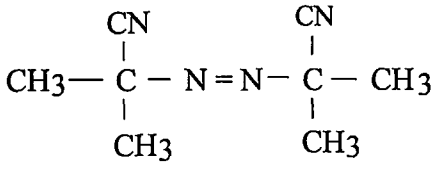

or

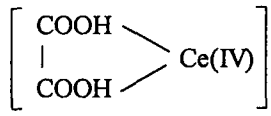

Mechanism:

m ≥ 1

$$I \longrightarrow I^{\cdot}$$

1) $$I^{\cdot} + NVCz \longrightarrow I(NVCz)^{\cdot}$$

$$I(NVCz)^{\cdot} + (m\text{-}1)\,NVCz \longrightarrow I(NVCz)^{\cdot}_{m}$$

$$I(AAm)^{\cdot}_{m} + NVCz \longrightarrow \text{Copolymer}$$

2) $$I^{\cdot} + AAm \longrightarrow I(AAm)^{\cdot}$$

$$I(AAm)^{\cdot} + (m\text{-}1)\,AAm \longrightarrow I(AAm)^{\cdot}_{m}$$

$$I(NVCz)^{\cdot}_{m} + AAm \longrightarrow \text{Copolymer}$$

NVCz

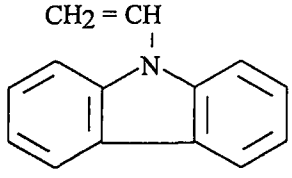

AAm

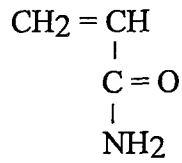

SCHEME 2

4.4 Electropolymerization of N-Carbazole and N-Ethylcarbazole in Acrylamide Medium

In order to understand the effect of acrylamide on carbazole structure, thermal, fluorescence and surface character of copolymers were studied.

4.4.1 Current-Potential Curve During Preparation of N-Carbazole Containing Polymers

The current - potential curve during preparation of the copolymerization strategy employed in the present study was to oxidise carbazole under diffusion limiting conditions. For this purpose a concentration of carbazole as low as 5.10^{-3} mol dm^{-3} was chosen, while that AAm was set at 0.5 mol dm^{-3} which kinetically the rates of polymerization of each monomer becomes comparable and allows copolymerization. When the amount of carbazole was increased, mainly PCz homopolymer was obtained. The current - potential curve was taken in these solutions at a potential swept rate 0.5 V s^{-1} which are given in Figure 4.4.1.1. The curve (a) concerns a current-potential curve for electropolymerization of AAm, curve (b) for NCz and curve (c) for NCz-AAm. Curve (a) and (b) add up to make the curve (c), supporting copolymerization takes place in these conditions.

4.4.2 Cyclic Voltammetry of N-Carbazole and N-Ethylcarbazole in the Presence of Acrylamide

The cyclic voltammogram of NCz in acetonitrile exhibits only one oxidation wave (Epa: 1.43 V vs SCE) in the first sweep, but the corresponding cathodic wave is very weak in intensity, a new band appearing instead (Figure 4.4.2.1). However when the sweep is repeated, the cyclic voltammograms show two anodic waves (Epa: 0.95 V vs SCE and Epa 1.42 V vs SCE), and the corresponding cathodic waves and the oxidation process tends to show reversible characteristic peaks. The gradual increase in the intensity of waves with repeated sweeps indicates that the reaction product is gradually deposited on the surface of the electrode.

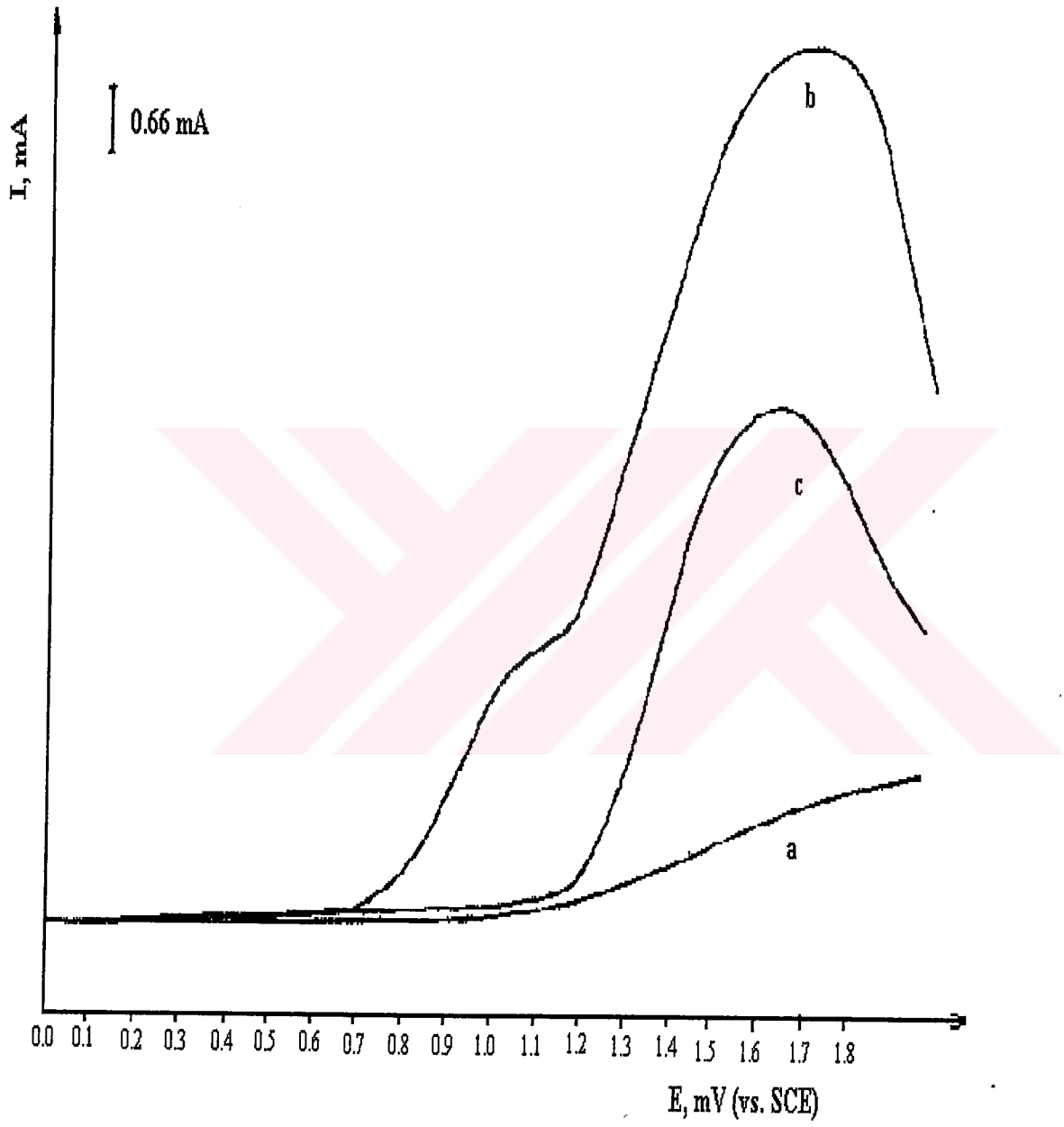

Figure 4.4.1.1 Current vs. Voltage of (a) $5x10^{-1}$ mol dm^{-3} AAm, (b) $5x10^{-3}$mol dm^{-3} NCz, (c) $5x10^{-1}$ mol dm^{-3} AAm + $5x10^{-3}$ mol dm^{-3} NCz in the ACN solution containing TEAP. Scan Rate: 0.05 V s^{-1}.

The first and second anodic waves are ascribed to the oxidations of the 3,3 bis carbazole and the isolated carbazole moieties respectively. It is suggested that the cationic polymerization of monomers be initiated either by the monomer cation radical or by the proton generated by the coupling reaction of cation radical of the carbazole. There are some differences in CV of NCz in the presence of AAm. By repeated cycles (Figure 4.4.2.2 cycles a, b and c) a shift in anodic peak as well as absences of reverse peak in cathodic direction indicate a reaction between NCz and AAm. In the first sweep (cycle a) oxidation of carbazole to cation radical takes place and the cathodic peak corresponds to its reduction. In the second sweep, cation radicals react with AAm. Upon multiple cycling of the solution, a new peak develops at a lower potential (E_a= 0.880 V, cycle b) due to deposition of electroactive product on the surface of the working electrode. By increasing the repeated cycles the peak shifts to the more anodic direction due to the reaction with AAm. This result leads to the conclusion that a different polymeric film in accordance with homopolymer of carbazole occurred at the surface. Further evidence for the formation of the polymer is the observation of a light green film on the surface. It is clear from the figure that successive cycles not only give very clear increases in both anodic and cathodic currents, but also that the ratio of anodic to cathodic charge in each cycle exceeds unity. This is shown in Table 4.4.2.1 where the anodic charge as a function of the sweep rate employed for polymer formation decreases with increasing sweep rate. It is also evident from the tabulated data that the anodic:cathodic ratio in all cases is superior to unity and that it too decreases with the increasing sweep rate.

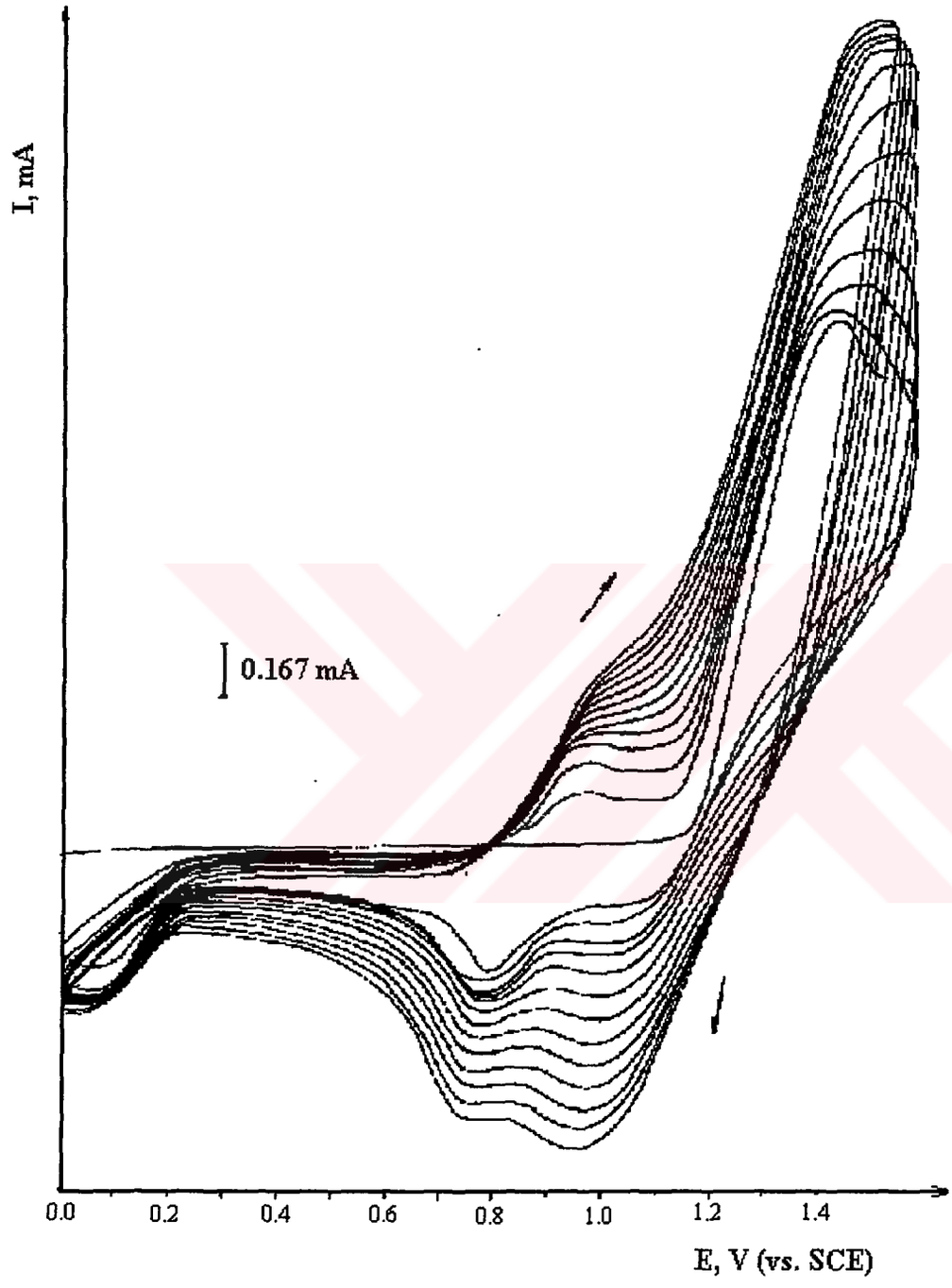

Figure 4.4.2.1 Cyclic Voltammogram of $1x10^{-2}$ mol dm^{-3} NCz electrochemically deposited onto Pt in the ACN solution containing $1x10^{-1}$ mol dm^{-3} TEAP as a supporting electrolyte. Scan Rate: 0.1 V s^{-1}.

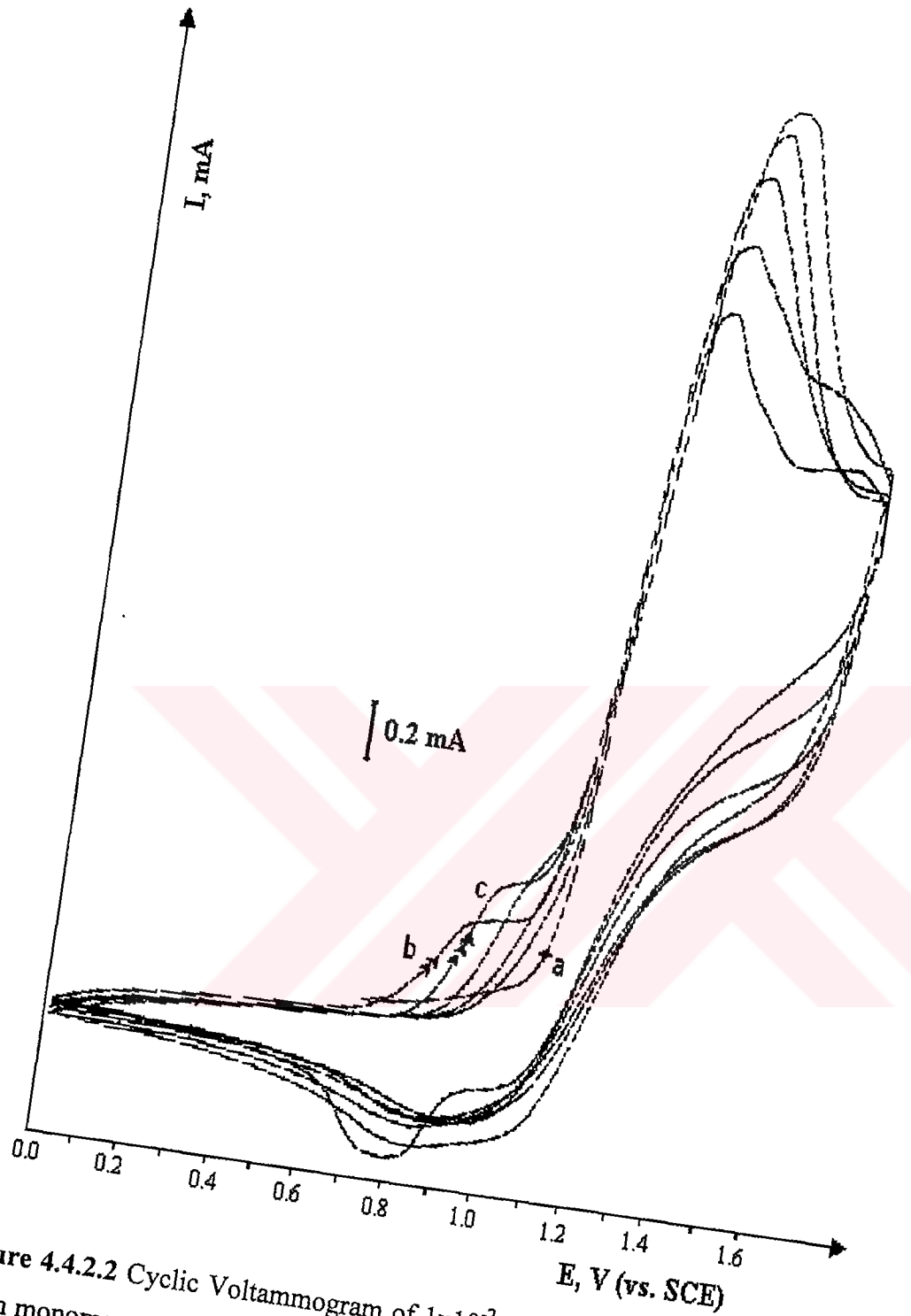

Figure 4.4.2.2 Cyclic Voltammogram of $1x10^{-2}$ mol dm^{-3} NCz and $5x10^{-1}$ mol dm^{-3} AAm monomers electrochemically deposited onto Pt in the ACN solution containing $1x10^{-1}$ mol dm^{-3} TEAP as a supporting electrolyte, Scan Rate: 0.05 V s^{-1}. a, b, c show the first, second and third cycle.

Table 4.4.1.1 The anodic charge and anode:cathode ratio for the electroformation of the copolymer of AAm and NCz as a function of the potential scan rate, AAm:NCz (50:1) in ACN containing $1x10^{-1}$ mol dm^{-3} TEAP.

Scan rate ($V\ s^{-1}$)	Anodic charge (Qa) x 10^{-3}	Anode:Cathode (charge ratio, Qa/Qc)
0.01	4.50	1.481
0.02	3.96	1.284
0.03	3.69	1.207
0.04	3.54	1.186
0.05	3.42	1.169
0.06	3.29	1.148
0.07	3.20	1.138
0.08	3.05	1.116
0.09	3.02	1.112
0.10	2.94	1.124

The achievement of PECz as a coherent film depends strongly on the nature of the substituent. It is known that N-ethyl and N-phenylcarbazoles in acetonitrile do not produce film [28]. NECz is synthesized electrochemically in the presence of AAm with the aim of forming a stable electroactive and electrically conducting polymer, which may exhibit properties of the different monomers, incorporated within.

The same electrochemical growth technique employed was that of repeated cycling between 0 and 1.8 V vs SCE for the ECz. There are significant differences in CV of NECz in the presence of AAm, as shown in Figure 4.4.2.3 a and b. The anodic oxidation of the NECz in ACN medium does not produce filming; the green colour ascribed to oxidized 3,3'-dicarbazyl units was seen to diffuse into the solution. During subsequent scans there were no differences in the cyclic voltammogram of ethylcarbazole (Ea_1=0.93 and Ea_2= 1.3 V) (Figure 4.4.2.3 a).

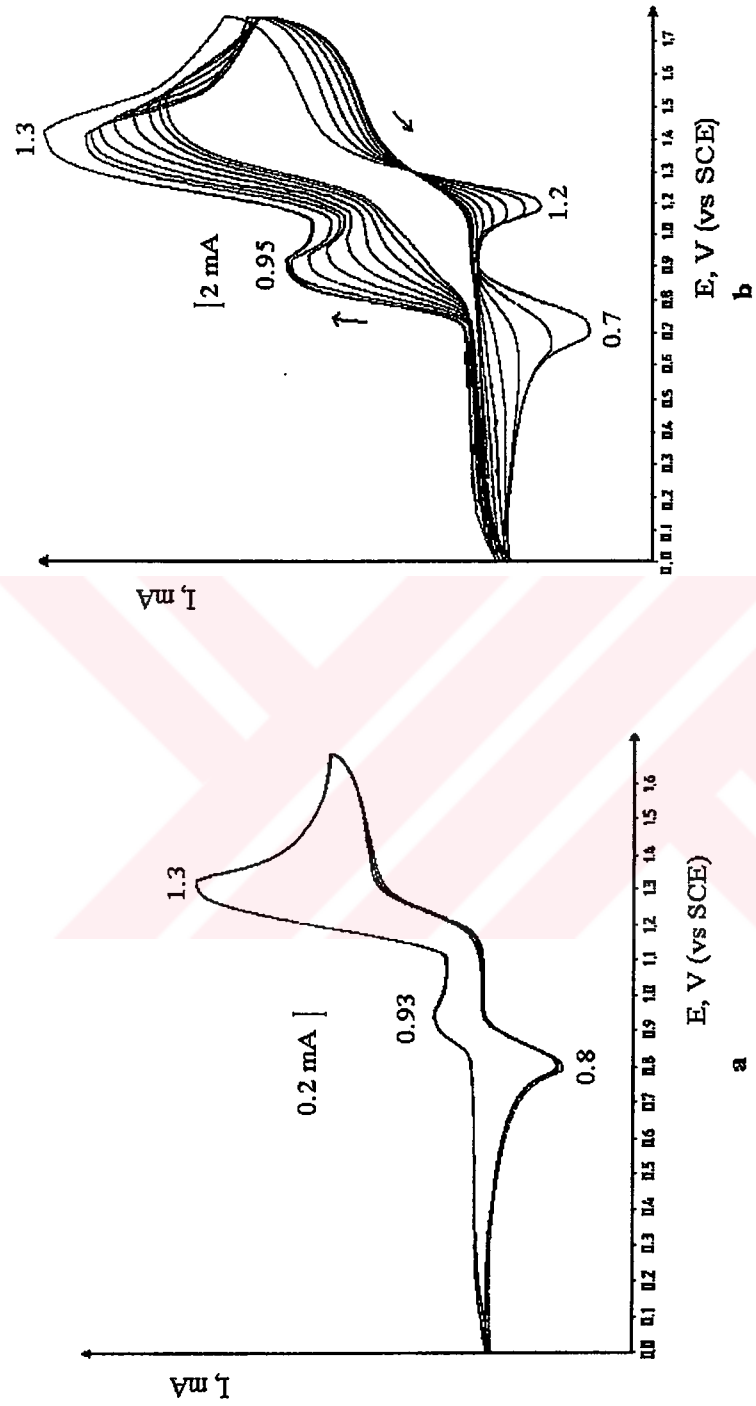

Figure 4.4.2.3 Cyclic voltammogram of (a) NECz (b) AAm:NECz onto the Pt in ACN solution. Scan Rate= 0.05 V s^{-1}, Supporting Electrolyte, $1x10^{-1}$ mol dm^{-3} TEAP.

However, in the presence of AAm, NECz is oxidized at Pt to form cation radical in acetonitrile which reacts further with AAm and results a green film on the electrode surface, in contrast to NECz alone (Figure 4.4.2.3b). The gradual increase in the intensity of waves (Ea_1= 0.85 and Ea_2= 1.3 V) with repeated sweeps indicates that the reaction product is gradually deposited on the surface of the electrode.

Solvents have a very strong influence both on the mechanism of electropolymerization and on polymer properties. In fact, solvents must simultaneously have a high dielectric constant to ensure the ionic conductivity of the electrolytic medium and a good resistance against decomposition at the potential required to oxidise the polymer ring. In addition, as polymerization proceeds via radical cations intermediates, the reaction is particularly sensitive to the nucleophilicty of the environment in the region near the electrode, where radical cations are generated. All these reasons introduce limitations in the choice of solvent.

Among organic solvents, acetonitrile has been the most commonly used. Films grown from dry acetonitrile are non-uniform and are poorly adhered to the electrode surface for carbazole [28]. In addition to acetonitrile, a wide variety of other aprotic solvents can be used as well as the nucleophilic aprotic solvents such as dimethylformamide, dimethylsulfoxide. A better morphology and adhesion of the electropolymer film to the electrode substrate could be achieved in DMF [120]. In addition to aprotic solvents, films have been prepared in acid media. The oxidation of carbazole in a protic acid medium has been shown to provide an easy and straightforward route for synthesizing films bound to an inert electrode substrate, which in a suitable acid electrolyte, could exhibit reasonable conductivity and stable redox properties [120]. The main problem concerning polyheterocylic compounds electrogeneration in water is associated with the excess of oxygen present in the polymer structure originated by degradation processes taking place during polymerization [121-123]. These degradation processes are associated with the nucleophilic character of the solvent.

As has been pointed out, acetonitrile has been the most used solvent to electro polymerise carbazole and the other heterocyclic compounds. From the experimental results that have been done for PCz and especially for PPy results the amount of water and acid effects on the polymers in different ways.

The effect of solvent on the electrochemical behaviour can be seen by comparing the cyclic voltammogram of Figure 4.4.2.4, carried out in a 1:1 CH_3CN: H_20 ($HClO_4$) mixture to that of Figure 4.4.2.4. A better definition of all the current peaks was found in the mixture, in particular in the reduction peaks for the electrochemically deposited polymer. This clearly signifies that the electrochemical activity of the polymer films in this medium has significantly improved, possibly due to the more highly mobile protons in the solution which could more readily compensate for the electroneutrality of the polymer film during its oxidation and reduction. It is also evident that with an increasing number of cycles, the relative heights of the two reduction peaks alter (Figure 4.4.2.5) with the second reduction process at *ca* 0.76 V becoming less prominent. This was also found for the repeated cycling and hence increasing film thickness in the ACN medium and may suggest that there is a relationship between in the mechanism for electroreduction of the film with thickness. This should not be too surprising since the reduction process involves electron injection into the conjugated polymer chain from the metal substrate and a corresponding loss of anion or gain of cation within the polymer matrix to maintain electroneutrality. Ejection of an anion into the solution from deep inside the polymer becomes a less likely scenario as film thickness increases and it is thus more likely that in this case, cation (notably proton) injection plays the dominant role.

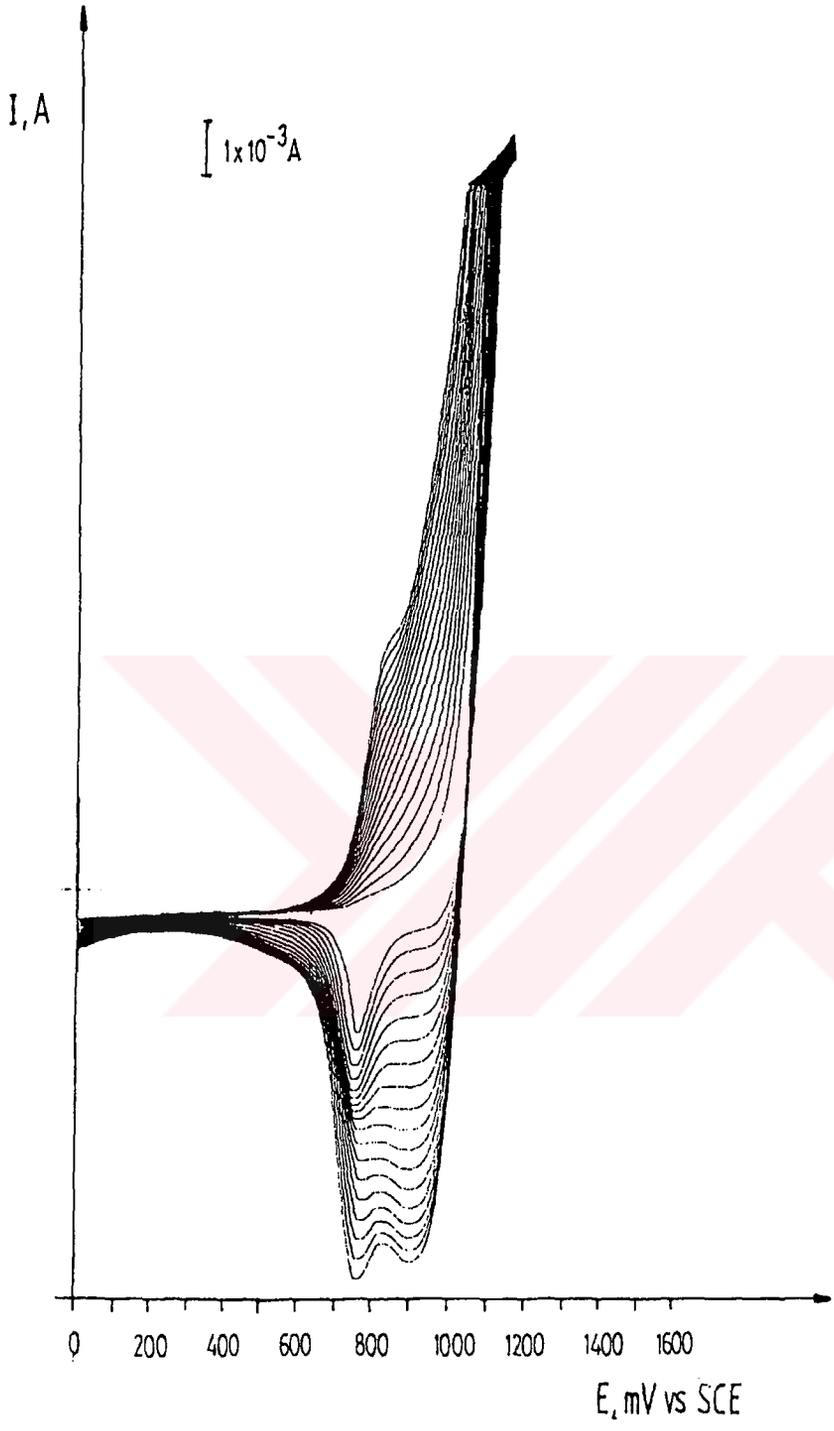

Figure 4.4.2.4 Electrodeposition of AAm:NCz copolymer films onto Pt in in ACN:H_2O (50:50) ($1x10^{-1}$ mol dm^{-3} $HClO_4$) solution. Scan Rate = 0.05 V s^{-1}.

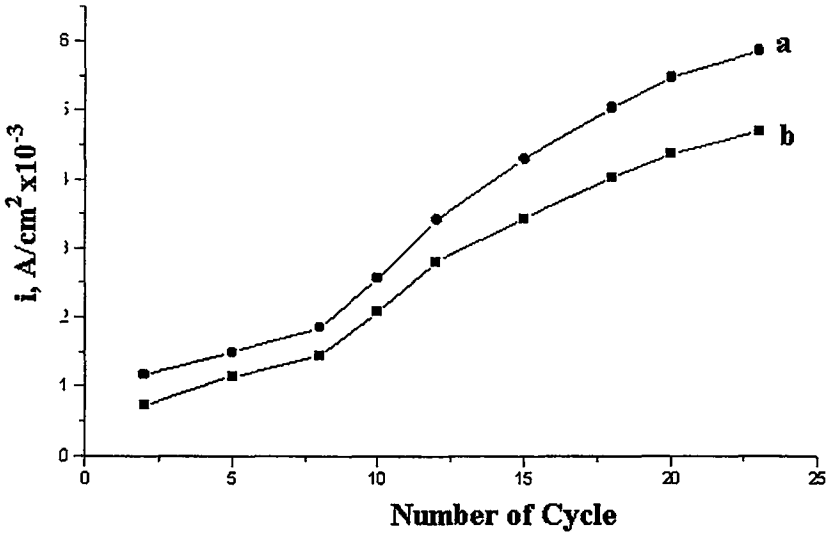

Figure 4.4.2.5 Changes of the cathodic peak current densities of NCz and AAm:NCz (50:1) with the number of cycles in ACN:H_20 ($1x10^{-1}$ mol dm^{-3} $HClO_4$), **A**- a) Ec_1= 0.860 V NCz b) Ec_1= 0.750 V NCz in the presence of AAm. Working and Counter Electrode: Pt, Reference Electrode: Calomel, Scan Rate: 0.05 V s^{-1}

The solvent effect of polymerization onto the anodic peak densities also supported the mechanism depicted in scheme.

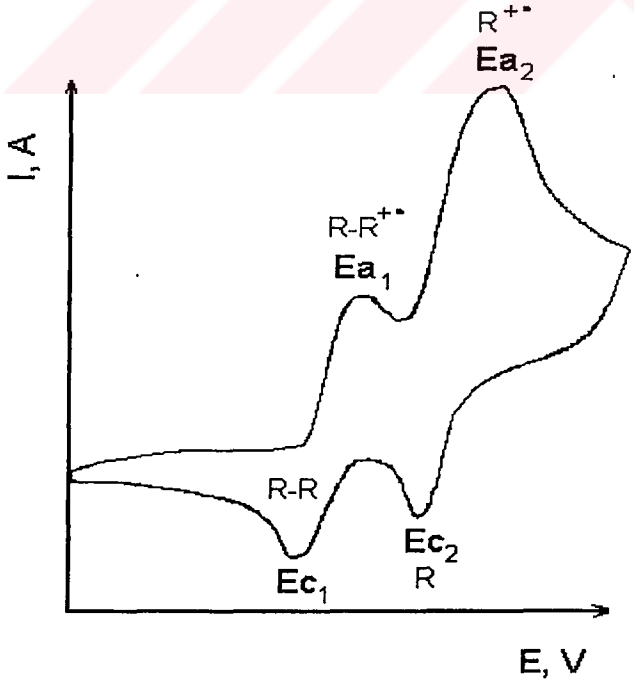

Scheme 1 Probable reaction formation that is showed with the scheme.

X: ClO_4^- (Et_4ClO_4, $HClO_4$), AAm **R:**

R' : H, $CH=CH_2$, C_2H_5

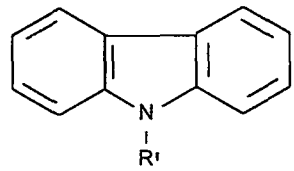

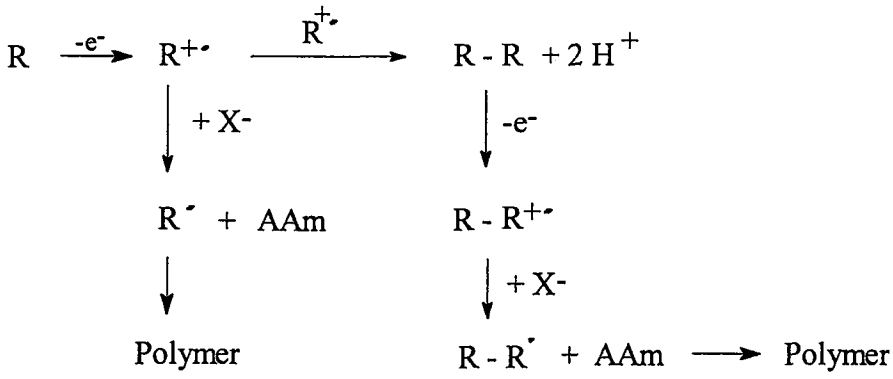

Scheme 2

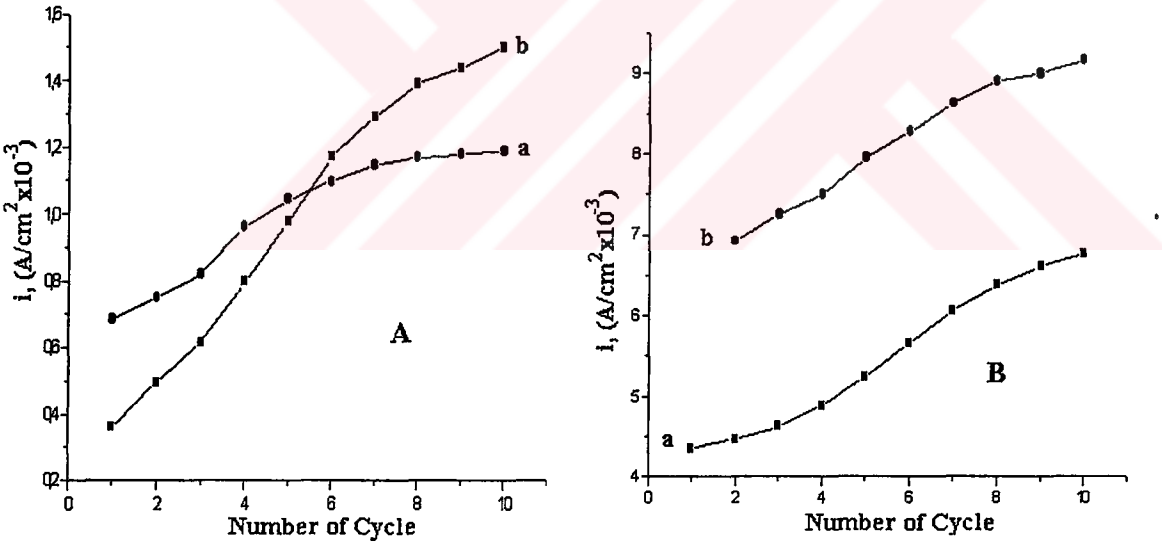

Figure 4.4.2.6 Changes of the anodic peak current densities of PCz and AAm:PCz (50:1) with the number of cycle in ACN ($1x10^{-1}$ mol dm^{-3} TEAP), **A**- a) Ea_1= 0.96 V PCz b) Ea_1= 0.9 V PCz in the presence of AAm; **B**- a) Ea_2= 1.35 V PCz b) Ea_2= 1.28 V PCz in the presence of AAm. Working and Counter Electrode: Pt, Reference Electrode: Calomel., Scan rate: 0.05 V s^{-1}

In the presence of AAm there is a decrease in the first anodic oxidation potential (Ea_1= 0.9 V) which is, a reaction of $R - R^{+\bullet}$ comparison to NCz (Ea_1= 0.96

V). Changes in the second oxidation potential (Ea_2) of NCz and AAm:NCz which are known as $R^{+\bullet}$ are linear with each other (Figure 4.4.2.6). This also shows AAm incorporated into the cation radical of the carbazole oligomer ($R - R^{+\bullet}$).

The solvent effect was also studied for NECz polymerization. The same figures were obtained for the ACN:H_20 ($HClO_4$) media (Figure 4.4.2.7). The faster polymer generation at rising proton concentrations in aqueous solution was observed. The protonated ethylcarbazole could transfer an electron to the electrode to form the cation radical which propagates the polymerization. This mechanism is able to explain the increase in polymerization rate with the acidification of the aqueous electrolytic solution.

Peak current densities show an almost linear increase with number of cycles for the perchloric acid medium to the ACN medium (Figure 4.4.2.7). This is reasonable because NECz does not produce a film in ACN. Protic acid as a solvent might affect the C_2H_5 group of NECz. Protonation of C_2H_5 group, which deactivates the radical cationic site on the NECz ring, results in the progress of polymerization that is shown in the FT-IR measurements section (Appendix A.3).

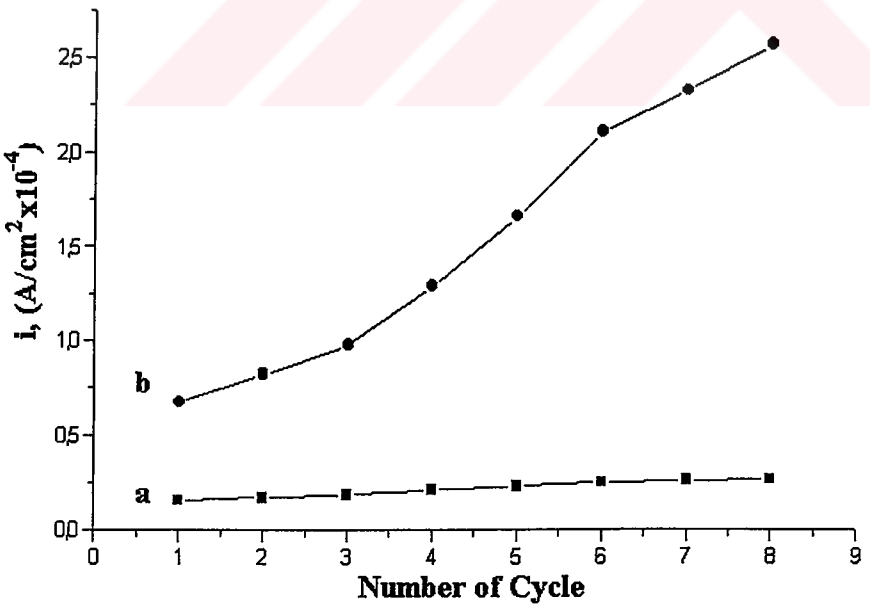

Figure 4.4.2.7 Changes of the anodic peak current densities of NECz with the number of cycles in different solvents, a) Ea_1= 0.96 V for ACN ($1x10^{-1}$ mol dm^{-3} TEAP) b) Ea_1= 0.64 V for ACN:H_2O ($1x10^{-1}$ mol dm^{-3} $HClO_4$). Working and Counter Electrode: Pt, Reference Electrode: Calomel. Scan Rate: 0.05 V s^{-1}.

4.4.3 FT-IR Measurements

The spectral features agree with the previously reported data that The carbazole monomer has bands at 3550, 1620, 1450, 1350, 1280, 940, 760 and 440 cm^{-1}. [124, 125]. When the carbazole monomer was electropolymerized, the bands at 1100 and 620 cm^{-1} appeared which was attributed to ClO_4^- [28]. For the bands in the range 750-900 cm^{-1} which correspond to 1,2,4, a substituted benzene ring appears in the FT-IR spectrum. Figure 4.4.3.1 shows the spectra of PCz and PCz in the presence of AAm.

The polymerization by co-monomer performed at two different potentials (1.2 V and 2.0 V) and different AAm/NCz (100 and 400) mole ratios. The change of applied potential shows no significant effect on the copolymer structure (Appendix A.2). In the FT-IR spectrum of the resulting polymers obtained both 2.0 V and 1.2 V, the band at 1650 cm^{-1} which is attributed to -C=0 group of AAm. In addition, the intensity of this band increased with increasing AAm feed, showing incorporation of AAm into the structure. In addition to this, –C=O band at 1650 cm^{-1} increased in the intensity of the bands at 1453 cm^{-1}, which correspond to –C-N bands of the substituted benzene ring at 805 and 750 cm^{-1} by increasing AAm feed, Appendix A5. This increase also supports the idea mentioned above. Therefore, the presence of the band at 3550 cm^{-1} which is attributed to -NH str. and the disappearance of the band at 1550 cm^{-1} which is due to aromatic –CH of the carbazole ring in the presence of AAm so that polymerization mostly goes through the NCz ring. In order to understand the type of incorporation of AAm into the final polymer, the copolymer formed at the mole ratio of $n_{AAm}/n_{Cz}=50$, and the composite was compared in accordance with their FT-IR characteristics. The final product dissolved in water to remove PAAm that might be formed on the outer side of the composite and may occur in the copolymer structure. The intensity of the band at 1650 cm^{-1} which is attributed to decreasing the -C=0 group of AAm can be seen from the FT-IR spectra of these polymers (Figure 4.4.3.2 a and b). As the PAAm was dissolved in water, washing the composite caused changing in the structure (Figure 4.4.3.2 a). While washing by water, there is no change at the same band for the copolymer (Fig. 4.4.3.2 b), which supports the possibility of copolymerization of AAm with NCz.

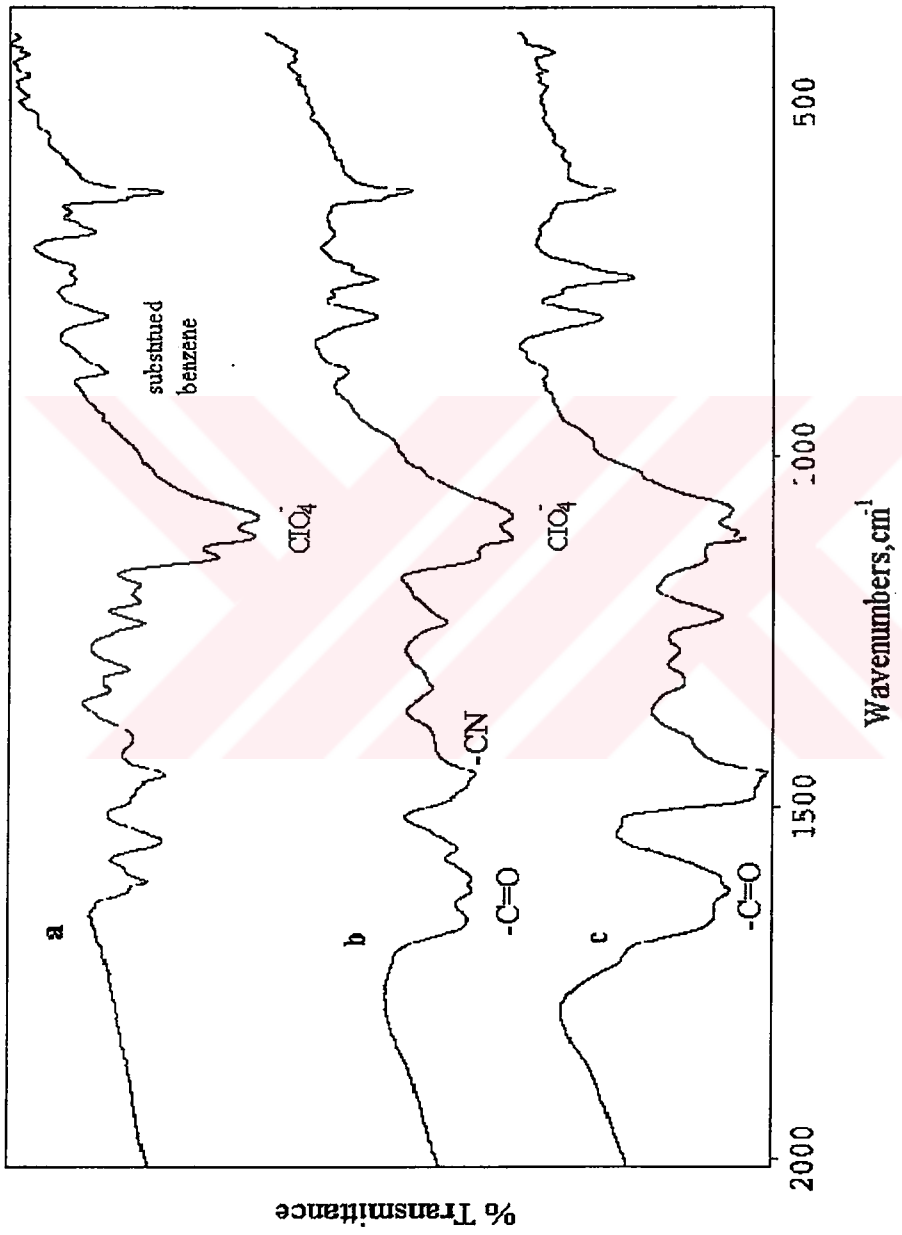

Figure 4.4.3.1 The FT-IR spectra of a) PCz, b) Copolymer, n_{AAm}/n_{NCz}= 10, c) , n_{AAm}/n_{NCz} =100.

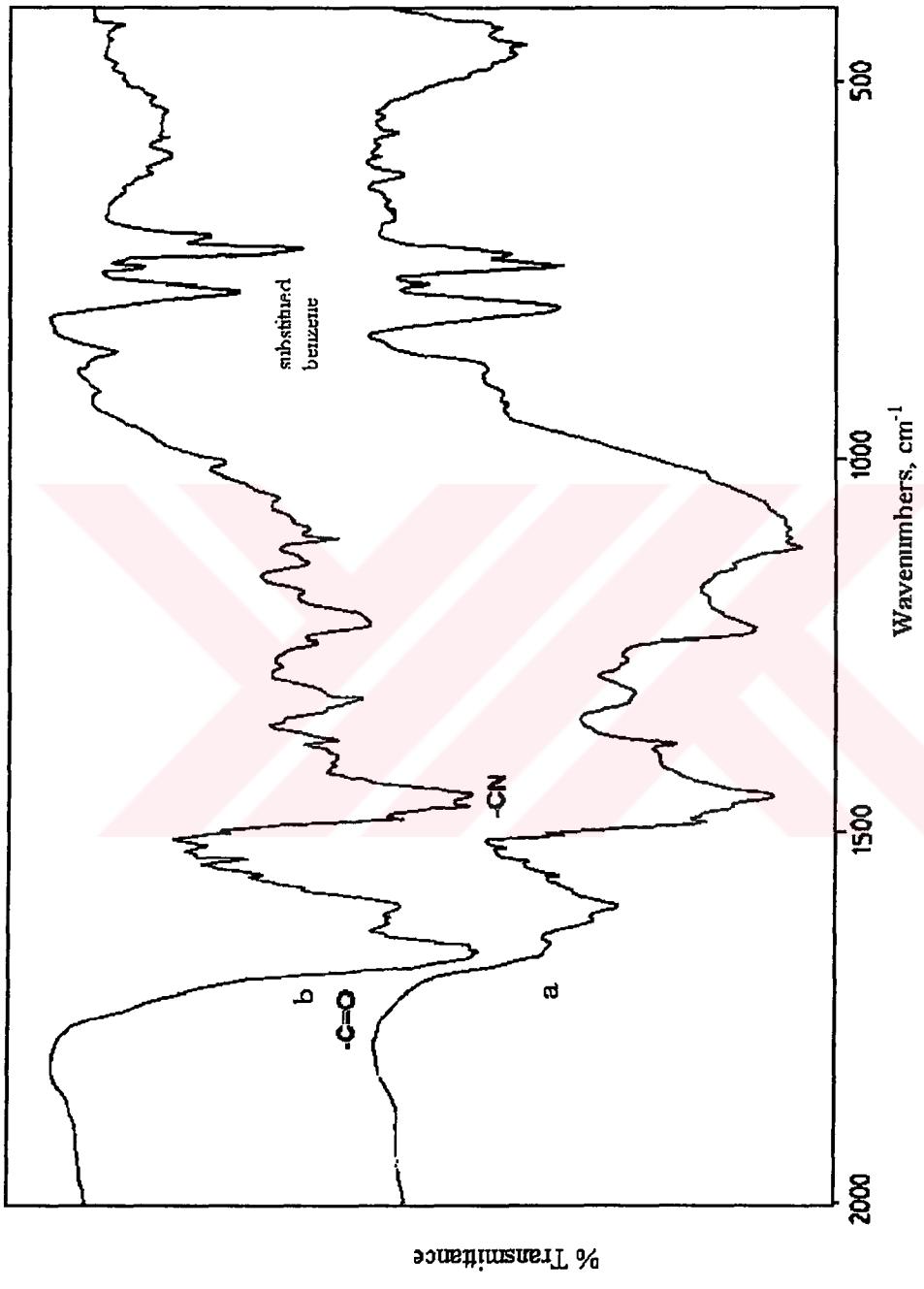

Figure 4.4.3.2 The FT-IR spectra of a) Composite, b) Copolymer, n_{AAm}/n_{NCz} = 50, Applied Potential: 1.2 V.

The FT-IR spectrum of the oxidised NECz film in protic acid medium is shown in Appendix A.3 a and b as compared with obtaining in the presence of acrylamide in acetonitrile solution. The perchlorate anion (1100-620 cm^{-1}) and –CH bending of 1,2,4-trisubstituted aromatic rings (795-835 cm^{-1}) may be identified in the PECz film. The 1380 cm^{-1} band due to C-CH_3 bending testifies that pendant ethyl groups remain unaltered. In addition, the characteristic corresponds to PECz in the presence of AAm –C=O group of AAm also appeared at 1650 cm^{-1} and the intensity of -CN band at 1450 cm^{-1}increases with incorporation of AAm groups, and the band at 1380 cm^{-1} disappeared.

4.4.4 UV-Visible Measurements

a) *Ex-Situ* Spectro-electrochemical Investigation

Figure 4.4.4.1 a shows the UV-Visible spectra of perchlorate doped PCz on Indium Tin Oxide (ITO). The characteristic absorption peaks such as those at 738, 400, 350 nm agree with the previously reported data [126, 127]. They arise from the bonding level to anti-bonding state of a polaron bonding level to the π^* conduction band, and valence band to conduction respectively.

In the presence of AAm, when the reaction media was ACN, the decrease in the intensity of 738 nm peak, due to the decrease in the number of redox sites, might be ascribed to the coexistence of AAm groups with Cz (Fig. 4.4.4.1 b). The increase in the intensity of this peak can be attributed to the enhanced concentration of carbazole radical ions formed as a result of the increased polymerization time (Figure 4.4.4.1 b-f).

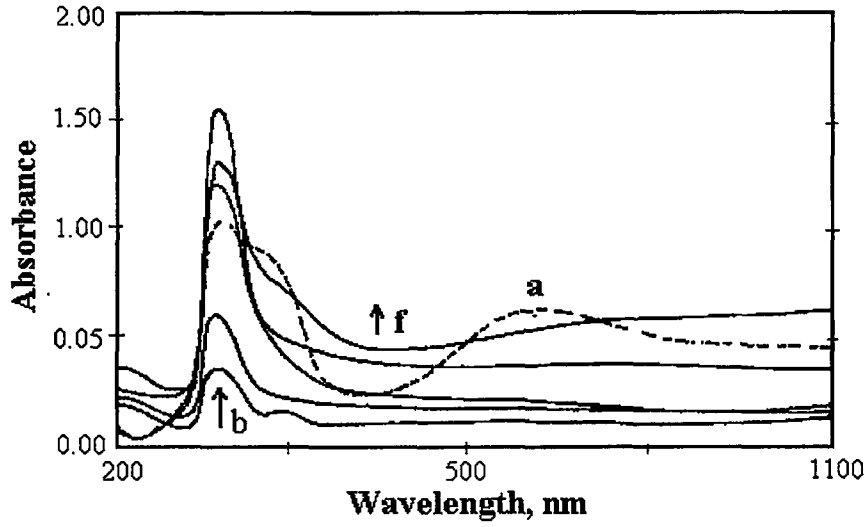

Figure 4.4.4.1 UV-Visible spectra of electrochemically prepared a) PCz film, b) AAm/NCz copolymer (n_{AAm}/n_{NCz} =10) film on ITO, and changes by increasing reaction time (b-f) at the 1.2 V applied potential in ACN. Curves were collected within time intervals at 2 min (a), 5 min (b-f).

It can be seen that the intensities of the 350 and 740 nm absorption peaks decrease with participation of AAm monomers to the structure in the protic acid media as well. This result can be attributed to the decreased concentration of quinone carbazole radical ions formed because of the incorporation of AAm monomer (Fig. 4.4.4.1).

In addition to the film, which occurred at the anode surface (ITO), the reaction in the solution was also followed spectroelectrochemically by UV-vis measurements. The characteristic peaks of the carbazole at 231, 260, 291, 321 and 340 nm (Figure 4.4.4.2) shifted and the intensity of the peak at 290 nm decreased in the presence of AAm (n_{AAm}/n_{NCz}=20), (Figure 4.4.4.2 b). The intensity of characteristic peaks of carbazole decreased with increasing reaction time (Figure 4.4.4.2 b – f) showing the incorporation of the AAm into NCz structure.

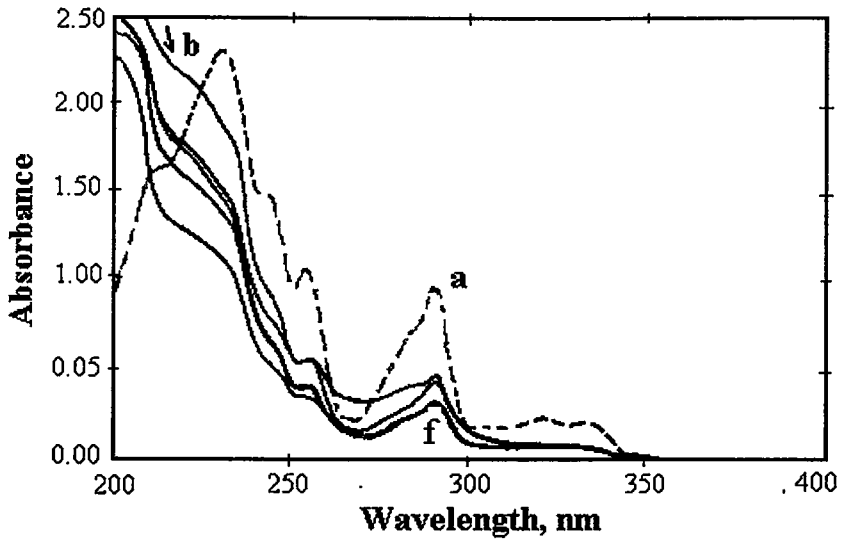

Figure 4.4.4.2 UV-Visible spectra of $1x10^{-2}$ mol dm^{-3} NCz (a), and changes in absorption spectra of reaction solution obtained during copolymerization at n_{AAm}/n_{NCz}=20 and 1.2 V applied potential by increasing time (b-f). Each curve corresponds to five minutes intervals.

Appendix B.1 shows the absorption spectrum of PECz in the presence of acrylamide. Although oxidation of ECz alone does not produce polymeric film on ITO, in the presence of AAm (n_{AAm}/n_{NECz}) = 100 a green film occurred on ITO in acetonitrile solution and a UV-visible spectrum of this film shows the characteristic peak of polycarbazoles at λ = 805, 393, 346, 256 nm [28]. But this increase is not as much as carbazole in the presence of AAm.

b) *In-Situ* Spectro-Electrochemical Investigation

To obtain further information *in-situ* spectro-electrochemical polymerization of NECz and 3,6-dibrECz in the presence of AAm was carried out. NECz and 3,6-dibrECz were selected since they might be also considered as model systems. The main difference between NECz and NCz (1.2 V vs. SCE in ACN/TEAP) is NECz does not polymerise under given conditions but forms a soluble 3'3-dimer [28, 39].

In the case of mono-substituted NCz derivative, coupling can occur at 3 and/or 6 position of carbazole ring and polymerization takes place as formation of a

green film on the anode. In contrast, for the dibromo derivative in the presence of two bromine atoms at 3 and 6 positions protons are released and inhibit the polymerization.

The electrochemical behaviour of the dihalogenated derivatives is completely different from unsubstituted ones. Voltammograms of 3,6'-diBrECz remained unchanged during consecutive scan cycles (Appendix D.1). No deposition or colouring takes place at the anode. Therefore no visible polymerization occurs at the electrode surface. To understand the interaction of acrylamide with NCz's (NECz, NCz, NVCz) in-situ spectroelectrochemical measurements for NECz and 3'6-dibrECz were compared.

In the case of unsubstituted NECz, coupling reactions between monomers can occur and the formation of some oligomers takes place in solution. The peak intensities between 500-1100 nm at ~800, 531 nm increased rapidly with the polymerization time (Figure 4.4.4.3). Under the same experimental conditions the same absorption at 800 nm was also observed for dibromo substituted NECz. Peak intensities of brominated ethylcarbazole at about 800 nm decreased, during the reaction as illustrated in Figure 4.4.4.4. The absorbance values were halved in accordance with the values of NECz. This is due to reaction going through only –2 and/or 7 position of the carbazole ring, since the –3 and/or 6 position are brominated. No peak observed at 531 nm. According to literature, data reported for 3,3'-dicarbazyl [35], the band at 410 nm, can be assigned to the radical cation (polaron), produced during the oxidation of the film. The peak at 531 nm may correspond to polaron of oligomer of NECz.

In the presence of AAm, absorption of the peak at ~800 nm increased as the acrylamide interacts and no peak observed at 531 nm. The peak at 800 nm increased with the polymerization time (Figure 4.4.4.5). It is suggested in literature that the peak at 800 nm corresponds to the 3,3'-dicarbazyl cation radicals (dimer radical cation) [35]. The shift during the properties of polymerization might be also due to the formation of oligomers.

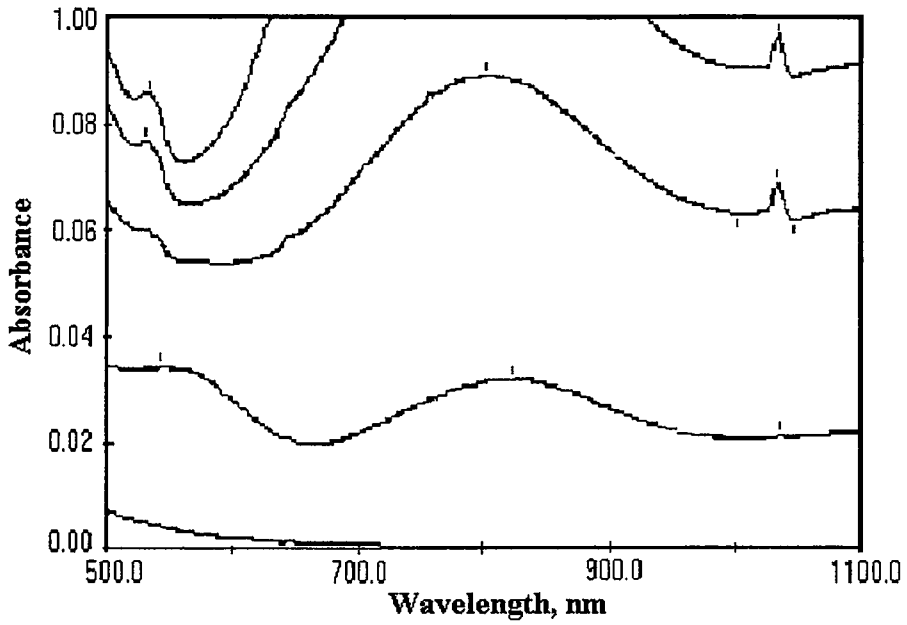

Figure 4.4.4.3 *In-situ* spectroelectrochemically obtained UV-visible absorption spectra of $5x10^{-2}$ mol dm^{-3} NECz in ACN solution using $1x10^{-1}$ mol dm^{-3} TEAP as a supporting electrolyte. Scan Rate: 0.05 V s^{-1}, Working and Counter Electrode: Pt, Reference Electrode: Ag/AgCI in 5 minutes intervals.

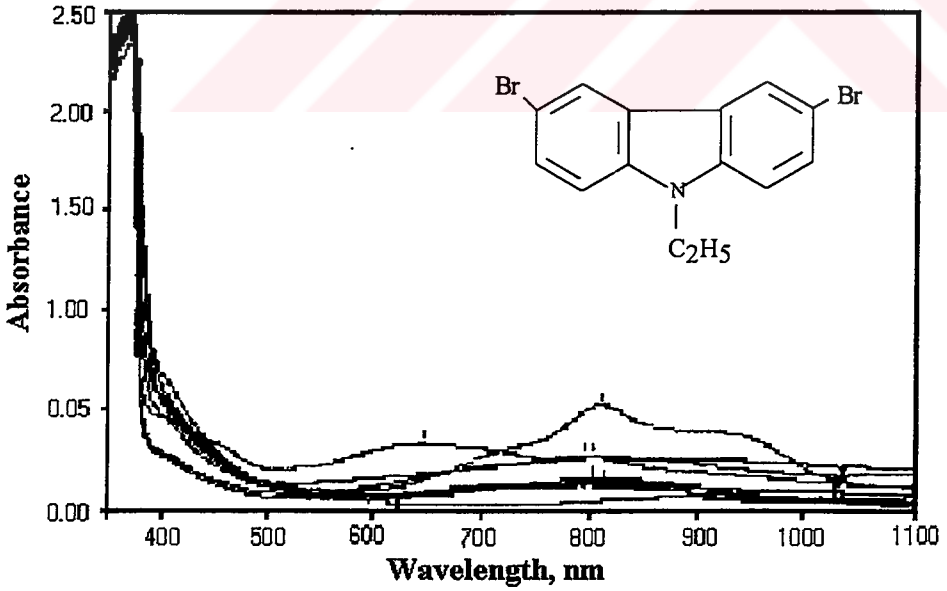

Figure 4.4.4.4 *In-situ* spectroelectrochemically obtained UV-visible absorption spectra of $5x10^{-2}$ mol dm^{-3} 3,6'-dibrECz in ACN solution using $1x10^{-1}$ mol dm^{-3} TEAP as a supporting electrolyte. Scan Rate: 0.05 V s^{-1}, Working and Counter Electrode: Pt, Reference Electrode: Ag/AgCI.

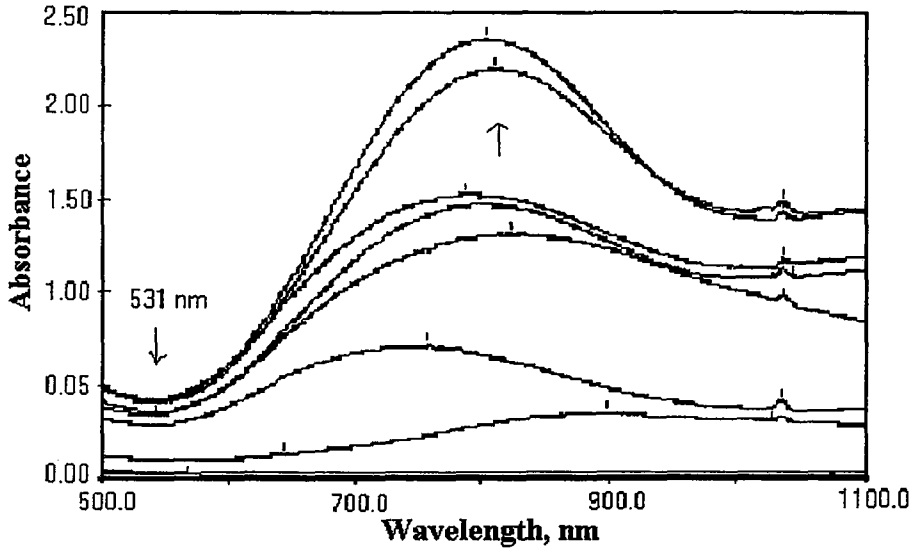

Figure 4.4.4.5 *In-situ* spectroelectrochemically obtained UV-visible absorption spectra of 20:1 (AAm: NECz) in ACN solution using $1x10^{-1}$ mol dm^{-3} TEAP as a supporting electrolyte. Scan Rate: 0.05 V s^{-1}, Working and Counter Electrode: Pt, Reference Electrode: Ag/AgCI in 8 minutes time.

This behaviour shows some parallelism with the electrochemical measurements (Figure 4.4.4.6 and 7). In the presence of AAm anodic peak currents were higher than in the case of NECz alone (Figure 4.4.4.6 and 7 a, c). The same behaviour was also observed for cathodic currents (Figure 4.4.4.6 and 7 b, d). On the other hand, anodic currents are greater than cathodic currents. This finding seems reasonable, due to the fact that formation of radical cationic species and successive fast chemical combination before reduction of these species.

On the contrary to the NCz, NECz, NVCz, for the dibromo derivative the presence of two bromine atoms at the 3 and 6 positions prevents proton release and inhibits the polymerization. In the presence of AAm, absorption values stayed constant at 800 nm, after 5 minutes (Figure 8 a and b). These results indicated the interaction AAm with the oligomer and dimer.

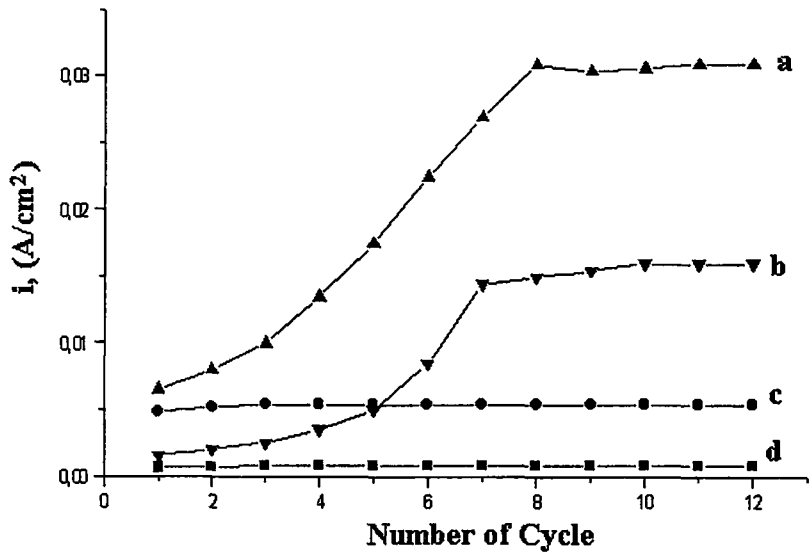

Figure 4.4.4.6 Results of Cyclic Voltammetric measurements with the time at the first oxidation (0.95 V); a) Ia for AAm:NECz, b) Ic for AAm:NECz, c) Ia for NECz, d) Ic for NECz; $1x10^{-2}$ mol dm^{-3} NECz, AAm:NECz (20:1) in ACN using $1x10^{-1}$ mol dm^{-3} TEAP as a supporting electrolyte. Scan Rate: 0.05 V s^{-1}, Working and Counter Electrode: Pt, Reference Electrode: Ag/AgCI.

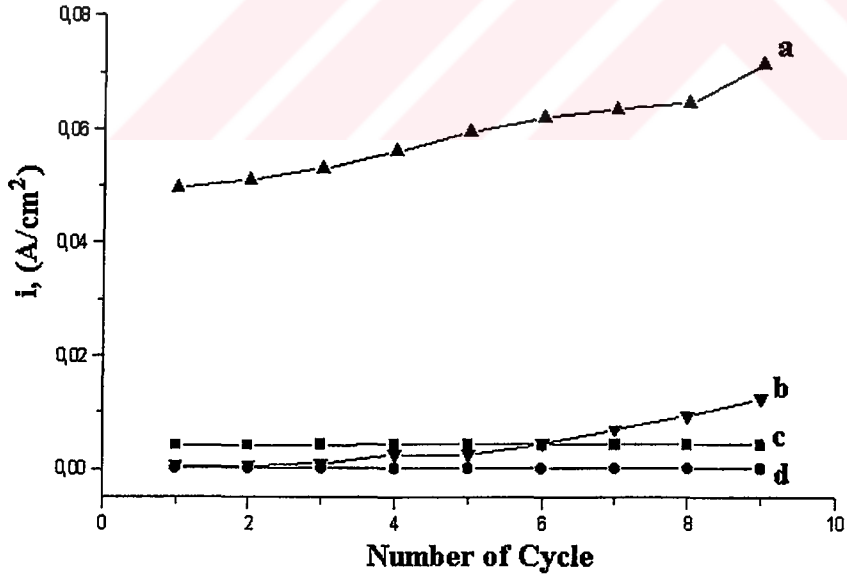

Figure 4.4.4.7 Results of Cyclic Voltammetric measurements with the time at the second oxidation (1.3 V); a) Ia for AAm:NECz, b) Ic for AAm:NECz, c) Ia for NECz, d) Ic for NECz; $1x10^{-2}$ mol dm^{-3} NECz, AAm:NECz (20:1) in ACN using $1x10^{-1}$ mol dm^{-3} TEAP as a supporting electrolyte. Scan Rate: 0.05 V s^{-1}, Working and Counter Electrode: Pt, Reference Electrode: Ag/AgCI.

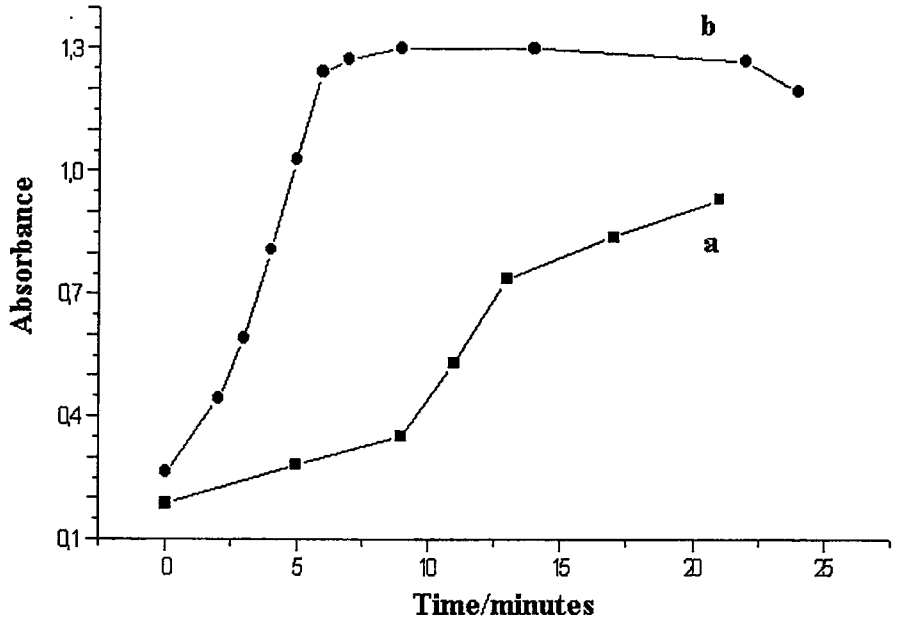

Figure 4.4.4.8 *In-situ* spectroelectrochemically obtained UV-Visible absorption spectra values at 800 nm a) NECz b) AAm:NECz (20:1) in ACN using $1x10^{-1}$ mol dm^{-3} TEAP as a supporting electrolyte. Scan Rate: 0.05 V s^{-1}, Working and Counter Electrode: Pt, Reference Electrode: Ag/AgCI.

In the case of 3,6'-dibrECz the absorbance values at 800 nm are higher than the absorbance values obtained in the presence of AAm (Figure 4.4.4.9 A curve a and b). On the contrary, at 362 nm, an increase in absorbance value was observed in when there was AAm in the medium (Figure 4.4.4.9 B curve a and b). On the other hand, absorbance values at 369 nm stayed constant by the virtue of AAm, although there was an increase in the absence of AAm (Figure 4.4.4.9 C curve a and b).

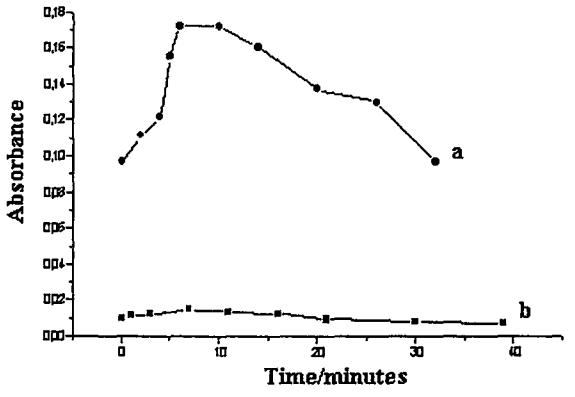

A

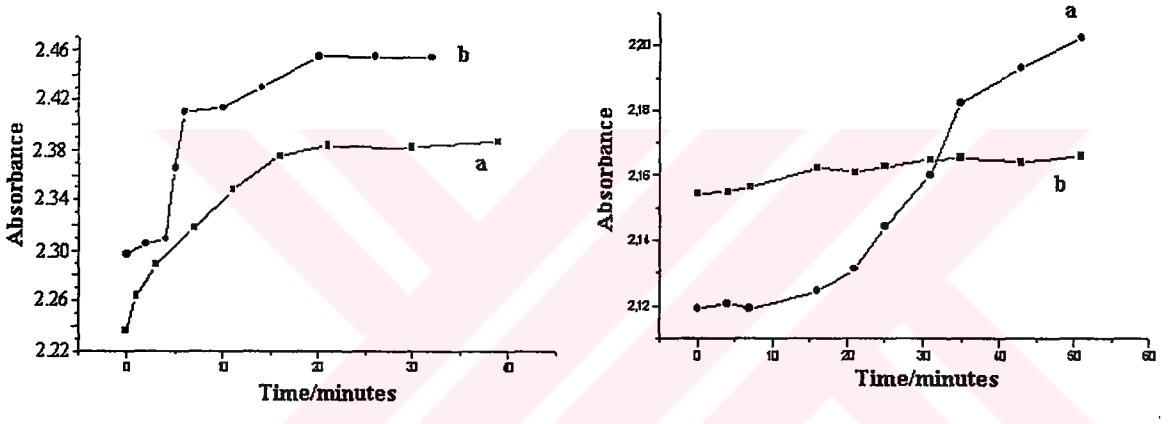

B C

Figure 4.4.4.9 *In-situ* obtained UV-Visible absorption spectra values at A) at 800 nm, B) at 362 nm, C) at 369 nm; a) $5x10^{-2}$ mol dm^{-3} 3,6'-dibrECz, b) 50:1 (AAm: 3,6'-dibrECz), in ACN using $1x10^{-1}$ mol dm^{-3} TEAP supporting electrolyte. Scan Rate: 0.05 V s^{-1}, Working and Counter Electrode: Pt, Reference Electrode: Ag/AgCI

4.4.5 Kinetic Study of Polycarbazole with Acrylamide

Most kinetic studies on conducting polymers were carried out by purely electrochemical methods [128-130]. Only a small portion of the papers published in this field were dedicated to the application of gravimetric techniques.

The use of gravimetric methods to follow polymer growth allows us to know the influence of each studied variable on the polymer production. No interference of possible parallel reactions, giving non-polymeric products, on the measured magnitude (the polymer weight) is expected. The ex-situ determination avoids uncertainties related to the density change of the solution as well as changes of the frequency of the coated product.

The method is based on the following of the weight of polymer grafted on the electrode surface, as a function of the conditions of synthesis. This following allows empirical kinetics to be obtained through the polymer weight generated under constant potentials of polymerization times. The weight of grafted polymer was produced by a unit of polymerization time. The formation and growth of PCz films and PCz in the presence of AAm on platinum electrodes were followed by a gravimetric *ex-situ* determination of the polymer grafted on the electrode. From the influence of monomer or electrolytic concentration empirical kinetics can be obtained.

$$Rp = k\,[\text{N-Carbazole}]^{\alpha}\,[\text{Electrolyte}]^{\beta} \qquad (4.4.5.1)$$

If the empirical kinetic rearranges for the AAm monomer in the medium:

$$Rp = k\,[\text{N-Carbazole}]^{\alpha}\,[\text{Electrolyte}]^{\beta}\,[\text{Acrylamide}]^{\gamma} \qquad (4.4.5.2)$$

N-Carbazole Concentration Influence

All the polymerization was carried out by a potential from 0 V to 1.2 V (vs SCE). The polymerization solution was $1x10^{-1}$ mol dm^{-3} TEAP and $5x10^{-1}$ mol dm^{-3} with different monomer concentrations in the $1x10^{-3}$ to 0.1 mol dm^{-3} range, in ACN.

The results obtained in $1x10^{-1}$, $7.5x10^{-2}$, $5x10^{-2}$, $1x10^{-2}$, $1x10^{-3}$ mol dm^{-3} NCz solutions at 25 °C is shown in Figure 4.4.5.1 A. The flow of increasing densities at greater concentrations of monomer and constant polymerization times promotes steeper slopes on the correlative straight. The physical meaning of the slopes is the rate of polymerization: i.e. polymer weight produced by units of time under the defined experimental parameters. Figure 4.4.5.1 shows an increase in polymerisaiton rate (Rp) at increasing monomer concentrations. In this way an order dependence on the monomer may be obtained:

$$Rp = k\,(Monomer)^{\alpha} \qquad (4.4.5.3)$$

A Logorithmic representation of the Rp against monomer concentration gives a straight-line slope whose slope is the order dependence. Figure 4.4.5.1 B shows such a linear variation; in this case the empirical reaction order is 0.50:

$$Rp = k\,(N\text{-}Carbazole)^{0.50} \qquad (4.4.5.4)$$

Electrolyte influence

PCz films were electrogenerated at 1.2 V in $1x10^{-2}$ mol dm^{-3} NCz, and different TEAP concentrations in ACN solution. Five different TEAP concentrations were studied: $1x10^{-2}$, $1x10^{-1}$, $2.5x10^{-1}$, $3x10^{-1}$, $6x10^{-1}$ mol dm^{-3}. The upper limit concentration is limited by the solubility of NCz in the ACN. The experimental results shown in Figure 4.4.5.2 A were obtained. The slope of each line is the polymerization rate. The existence of an order dependence of the polymer production relative to the TEAP concentration can be observed according to:

$$Rp\ \alpha\ [TEAP]^{\beta} \qquad (4.4.5.5)$$

A representation of log Rp against log [TEAP] implies a straight line, as was obtained experimentally (Figure 4.4.5.2 B). The order dependence for TEAP, determined from the slope is 0.625.

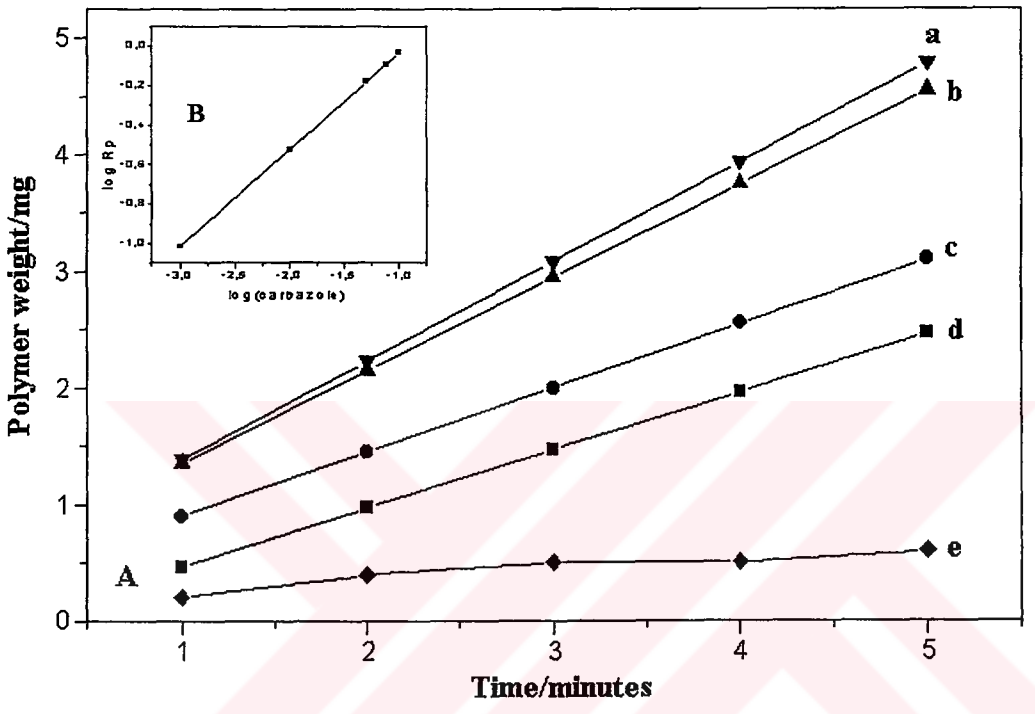

Figure 4.4.5.1 **A-** Evolution of PCz film weight with polymerization time for different NCz concentrations employed in synthesis at 1.2 V [NCz]: a) $1x10^{-1}$, b) $7.5x10^{-2}$, c) $5x10^{-2}$, d) $1x10^{-2}$, e) $1x10^{-3}$ mol dm^{-3}; [TEAP]: $1x10^{-1}$ mol dm^{-3}, T: 25 °C; **B-** Determination of the reaction order relative to carbazole concentration from gravimetric results (Rp values were obtained from the slopes of the weight-time lines for different carbazole concentrations).

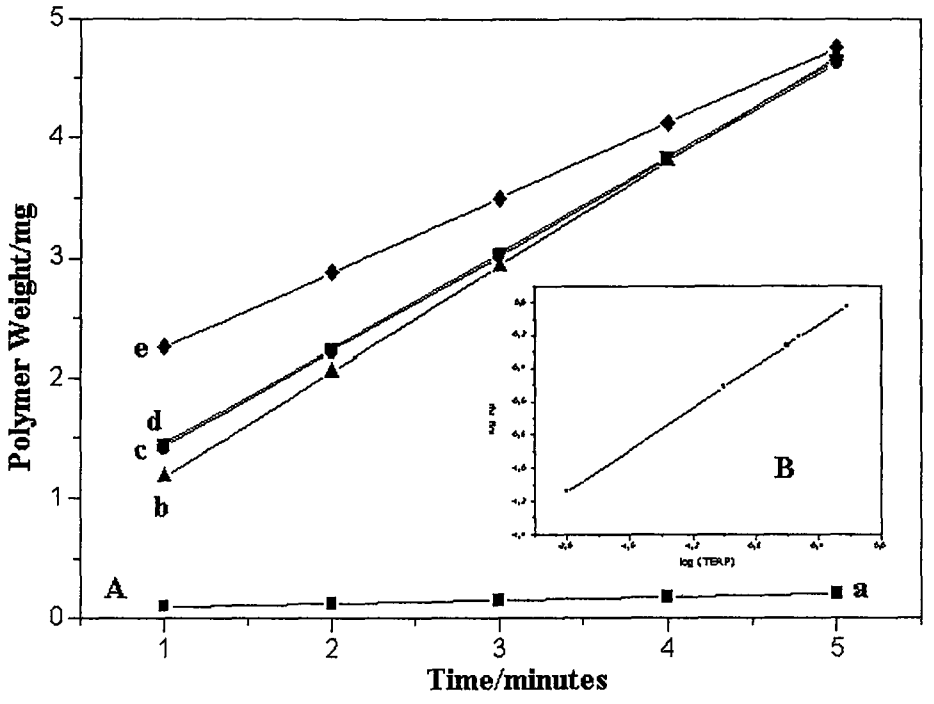

Figure 4.4.5.2 A- Evolution of PCz film weight with polymerization time for different TEAP concentrations employed in synthesis at 1.2 V [TEAP]: a) $1x10^{-2}$, b) $1x10^{-1}$, c) $2.5x10^{-1}$, d) $3x10^{-1}$, e) $6x10^{-1}$ mol dm^{-3}; [NCz]: $1x10^{-2}$ mol dm^{-3}, T: 25 °C; **B-** Determination of the reaction order relative to TEAP concentration from gravimetric results.

The experimental results allow us to write the empirical kinetics for the process, followed by gravimetric determination of the polymer generated on the electrode. Thus,

$$Rp = k\,[\text{N-Carbazole}]^{0.50}\,[\text{TEAP}]^{0.625} \qquad (4.4.5.6)$$

Carbazole Concentration Influence in the Presence of Acrylamide

The results were obtained at $5x10^{-1}$ mol dm^{-3} AAm monomer and $1x10^{-1}$mol dm^{-3} electrolyte concentration and same NCz concentrations were used. An increase in the polymer production is observed by increasing NCz concentrations. As it was seen from the figure 4.4.5.3 A, the slope of each line is the polymerization rate. Figure 4.4.5.3 B also shows the order of dependence. In the presence of AAm, the reaction order is obtained as 0.54.

$$Rp = k\,[\text{N-Carbazole}]^{0.54} \qquad (4.4.5.7)$$

Electrolyte Concentration Influence in the Presence of Acrylamide

PCz films were produced in the presence of $5x10^{-1}$ mol dm^{-3} AAm concentration and $1x10^{-2}$ mol dm^{-3} NCz and different TEAP ($1x10^{-2}$, $1x10^{-1}$, $2.5x10^{-1}$, $3x10^{-1}$, $6x10^{-1}$ mol dm^{-3}) concentrations in ACN solution. The experimental data shown in Figure 4.4.5.4 A. Linear variations of the polymer weight against polarisation time were observed. Increasing polymer weights were obtained by increasing TEAP concentrations: the polymerization process is favoured by the increase of the TEAP concentrations. The order dependence of TEAP, determined from the slope, is 0.50 (Figure 4.4.5.4 B).

$$Rp = k\,[\text{N-Carbazole}]^{0.54}\,[\text{TEAP}]^{0.50} \qquad (4.4.5.8)$$

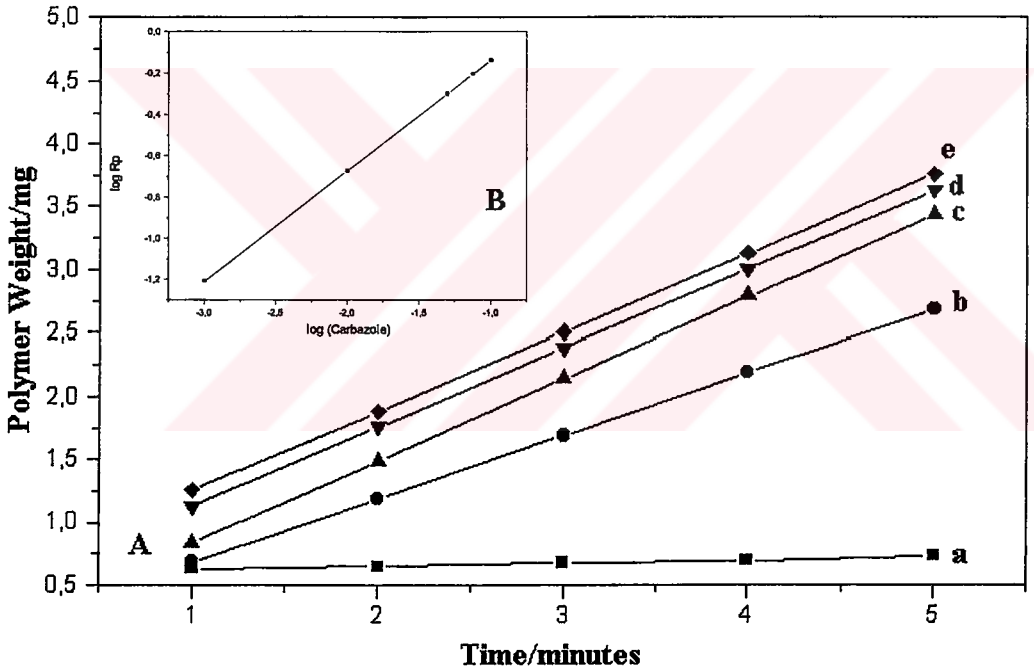

Figure 4.4.5.3 **A-** Evolution of PCz film weight in the presence of $5x10^{-1}$ mol dm^{-3} AAm with polymerization time for different NCz concentrations employed in synthesis at 1.2 V [NCz]: a)$1x10^{-3}$, b) $1x10^{-2}$, c) $5x10^{-2}$, d) $7.5x10^{-2}$, e) $1x10^{-1}$ mol dm^{-3}; [TEAP]: $1x10^{-1}$ mol dm^{-3}, T: 25 °C; **B-** Determination of the reaction order relative to NCz concentration from gravimetric results.

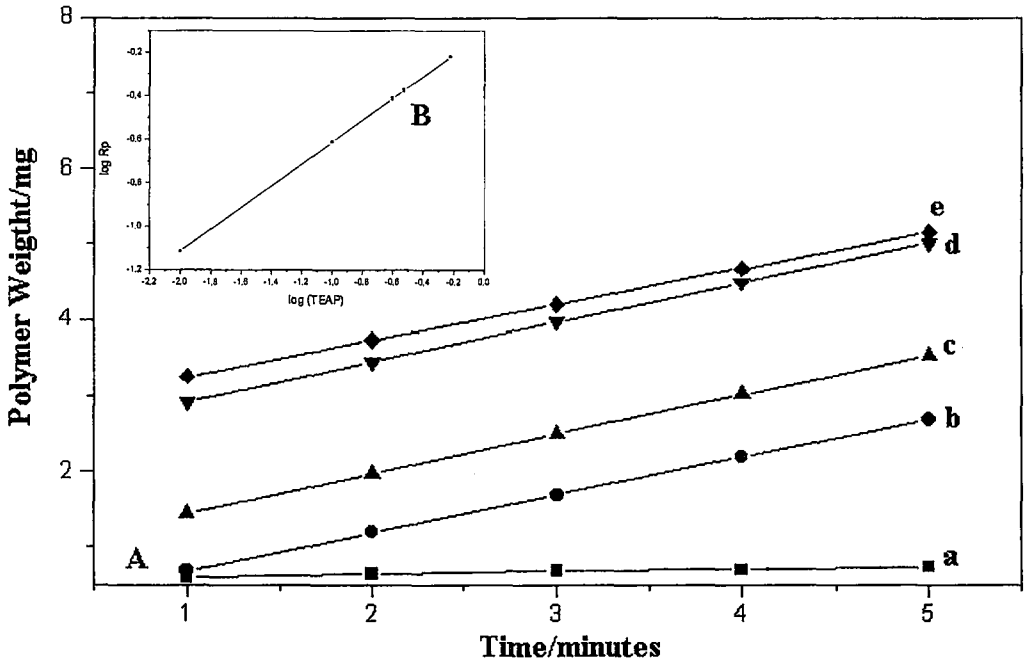

Figure 4.4.5.4 A- Evolution of PCz film weight in the presence of $5x10^{-1}$ mol dm^{-3} AAm with polymerization time for different TEAP concentrations employed in synthesis at 1.2 V [TEAP]: a) $1x10^{-2}$, b) $1x10^{-1}$, c) $2.5x10^{-1}$, d) $3x10^{-1}$, e) $6x10^{-1}$ mol dm^{-3}; [NCz]: $1x10^{-2}$ mol dm^{-3}, T: 25 °C; **B-** Determination of the reaction order relative to TEAP concentration from gravimetric results.

Acrylamide Concentration Influence

Working with $1x10^{-2}$ mol dm^{-3} NCz and $1x10^{-1}$ mol dm^{-3} TEAP in ACN solution, *ex-situ* gravimetric kinetics were followed at different AAm concentration ($1x10^{-3}$, $5x10^{-2}$, $1x10^{-1}$, $5x10^{-1}$ mol dm^{-3}). Figure 4.4.5.5 shows an increase in the polymer yield observed by increasing AAm concentrations. Also, the order dependence of for TEAP, determined from the slope (Figure 4.4.5.5 B),

$$Rp = k\,[\text{N-Carbazole}]^{0.54}\,[\text{TEAP}]^{0.50}\,[\text{Acrylamide}]^{0.10} \qquad (4.4.5.9)$$

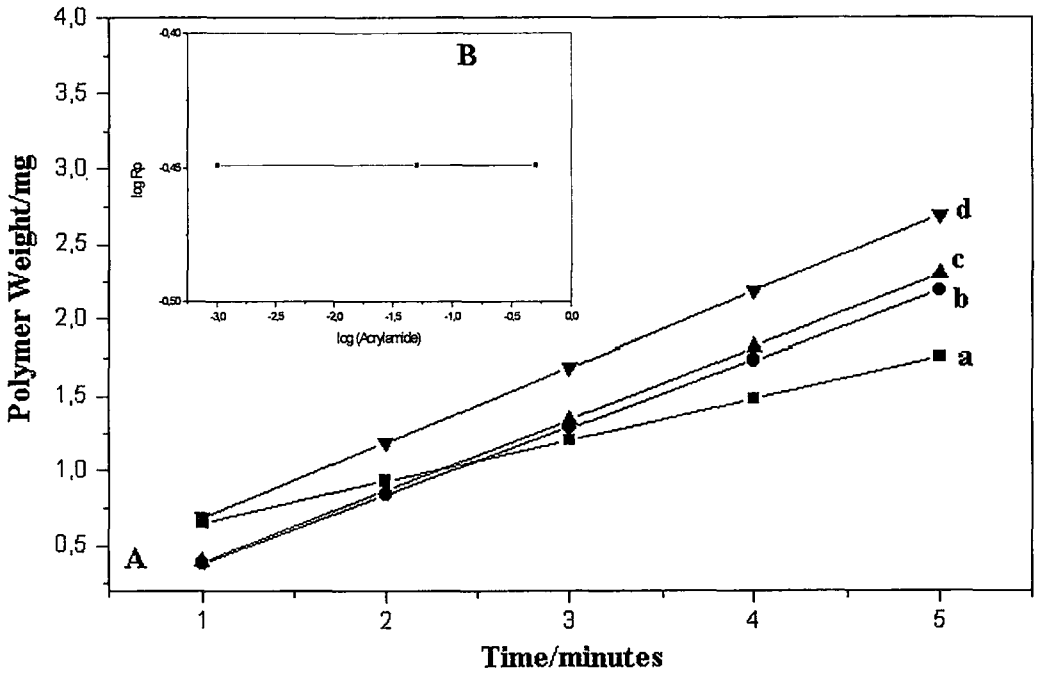

Figure 4.4.5.5 A- Evolution of PCz film weight in the presence of different AAm concentrations with polymerization time employed in synthesis at 1.2 V [AAm]: a) $1x10^{-3}$, b) $5x10^{-2}$, c) $1x10^{-1}$, d) $5x10^{-1}$ mol dm^{-3}; [NCz]: $1x10^{-2}$ mol dm^{-3}, [TEAP]: $1x10^{-1}$mol dm^{-3}, T: 25 °C; **B**- Determination of the reaction order relative to AAm concentration from gravimetric results.

There is such a high reaction order relative to the electrolyte decrease in the presence of AAm. This decrease is almost equal to the AAm reaction order. It might be concluded that AAm effects reaction of ClO_4^- anions or the amount of ClO_4^- anions with resulting polymer.

4.4.6 Fluorescence Excitation and Emission Characteristics

The steady-state fluorescence spectra of electrochemically deposited PCz and PCz in the presence of AAm a part of was dissolved in ACN are shown in Figure 4.4.6.1 and 4.4.6.2. The electrosynthesised PCz and PCz with AAm were prepared in a monomer solution which was performed at 1.2 V. It can be seen that fluorescence spectra of both PCz and PCz with AAm occur in the same region between 340 and 500 nm. The fluorescence spectrum of PCz is slightly different in the presence of AAm. Both of them exhibit only one broad emission band at about 400 nm. Nevertheless, their intensities are different from each other. As seen in Figure 4.4.6.1, fluorescence intensity of electropolymerized PCz to be dissolved is more decreased than that of the copolymerized NCz in the presence of high ratio of AAm. Since the molecular motion of NCz is restricted when it is bound to a polymer chain, self quenching of the carbazole chromophore is reduced because of the separation by the comonomeric groups, or it might be specific interactions which also occur between the oxidized PCz films exicited state and diffused anionic groups of AAm as counterions such as doped PCz with perchlorate counterions, a similar phenomenon was described for poly(thiophene) by Hayashi et al. [131].

In order to understand the solvent effect, electropolymerized films were tried to be dissolved in water. Fluorescence also allows differentiation between acetonitrile and water. The behaviour of polymers obtained in water is quite different from in ACN media. Intensities of PCz and co-PCz are decreased, due to the insolubility in water which can be seen that Figure 4.4.6.2, there is a slight increase in the presence of AAm.

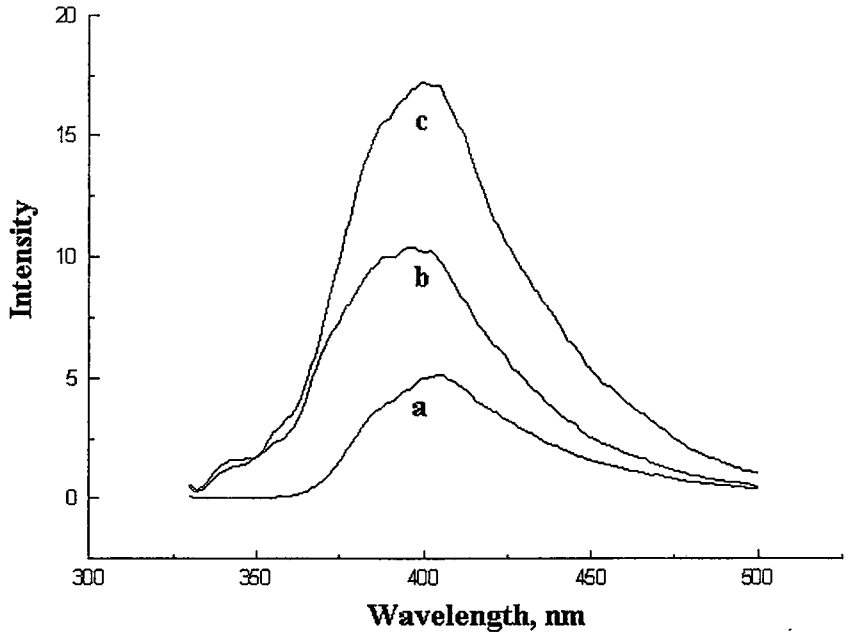

Figure 4.4.6.1 Fluorescence spectra of (a) a part of dissolved PCz in ACN, (b) and (c) AAm:NCz (n_{AAm}:n_{NCz}= 100, n_{AAm}:n_{NCz}=50).

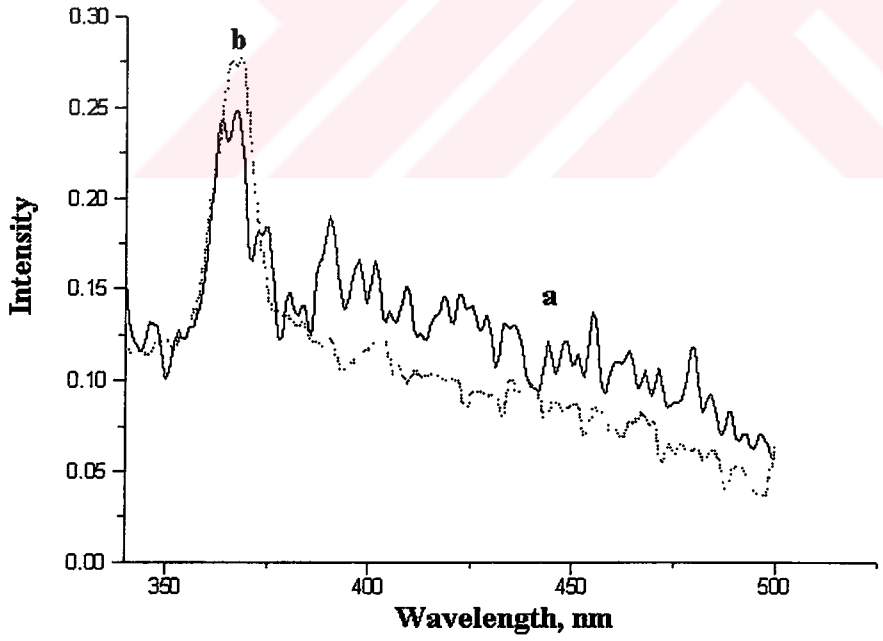

Figure 4.4.6.2 Fluorescence spectra of (a) dissolved PCz in H_20, (b) dissolved AAm:Cz (n_{AAm}:n_{NCz}=50) in H_20.

NCz monomer shows fluorescence behaviour as is known. In order to understand the unreacted monomer effect absorbed on the surface, and compare the fluorescence behaviour, after polymerization performed on the Pt surface, samples were washed with ACN to remove the monomer. They did not show significant behaviour. There is a slight blue-shift of the emission band which is located at about 400 nm for the unwashed samples (Figure 4.4.6.3).

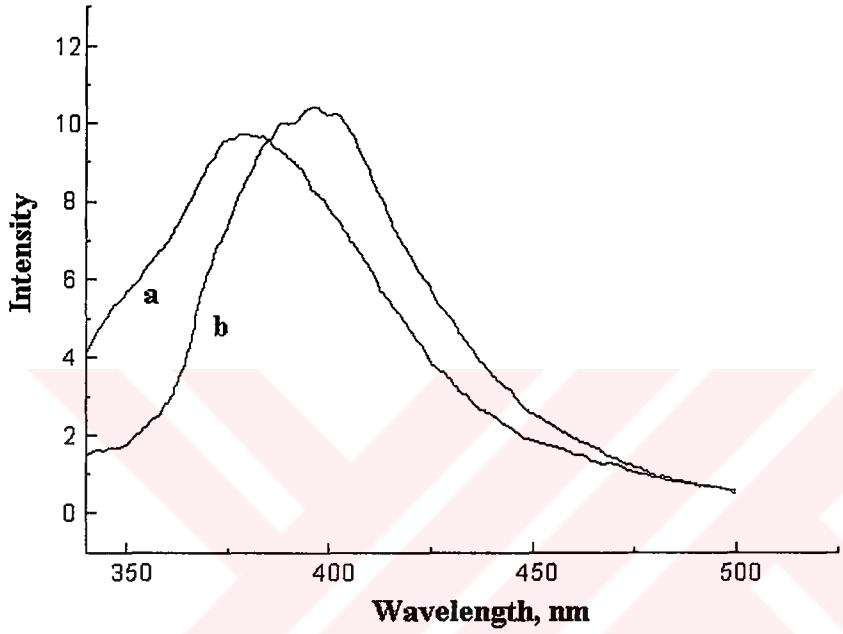

Figure 4.4.6.3 Fluorescence spectra of (a) washed PCz in ACN, (b) unwashed PCz in ACN.

4.4.7 Ellipsometric Studies

The electrochemical growth of the copolymers was followed using *in-situ* ellipsometry. Figure 4.4.7.1 shows the Δ-ψ signature recorded for the growth of the polymer using linear sweep voltammetry from a solution containing 50:1 AAm:NCz in ACN solution. The potential here was scanned from the open circuit potential of 0 V to 1.2 V at a sweep rate of 0.001 V s^{-1} and then held constant at the higher limit for the remaining period of the growth. In Figure 4.4.7.1 is the modelled fit for the growth based on the Drude equation is also included [132]. It can be seen from the model that the refractive index of the layer shows only a slight decrease over the ~1.45 μm overall thickness of the layer. This can be attributed to a less dense film being formed in the latter stages of growth and is entirely consistent with the three-

dimensional growth of the layer. The extinction coefficient, on the other hand, shows no significant trend with film thickness with the value recorded being in the range 0.01 to 0.02 over the whole of the thickness of layer. The Δ-ψ signature for the growth from a 20:1 AAm:NCz monomer mixture in ACN is shown in Figure 4.4.7.2 a. The Growth of the film here was more rapid and the ellipsometry signal quickly deteriorated, indicative of a diffuse surface, after a thickness of only 2303 Å. The refractive index for the film grown in this medium was slightly lower than that measured for the film grown in ACN alone but as before, there was virtually no change in the extinction coefficient. In Figure 4.4.7.2 b, growth from the mixed ACN:H_20 ($HClO_4$) solvent containing the same AAm:NCz ratio as in Figure 4.4.7.2 a, *.i.e.* 20:1 is shown. In the presence of the perchloric acid, the rate of polymerization is faster again and only 816 Å of the growth could be recorded before loss of the ellipsometry signal occurred due to surface roughness. A more rapid rate of growth would most likely be dominated by growth in three dimensions as opposed to growth in two dimensions, parallel to the surface. The former would thus lead to a much poorer optical. Table 4.4.7.1 shows the modelled data obtained for these samples as well as other data recorded at faster sweep rates and the use of AAm:NCz ratios of 10:1 and 1:1 (Appendix E.1-3). It would appear that the potential scan rate has no effect (at least at these low values employed) on the optical constants for the film, but decreasing the ratio of AAm:NCz leads to a larger value for *n* and an increasing roughness of the polymer surface.

The variation in the optical constants as a function of AAm:NCz ratio indicates a general increase in the value of the extinction coefficient *k* with increasing NCz content. This is to be expected from an examination of the UV-vis spectra of carbazole and of the carbazole copolymer with AAm since a broad peak centred at 800 nm can be observed in both spectra. This suggests that more carbazole is incorporated into the matrix as its monomer concentration increases. This should not be surprising since the whole polymerization process is initiated by the formation of the Cz cation radical through electrooxidation. Hence when the NCz monomer concentration is low, such as in the 50:1 mixture, the measured extinction coefficient is similarly low signifying that the $Cz^{+\bullet}$ initiates the polymerization of the AAm but that its rate of incorporation into the polymer matrix is low. Another aspect of the data present in the table, which warrants further

discussion is the almost constant n-value, measured for all the monomer ratios apart from the 1:1 mixture. In the latter, a much higher refraction index was obtained. The n = 1.58 value is in good agreement with those measured for polyaniline (n = 1.4-1.6) and polypyrrole (n=1.4-1.6) [133] films, the observed value depending on the medium used for growth as well as on the growth conditions themselves. It appears therefore that the determining factor in the magnitude of n is the electronic configuration of the –C-C- bonding along the polymer backbone. However, the increase in *n* from 1.58 ±0.01 to 1.62 for the 1:1 mixture signifies a more compact film structure with less solvent incorporation in the polymer matrix in the latter.

Table 4.4.7.1 N_f, K_f, D_f, Values of Different Ratio of Copolymers obtaining in ACN using $1x10^{-1}$ mol dm^{-3} TEAP as a supporting electrolyte and [a] $HClO_4$ medium ACN:H_2O (50%:50%) ($1x10^{-1}$ mol dm^{-3} $HClO_4$).

Sample AAm:NCz	**Scan Rate V s^{-1} x 10^{-3}**	**N_f**	**K_f**	**D_f, A°**
50:1	2	1.59	0.015	4780
10:1	2	1.59	0.056	2335
10:1	1	1.59	0.033	2613
1:1	1	1.62	0.055	2038
20:1	2	1.57	0.052	2375
20:1	1	1.57	0.064	2303
20:1[a]	1	1.58	0.074	816

The modelled data could not be obtained for NECz and incorporation with AAm inside such as carbazole in the presence of AAm as was seen in the *in-situ* section, the rate of polymer was high in the presence of AAm in comparison to NCz. And no proper growth could be recorded due to surface roughness.

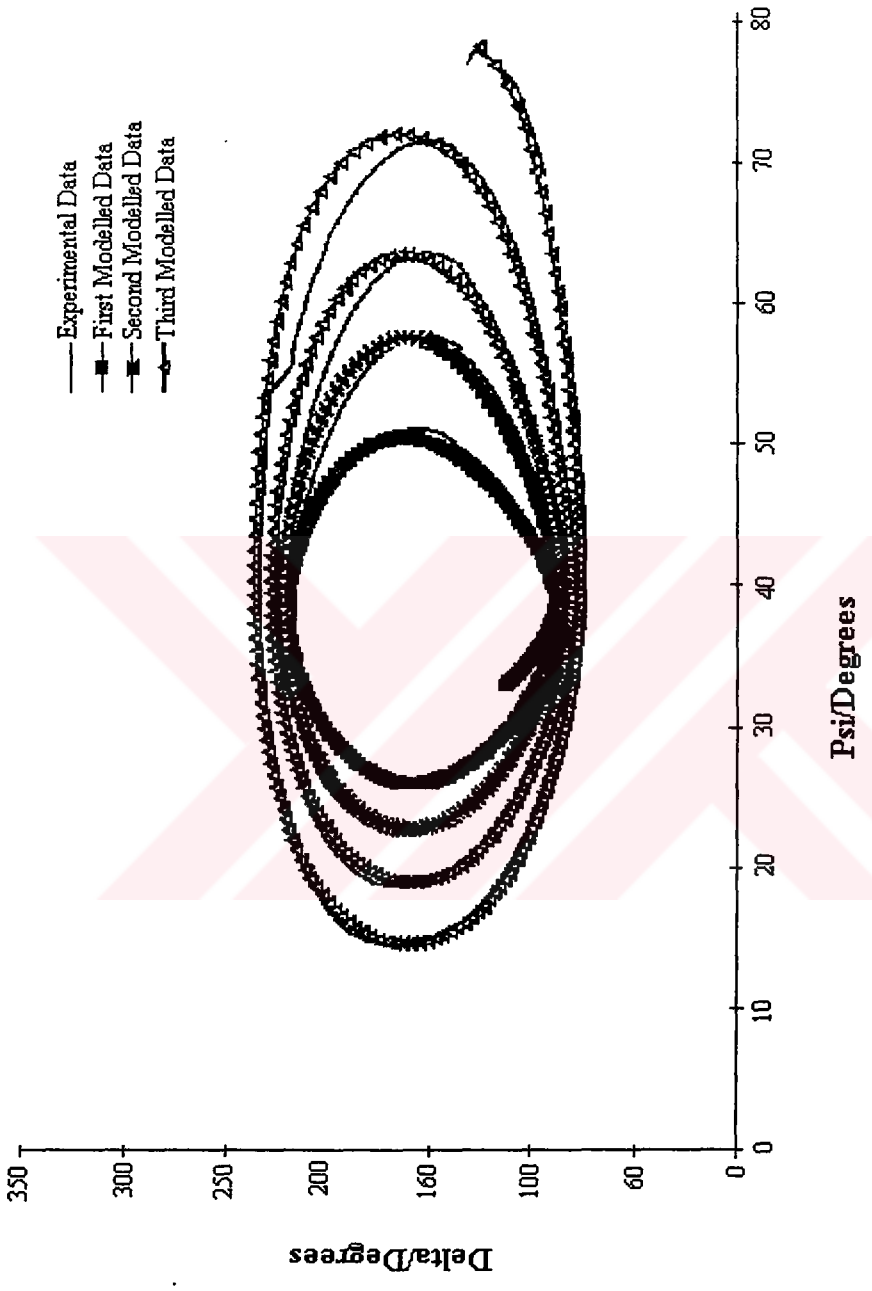

Figure 4.4.7.1 Ellipsometric Δ-ψ curves recorded during the growth of the copolymer films from a solution of 50:1 AAm:NCz in ACN using $1x10^{-1}$ mol dm^{-3} TEAP as a supporting electrolyte. Scan Rate: 0.002 V s^{-1}.

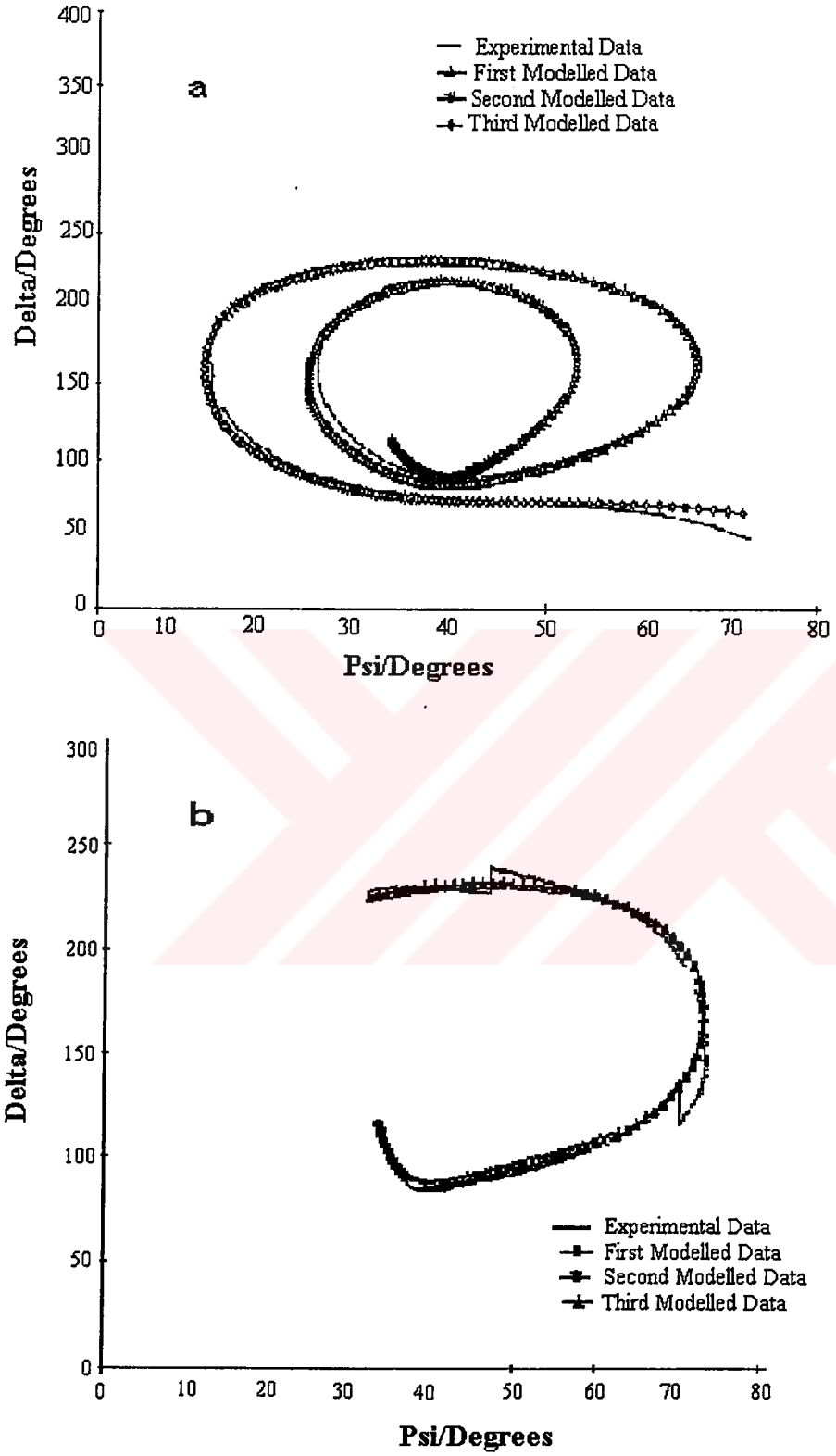

Figure 4.4.7.2 Ellipsometric Δ-ψ curves recorded during the growth of the copolymer films from a) 20:1 AAm:NCz in ACN using $1x10^{-1}$ mol dm^{-3} supporting electrolyte. Scan Rate: 0.002 V s^{-1}, b) 20:1 AAm:NCz in ACN:$HClO_4$. Scan Rate: 0.001 V s^{-1}.

4.4.8 Thermal Analysis Studies

Thermogravimetric Analysis (TGA) was performed on a number of the copolymer samples prepared by the electrochemical oxidation method. The technique was used in order to establish the thermal properties of the material as well as to assess the amount of solvent incorporated within the film. A typical TGA curve obtained on heating the sample at 10 K min^{-1} from 25 °C to 400 °C in an inert He atmosphere is shown in Figure 4.4.8.1.

The TGA data recorded for the AAm:NCz co-polymers, were on the whole, in good agreement with that presented by Saraswathi and co-workers [135] for the decomposition of polycarbazole in N_2 and air. Over the temperature range 25°C to 400°C, these authors also reported a weight loss of *ca.* 25%. The relative weight loss generally depended on the composition of the polymer analysed and the results obtained are tabulated in Table 4.4.8.1. The table also includes data showing the effect of the positive potential limit employed for the growth. This parameter is important since it determines not only the rate of polymer formation but also, as discussed above, the degree of over-oxidation that occurs during polymerization and so leading to loss of conjugation. The weight loss over the temperature region up to 400°C is divided into two events, that between 100-280°C and the other above it. The same samples were also analysed for their thermal response by differential scanning calorimetry (DSC) over the same temperature range under an inert N_2 atmosphere. The enthalpies recorded for the major enthalpy event as well as the peak temperatures are shown in Table 4.4.8.1. The TGA data indicate that in the first thermal region (100-280 °C), there is no significant difference in the weight loss experienced by the polymer containing AAm and that which does not. This would therefore imply that any weight loss in this region must be linked to the carbazole moiety and/or solvent loss from the polymer. In the next thermal region (280-400°C), the weight loss from the polymers, in which carbazole was at least the equal if not the major component in the forming solution, was a factor of 2 greater than those found from the higher AAm:NCz ratios of copolymers. This again suggests that weight loss in this temperature range was due to the carbazole moieties within the film. It is noticeable nevertheless that an enhanced thermal stability was found as more AAm units were incorporated into the matrix.

It would be tempting to attribute the weight losses to thermal degradation. Thus, in this scenario, the first event could be attributed to the loss of carbazole moieties (dimers, small oligomers) entrapped within the polymer matrix, and the second event to further loss of material possibly from the breakdown of the polymer matrix. However, the DSC data over the same temperature range (100-400°C), shown in Figure 4.4.8.2, indicate only exothermic processes, *i.e.* a stabilisation process rather than the break down of the polymer. The broad exotherms between 100 °C and 400 °C show evidence of at least three individual processes.

The thermal analysis data would lead us to conclude therefore that the weight loss observed in the TGA analysis is linked to the stabilisation of the polymer matrix through cross-linking, with the observed weight loss due to the leaving group. It is not possible at this stage to assign these individually but they may correspond to different leaving groups during the cross-linking process and hence to different levels of stability attained by the resulting polymer. This interpretation of the weight loss in terms of an increased stability is in marked contrast to the explanation put forward by Saraswathi and co-workers [134]. They attributed weight loss over the temperature range 70 °C to 350 °C to loss of the perchlorate dopant in the film whereas above 450 °C, the decomposition of the PCz backbone occurred. It is evident however from the DSC data of Figure 4.4.8.2 that only exothermic processes are found over this temperature range and this point to a stabilisation (through crosslinking) rather than the breakdown of the polymer, which would be strongly endothermic. From Table 4.4.8.1, it is evident that there is an increase in the enthalpy associated with the crosslinking with increasing carbazole concentration suggesting that this component plays a dominant role in that process. Cation radicals react by deprotonation coupling to form the 9,9' and 3.3' bicarbazyls between the carbazole units in ACN solution. According to Maitland and Tucker [135], the reaction medium affects the isomer distribution drastically. In the presence of sulfuric acid, only the 3,3'- dicarbazyl is obtained whereas in the absence of sulfuric acid the 9,9'- carbazyl is also formed [38]. The 9,9'- dimer was only formed very early during electrolyses, before the proton concentration build up. The addition of H_2SO_4 suppressed the formation of the 9,9'- dimer altogether, whereas the addition of a base such as a proton scavenger (pyridine) increased its yield significantly. We note that for PCz films grown in perchloric acid, the enthalpy associated with

crosslinking is much reduced since the protonation of the amine group of the carbazole moiety prevents coupling at this position.

Table 4.4.8.1 Thermal properties of the AAm:NCz Copolymers prepared electrochemically at 1.2 V in ACN using $1x10^{-1}$ mol dm^{-3} TEAP as a supporting electrolyte and [a] ACN:H_2O (50%:50%) ($1x10^{-1}$ mol dm^{-3} $HClO_4$). Scan Rate: 0.05 V s^{-1}.

Monomer ratio	**Weight % loss**		**Enthalpy**	**Exothermic max.**
(AAm:NCz)	**100-280°C**	**280-400°C**	**(J g^{-1})**	**(°C)**
100:1	10	7	548	249
80:1	15	7	536	265
50:1	17	8	622	307
20:1	8	7	1539	276
20:1[a]	14	6	1621	275
10:1	10	6	1249	309
1:1	11	10	1501	211
1:10	13	19	7200	194
NCz	13	14	1418	317
NCz[a]	7	10	842	215

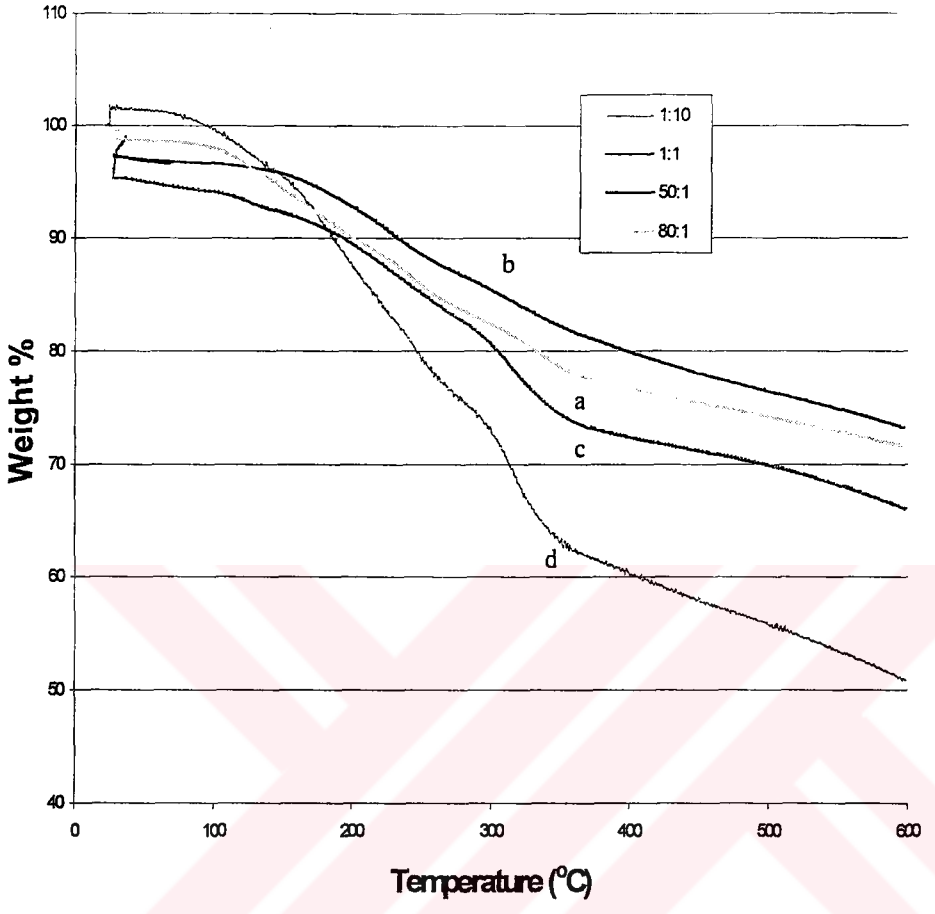

Figure 4.4.8.1 TGA curves for different ratios of AAm:NCz copolymers grown at 1.2 V in ACN using $1x10^{-1}$ mol dm^{-3} TEAP as a supporting electrolyte. *a)* 80:1, *b)* 50:1, *c)* 1:1, *d)* 1:10. Scan Rate: 0.05 V s^{-1}

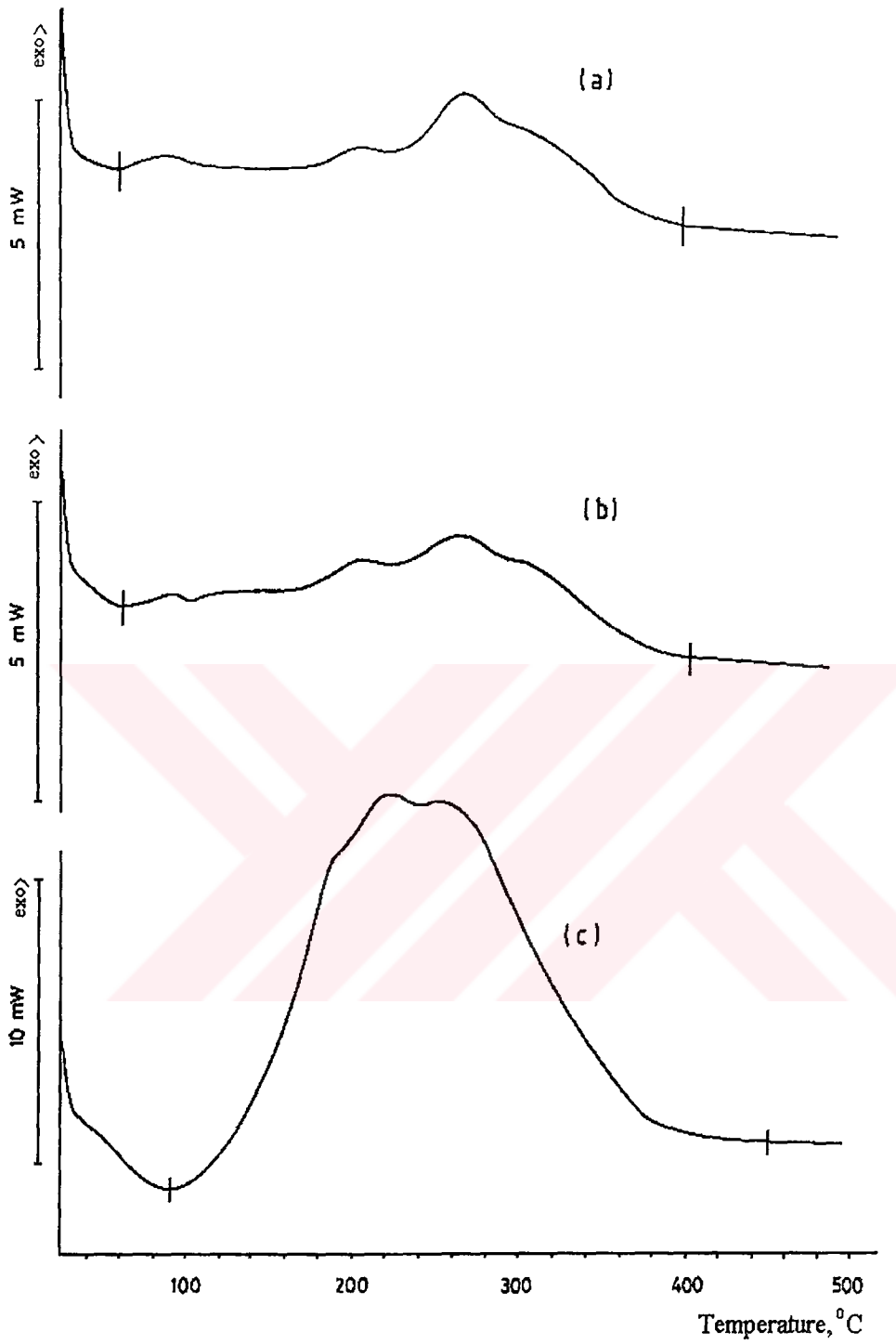

Figure 4.4.8.2 The DSC curves for different ratios of AAm-NCz copolymers grown at 1.2 V in ACN using $1x10^{-1}$ mol dm^{-3} TEAP as a supporting electrolyte, *a)* 80:1, *b)* 50:1, *c)* 1:10. Scan Rate of 0.05 V s^{-1}.

4.4.9 Morphology of Polymers

In order to understand the surface appearance of the copolymer film coated on platinum, Scanning Electron Microscopy (SEM) was used. The SEMs for the electrochemically oxidised copolymer and polycarbazole film in ACN/H_20 (0.1 mol dm^{-3} $HClO_4$) are shown in Figure 4.4.9.1 and in ACN are shown in Figure 4.4.9.2. For copolymer carbon paste was used as a substrate for the analyses. Polycarbazole has been known as a cauliflower structure [136]. The SEM microphographs of electrochemically prepared polymers in ACN and in protic acid show structurally different morphology (Figure 4.4.9.1 and 4.4.9.2 a). At the higher magnification clusters of globules with void space in between can be seen clearly. Figure 4.4.9.1 and 4.4.9.2 b, show the incorporation of AAm into the copolymer structure. The SEM photographs are also shown for electrochemically synthsized ECz and AAm:NECz (20:1) synthsized in Figure 4.4.9.3 a and b). The PCz and PECz surface crystallinity obtained in AAm media were completely different compared to each other.

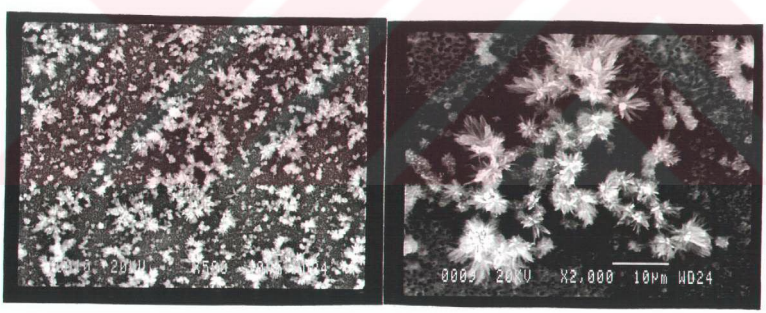

a b

Figure 4.4.9.1 Scanning electron micrographs of AAm/NCz copolymer (n_{AAm}/n_{NCz}=50) obtained in ACN/H_20 ($1x10^{-1}$ mol dm^{-3} $HClO_4$) at different magnifications, a) X500, b) X2000 magnification .

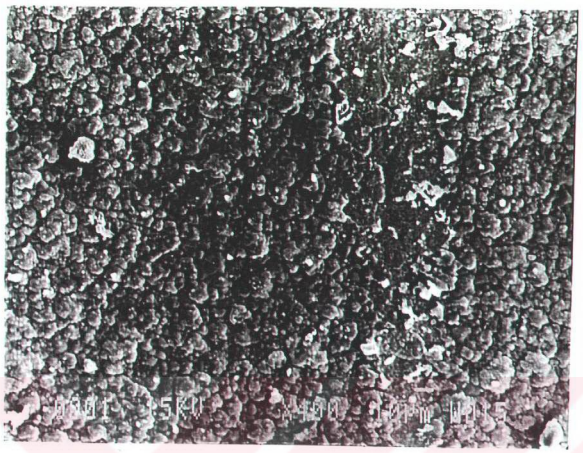

a

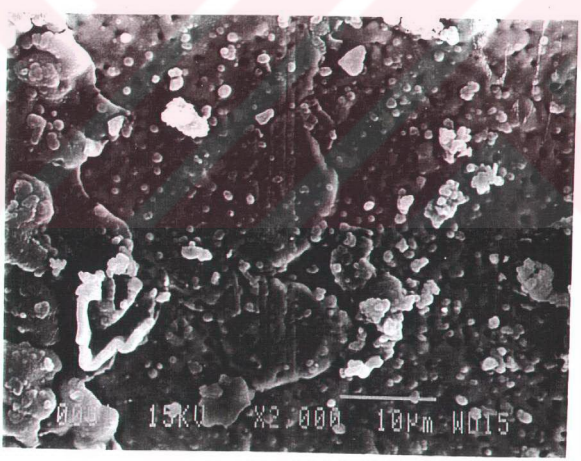

b

Figure 4.4.9.2 Scanning electron micrographs of AAm/NCz copolymer (n_{AAm}/n_{NCz}=50) obtained in ACN ($1x10^{-1}$mol dm^{-3} TEAP) at different magnifications, a) X400, b) X2000 magnification .

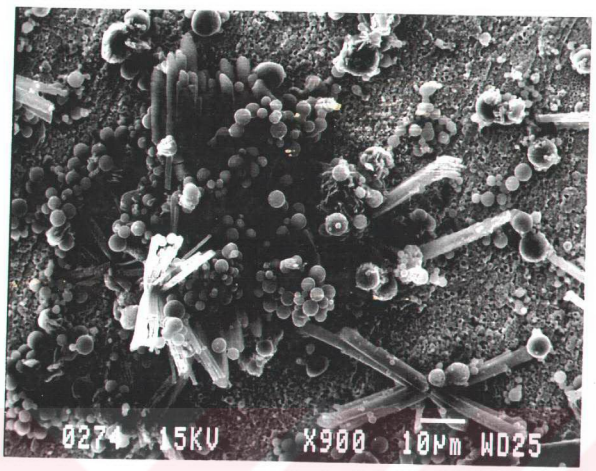

a

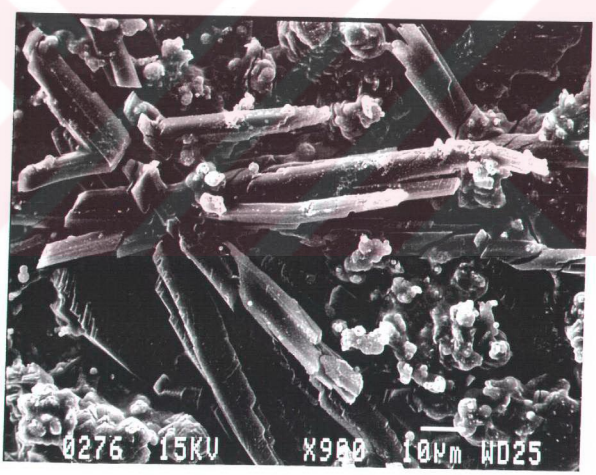

b

Figure 4.4.9.3 Scanning electron micrographs of a) $1x10^{-2}$ mol dm^{-3} NECz b) AAm/NECz polymer (n_{AAm}/n_{NECz}=50) electrochemically obtained in ACN/H_20 ($1x10^{-1}$ mol dm^{-3} $HClO_4$) at X900 magnification.

4.4.10 Conductivity Measurements

The conductivities of copolymers and composites are given in Table 4.4.10.1. The electrocopolymerization of carbazole derivatives with AAm can cause some decreases. In the presence of PAAm in a composite structure also has a negative effect on the conductivites of the composite. The decrease in conductivity in the case of copolymer and composite suggests a reaction between NCz an AAm. When $n_{AA}/n_{NCz}=1$ conductivity of the copolymer is almost the same with the homopolymer of PCz, because in this case copolymer formation is less possible due to kinetic reasoning. In the $HClO_4$ media, conductivity was increased as the addition of the $HClO_4$ suppressed the formation of the 9,9'-carbazyl, only the 3,3'-dicarbazyl is obtained.

Table 4.4.10.1 Conductivity of Polymers

Polymer n_{AAm} / n_{NCz}	**Medium**	**Conductivity** (S cm^{-1})
Composite	ACN	$1.27x10^{-6}$
50	ACN	$1.84x10^{-6}$
1	ACN	$3.6x10^{-3}$
1	ACN/H_2O($HClO_4$)	$8.4x10^{-3}$
Polycarbazole	ACN	$1.3x10^{-3}$
Polycarbazole	ACN/H_2O($HClO_4$)	$1.3.10^{-2}$

4.4.11 Yield of Polymers

An increase in the applied potential and the AAm:NCz mole ratio results in an increase in the copolymerization yield (Table 4.4.11.1). In the FT-IR spectra of copolymers, the increasing intensity of the band at 1650 cm^{-1} is due to -C=O group of AAm supports the idea that the increase in yield is due to incorporation of AAm into the structure.

With the addition of $2.8x10^{-4}$ mol dm^{-3} water, only a minor alteration in yield can be detected at 1.2 V applied potential; the highest yield can be obtained at

n_{AAm}/n_{NCz}=400 mole ratio (Table 4.4.11.1) in the case of higher applied potential. The observation of the highest intensity of the -C=0 band at 1650 cm^{-1} at 2.0 V applied potential in the presence of water also supports the idea above.

Table 4.4.11.1 Effects of AAm:NCz mole ratio, applied potential and water on the copolymerization yield. Supporting Electrolyte: $1x10^{-1}$ mol dm^{-3} TEAP, Temperature: 20 °C, * $[H_2O]= 2.8x10^{-4}$ mol dm^{-3}

n_{AAm}/n_{Cz}	Reaction Medium	Applied Potential (V)	Yield %
100	ACN	1.2	3.0
400	ACN	1.2	4.2
100	ACN	2.0	Trace
400	ACN	2.0	5.1
100	ACN:H_2O*	1.2	6.0
400	ACN:H_2O*	1.2	5.0
100	ACN:H_2O*	2.0	1.7
400	ACN:H_2O*	2.0	8.6

4.4.12 Elemental Analysis Measurements

Elemental analysis of PCz and NCz polymerised in AAm solution was carried out and given in Table 4.4.12.1. These results allow us to determine the composition of NCz polymerized in the presence of AAm. The calculated structure for $C_{10.87}H_{6.90}N_{1.0}$ fits the assumption of 20 Cz units combined with 1 AAm unit. And on the other hand NCz polymerised in the presence of AAm in ACN/H_20 (0.1 mol dm^{-3} $HClO_4$), calculated structure for $C_{15.56}H_{7.68}N_1$, and fits the assumption of 15 NCz units combined with 1 AAm unit.

Table 4.4.12.1 Elemental analysis results of PCz and PCz formed in the presence of AAm.

PolymerRatios n_{AAm}/n_{NCz}	Medium	Molecular Structure
1/15	ACN:H_2O ($HClO_4$)	$C_{183}H_{110}N_{16}O$
1/20	ACN	$C_{243}H_{154}N_{22}O$
Carbazole	ACN	$C_{12}H_7N$

4.5 Application of Electropolymerized N-Carbazole Film in Acrylamide Medium as Electrode

To understand the redox properties of the film, a current-voltage curve is recorded. The redox behaviour of the ferrocene on the electropolymer can be clearly seen in figure 4.5.1 despite the fact that a 100-fold change in the current was found compared to that of a bare Pt electrode (Figure 4.5.2). The peak separation changes from 0.06 V for bare Pt to 0.07 V for the film, obtained by electrolytic method, signifying a decrease in the kinetics of electron transfer on the polymer modified Pt surface. The increase in the anodic current beyond 1.1 V corresponds to the oxidation of the electropolymer itself. The large difference in the current between bare Pt and the film-covered Pt surface could at first suggest that the electrochemistry was still only happening on the exposed parts of the Pt surface, (*i.e.* those not covered by the polymer film) to which the electroactive species could reach through pinholes within the polymer film. In such instance however, the rate of mass transport of the ferrocene through the pores would be severely impeded and the clear diffusion peaks observed in figure 4.5.1 would not have been detected. A more likely explanation therefore for the reduction in the current on the polymer surface must be the poor conducting nature of the electropolymer in the potential region where the redox properties of the ferrocene are found.

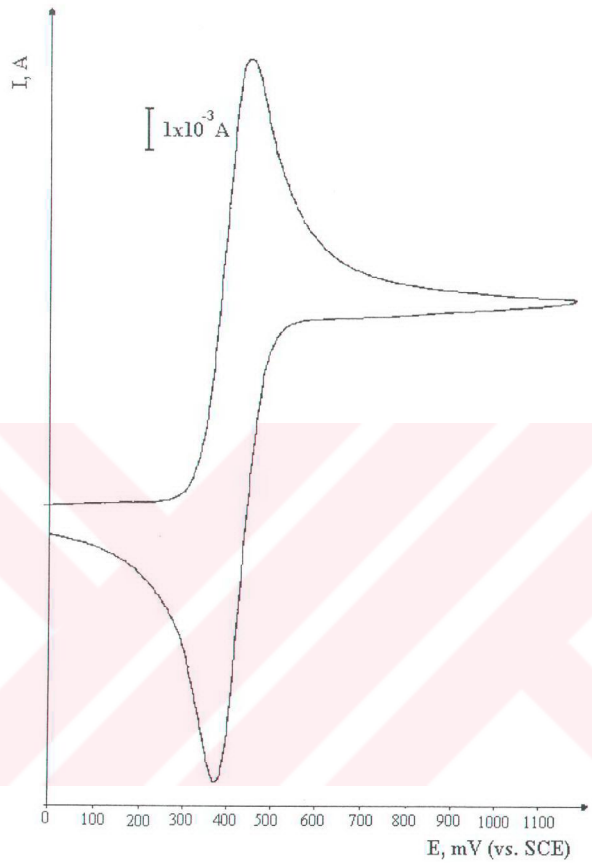

Figure 4.5.1 The electrochemical behaviour of Pt in $4x10^{-3}$ mol dm^{-3} Ferrocene in acetonitrile solution. Scan Rate 0.05 V s^{-1}, Supporting Electrolyte, 0.1 mol dm^{-3} TEAP.

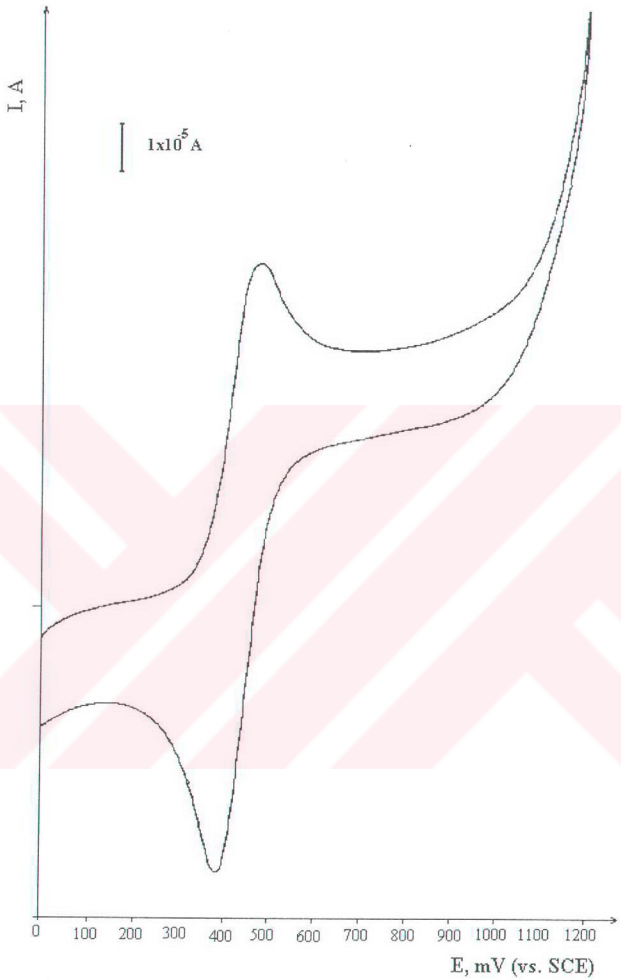

Figure 4.5.2 The electrochemical behaviour of AAm:NCz electrode in $4x10^{-3}$ mol dm^{-3} Ferrocene in ACN solution. Scan Rate: 0.05 V s^{-1}; Supporting Electrolyte, $1x10^{-1}$ mol dm^{-3} TEAP.

As the cyclic voltammetric measurements show the response to dopamine at platinum, NCz-AAm copolymer electrode in the phosphate buffer of pH=7.35 in the presence of $1.8x10^{-2}$ mol dm^{-3} dopamine were also prepared and tested (Figure 4.5.3-A and B). In the case of Pt electrode, an irreversible behaviour was observed (Figure 4.5.3-A) as given in literature [48]. According to the voltammetric measurements shown in Figure 4.5.3-B, polymer obtained in the presence of AAm electrode, redox process (E_a= 0.15 V, E_c= 0.25V) can be distinguished from a solution of dopamine in the buffer and the reversibility of copolymer electrode (Figure 4.5.3-B curve a) showed better behaviour than the naked Pt (Figure 4.5.3-A).

The stability of the polymer electrode was tested by leaving the electrode in vacuum during for three days, and CV of electrode was taken at different time intervals. During this time, the intensity of peak currents was decreased and the anodic shift in peak potential occurred. After three days the electrode became almost stable and no shift was observed in the peak potential. The CV of electrode after three days leaving in vacuum is given in Figure 4.5.3-B curve b.

The copolymer electrode seems to respond very significantly to dopamine and was stable after three days (Figure 4.5.3-B).

The electrochemical oxidation of dopamine on the prepared polymer electrode was also examined as a function of sweep rate 0.05-0.2 V s^{-1}. As expected, the intensity of peak current increases with increasing sweep rate. It is known that for the polycarbazole electrode, peak separation is quasi-reversible at slow sweep rates [26]. In our case even at slower rates, it was possible to obtain reversible peak response, which exhibits the advantage of the polymer electrode synthesized in this way.

These results suggest that the electrode respond in a reproducible manner and that electrode is sensitive and has reversible behaviour.

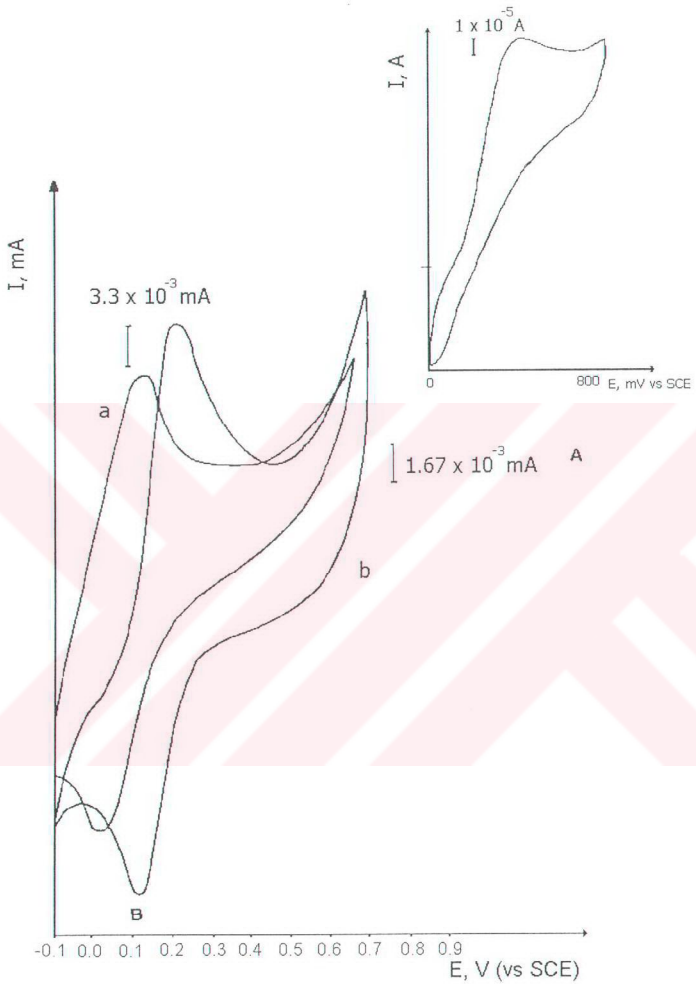

Figure 4.5.3 Cyclic Voltammograms, obtained for $1.8x10^{-2}$ mol dm^{-3} Dopamine in buffer solution (pH= 7.4); **(A)** on the Pt electrode, **(B)** AAm:NCz copolymer (n_{AAm}/n_{NCz}=50) electrode, a) newly prepared electrode, b) after three days. Scan Rate: 0.05 V s^{-1}.

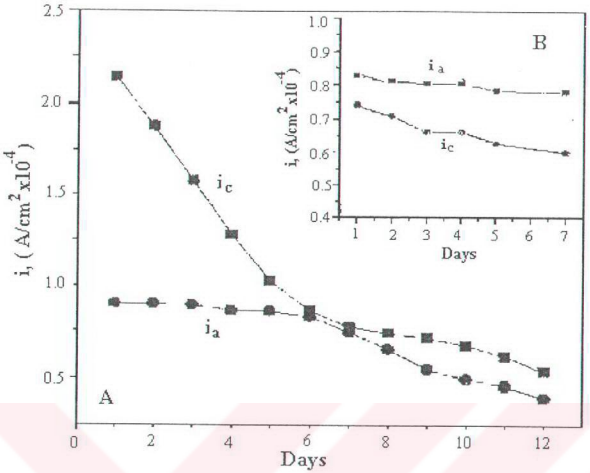

Figure 4.5.4 Changes in anodic (I_a) and cathodic (I_c) peak current response of copolymer electrode to Ferrocene left, (A) in ACN for 12 days; (B) in 1 mol dm^{-3} H_2SO_4 medium for 7 days. Supporting Electrolyte: $1x10^{-1}$ mol dm^{-3} TEAP, [Ferrocene]= $4x10^{-3}$ mol dm^{-3}, Scan Rate: 0.05 V s^{-1}.

The reproducibility of the current response of the AAm:NCz electrode for sensing ferrocene was assessed by recording the cyclic voltammetric responses everyday for a period of 15 days; the electrode was left in ACN and 1 mol dm^{-3} H_2SO_4 after each days. Figure 4.5.4-A and B show the plot of current densities response as a function of time. When the electrode is left in ACN at the beginning, although, the cathodic current shows a decreasing trend, they become almost constant after four days (Figure 4.5.4-A). Later, there is less change in anodic current densities. In addition to these experiments, the electrode was left in 1 mol dm^{-3} H_2SO_4 and the anodic and cathodic peak current densities of copolymer electrode in the presence of ferrocene were tested by recorded (Figure 4.5.4-B). The current densities almost become constant at the end the 7 days, indicating that the stability of the electrode is better under these conditions.

To understand the redox properties of the NECz film, a current voltage curve was also recorded. The anodic and the cathodic potential were slightly shifted to the cathodic potential (E_a= 0.455 V, E_c= 0.325 V) in the case of AAm containing ECz electrode in comparison to naked Pt (E_a= 0.455 V, E_c=0.375 V). The co-polymer film also represents reversible behaviour in the presence of ferrocene (Figure 4.5.5).

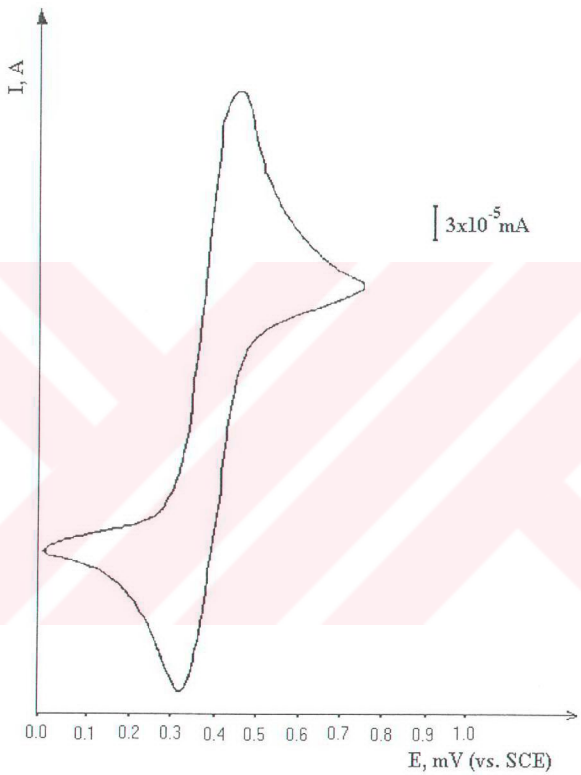

Figure 4.5.5 The electrochemical behaviour of AAm/NECz electrode in $4x10^{-3}$ mol dm^{-3} in acetonitrile using $1x10^{-1}$ mol dm^{-3} TEAP as a supporting electrolyte. Scan Rate= 0.05 V s^{-1},

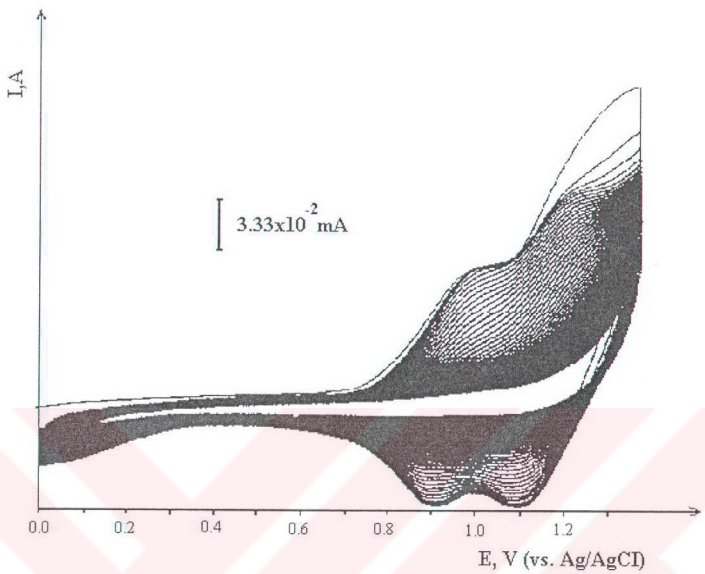

Figure 4.5.6 Cyclic Voltammogram of copolymer prepared by casting from DMF+THF+H_2O solution on Pt in ACN using $1x10^{-1}$ mol dm^{-3} TEAP as a supporting electrolyte. Counter and Reference Electrode: Pt and Ag/AgCI, Scan Rate: 0.05 Vs^{-1}.

The response of PVCz/AAm electrodes, which were synthesized by using an AIBN initiator to dopamine and ferrocene was prepared by casting from DMF+THF+H_2O (% 45+ % 45+ % 10) solution on Pt substrate, was also studied. To remove the solvent, they were heated at 383°K in vacuum of 10^{-3} Pa for 5 hours. The film-coated electrode was immersed in ACN containing 0.1 mol dm^{-3} TEAP, the white coloured polymer soluble in the solvent. The film electrode was used as the working electrode (anode) and subsequent cycling was performed in the range of 0-1.4 V. The white polymer was gradually converted into a conducting green PVCz film. The conversion was monitored by CV measurements (Figure 4.5.6). In the second cycle (Figure 4.5.7), oxidation of carbazole ring occurred at 1 V and the corresponding cathodic curve was at 0.85 V. Upon multiple cycling, the current of these peaks decreased down to the baseline (Figure 4.5.6).

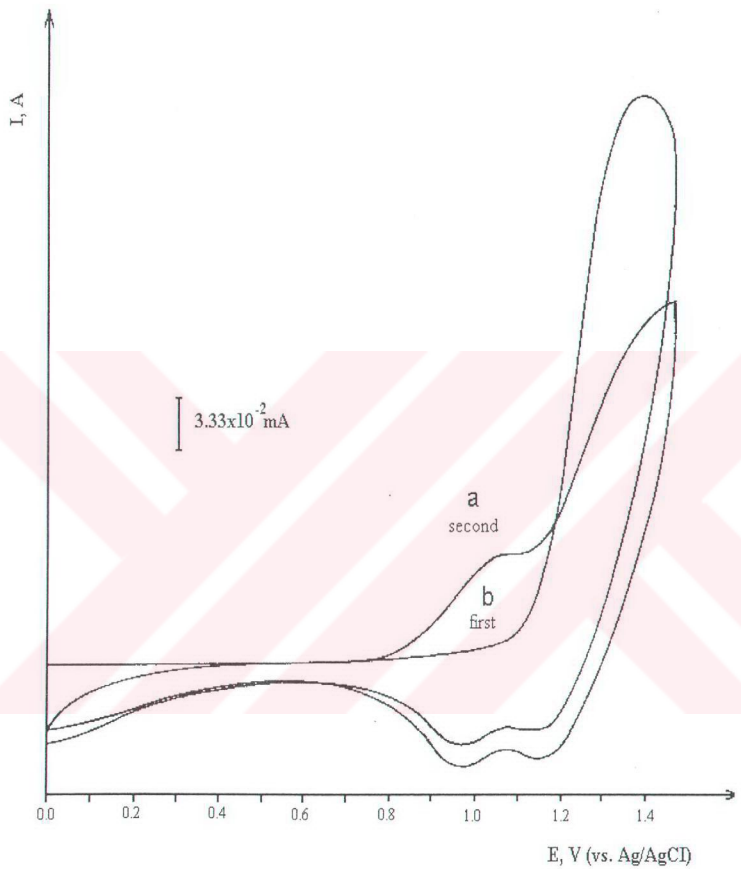

Figure 4.5.7 Cyclic Voltammogram of copolymer prepared by casting from DMF+THF+H_2O solution on Pt in ACN using $1x10^{-1}$ mol dm^{-3} $1x10^{-1}$ mol dm^{-3} TEAP, a) in the second cycle, b) in the first cycle. Counter and Reference Electrode: Pt, Ag/AgCI, Scan Rate: 0.05 V s^{-1}.

As the cyclic voltammetric measurements for the AAm:NCz copolymer electrode shows a reversible response to dopamine in the phosphate buffer of pH=7, the PVCz copolymer electrode were also tested for dopamine. Results suggest that depending on conditions (i.e scan rates, thickness of film) the electrode response may be reversible or quasi-reversible behaviour. At slow scan rates copolymer electrodes seem more reversible than naked Pt (Figure 4.5.8).

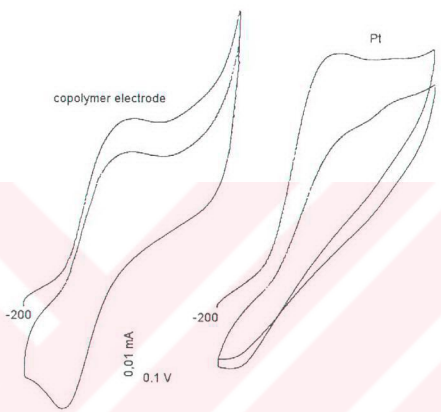

Figure 4.5.8. Cyclic voltammograms of copolymer electrode (area= 2 cm^2) and naked Pt (area= 0.2 cm^2) in $1.8x10^{-3}$ mol dm^{-3} Dopamine containing buffer solution (pH =7). Scan Rate 0.1 V s^{-1}, (The first and second cycle in anodic direction).

The corrosion inhibition of chemically and electrochemically coated polyvinylcarbazole electrodes was studied previously [137] and it was found that this polymer can display promising protective coating showing photoactivity. In this respect, corrosion inhibition of copolymer coating was investigated for stainless steel electrode. In accordance with the corrosion inhibition measurements, copolymer coating can inhibit the corrosion of stainless steel up to 64 %.

5. MECHANISM AND CONCLUSIONS

-Physical properties of the resulting polymers formed from both acrylamide and carbazole derivatives were improved and to investigate the mechanism of such reactions were tried to be enlightened.

-NVCz with AAm copolymers were polymerised in DMF and DMF/water mixtures by using Ce (IV)-OA redox pair or AIBN by electrochemically and chemically, respectively. N-Vinylcarbazole is one of the speciality material of considerable academic and industrial interest because of its unusual electrical and photoelectrical thermal properties. As expected, the resulting polymers obtained under these conditions exhibited good properties, except very low yield polymers were found in the case of when Ce (IV)-OA redox pair was used. The solvent effect on the reaction mechanism was investigated, nucleophilic solvents such as H_2O can attack the cationic site of the produced radical cations or dications during oxidation leading to degradation of the polymer. In DMF/water mixture, polymerization of NVCz in the presence of AAm caused a slightly high yield of polymer compared to the polymer obtained in DMF media itself due to the change of reaction conditions i. e. polarity, charge delocalisation and reaction of DMF to the dimethylamine and to the formic acid in the presence of water (Scheme 1).

-Polymerization of NCz and NECz was carried out in the presence of acrylamide in ACN and ACN:H_2O ($HClO_4$) media electrochemically not only to improve polycarbazoles' properties but also to give better properties to the acrylamide polymers. The oxidation of carbazole in protic acid medium has been shown to provide an easy and straightforward route for synthesizing films bound to an inert electrode substrate. The presence of water normally deactivates the polymerization. Polymer passivation can be accepted taking into account water-acetonitrile interactions. Both solvents interact forming hydrogen bonds and giving an intercomponent complex (Scheme 2). Passivation is explained in terms of a direct water discharge by reaction of the electrogenerated oxygen radicals with polarons on

the polymer in ACN comparison to the DMF:Water solution mixture. This comparison can be explained with the average bond energy of C≡N of acetonitrile. C≡N has a higher average bond energy (210 kcal mol^{-1}) than C-N (70 kcal mol^{-1}) [138]. While ACN and water interact forming hydrogen bonds and giving an intercomponent complex, DMF does not react with water but decomposes to dimethylamine and formic acid which were incorparated to the polymer matrix (Scheme 1). In the presence of protic acid in ACN/water mixture, protonated carbazole could easily transfer an electron to the electrode to form the cation radical, which propagates the polymerization. This mechanism is able to explain the increase in polymerization rate with the acidification of the aqueous electrolytic solution.

The polarity of solvent and/or solvent mixture (i.e. H_2O, ACN:H_20) should have an effect on the cationic site of the carbazole ring which might result in polymer passivation by preventing radical cation coupling (Scheme 2).

On the other hand, the solvent mixture has some effect on the cationic site of NCz ring and might favor radical formation which results more free radical character reactions, and that will allow AAm copolymerization on the ring of carbazole a certain extent, in addition to crosslinking of AAm between NCz chains and doping effect of AAm itself on the cationic site (although it is less possible in the presence of higly charged inorganic dopants). And in addition to these, in the case of vinylcarbazole there is another possibility which is namely polymerization of AAm through the vinyl group which could be followed by crosslinking of the AAm onto the aromatic sites of the benzene ring of carbazole, in addition to N-H group.

As suggested in literature [139], during polymerization in DMF/water mixture cause a decomposition of DMF to formic acid (FA) and dimethylamine (DMA) . DMA may also produce radical as to DMF does. Because in the presence of water integral areas of $-CH_3$ protons is higher in accordance with DMF.

I: AIBN

$I \longrightarrow I^{\bullet}$

$R^{\bullet}$: $I^{\bullet}$, $DMF^{\bullet}$, $DMA^{\bullet}$

$I^{\bullet} + DMF \longrightarrow DMF^{\bullet}$

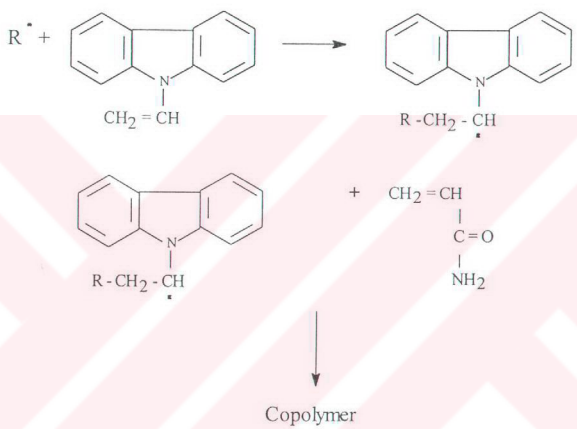

SCHEME 1

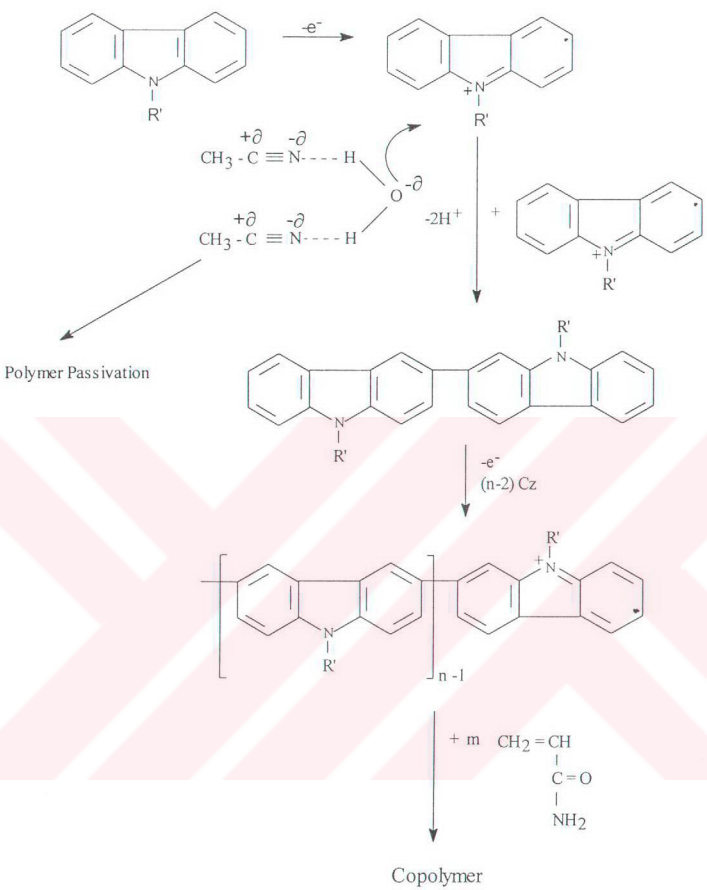

SCHEME 2

-Optical properties of electrochemical polymerization product of NCz in the presence of AAm were investigated, by determining absorption coefficient, refractive index, thicknesses by Ellipsometry. Since the whole polymerization process is initiated by the formation of the Cz cation radical through electrooxidation ellipsometric results suggest that more carbazole is incorparated into the matrix as its monomer concentration increases. Beside that, these measurements revealed that

incorparation of acrylamide to the structure caused a slow down of carbazole polymerization.

-Thermal analysis studies over the temperature range 25-400 °C indicated that the weight loss observed in the TGA analysis is linked to the stabilization of the polymer matrix through crosslinking, with the observed weight loss due to the leaving group, and they may correspond to different leaving groups during the cross-linking process, and hence to different levels of stability attained by the resulting polymer. This stabilty increases with incorparated AAm units within the polymer matrix (Figure 5.1). Even though AAm has a low degradation temperature, percentage weight loss of copolymers are 5 % even at 400 °C. It is also evident that there is an increase in the enthalpy associated with the crosslinking with increasing carbazole concentration, suggesting that this component plays a dominant role in that process (Figure 5.2). At high H^+ concentration, less possibility of crosslinking through N (9-9 coupling) eases the conjugated homopolymerization of carbazole and copolymers of AAm:NCz which results in decrease in enthalpy.

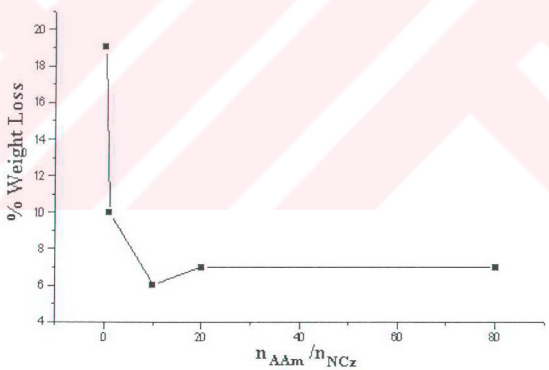

Figure 5.1 Weight losses obtained by TGA between 280- 400 °C temperatures for different ratios of AAm/NCz copolymers.

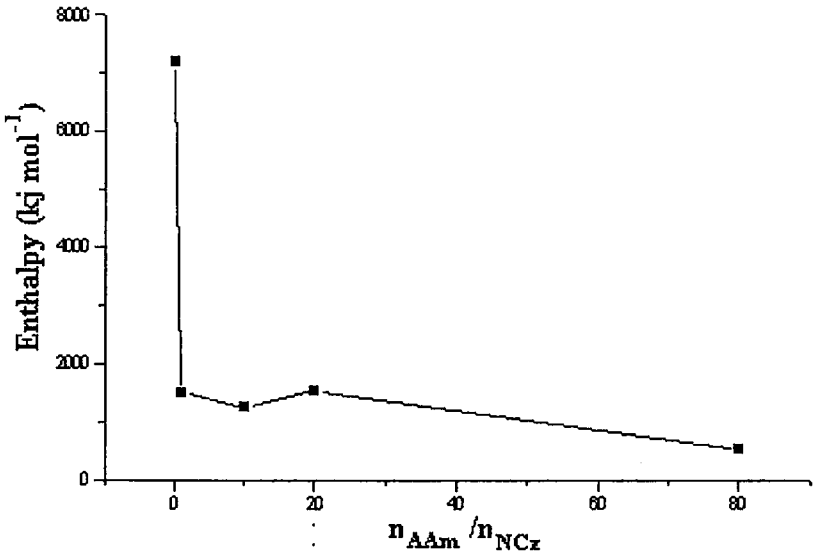

Figure 5.2 Enthalpy values obtained by DSC for different mole ratios of copolymers.

The negativeness of the PCz electrodes, which cause the pinholes (nonsmooth deposits) and weakly adhering nature of the deposits, was improved by introduction of AAm into the structure. The redox behaviour was checked on ferrocene and dopamine containing solution by cyclic voltammetry. According to the cyclic voltammetric results of AAm:NCz electrode in dopamine, exhibits response in a reproducible manner and this electrode is sensitive and has reversible behaviour. In the determination of dopamine solution, incorporation of acrylamide into the structure, polycarbazole showed better stability and flexibility as an electrode than the polycarbazole electrode and Pt itself.

The response of AAm:NVCz electrodes to dopamine and ferrocene, which were synthesized by using AIBN initiator were prepared by casting from DMF+ THF+H_2O solution on Pt, was suggested that depending on the conditions (i.e scan rates, thickness of film) the electrode response may behave also in a reversible or quasi-reversible manner.

Formation of conducting PVCz at the electrode surface takes place as suggested in literature [140] and in our case, with analogy a possible structure could be given as in Scheme 3.

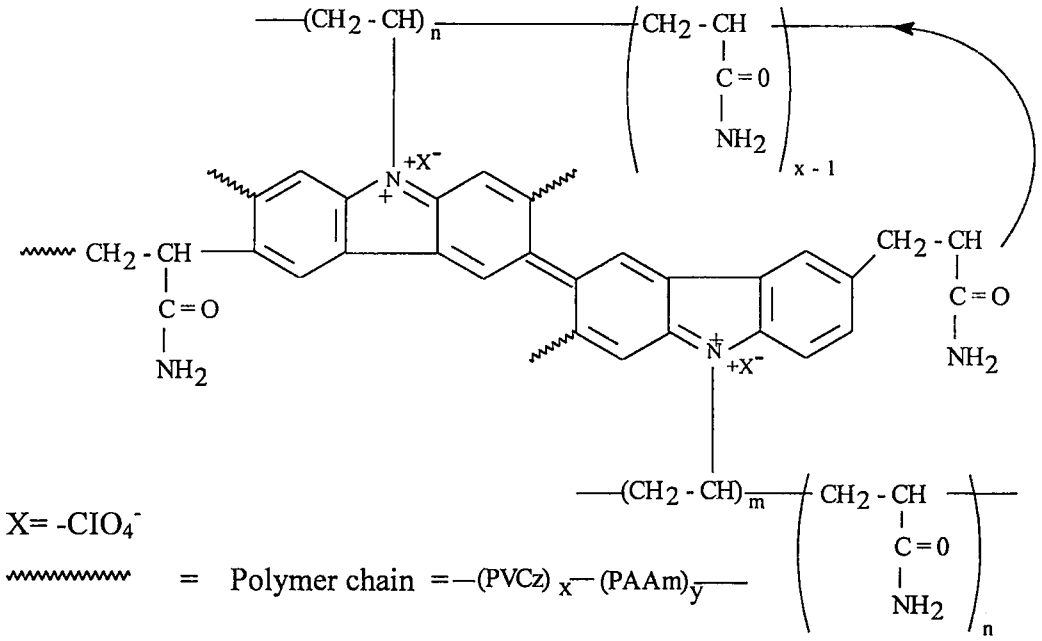

SCHEME 3

- *In-situ* spectro-electrochemical measurements were followed in solution to understand the interaction between acrylamide and carbazoles. For that reason, NECz and 3,6'-dibrECz were used as a model compound. In the case of unsubstituted ECz, reactions between monomers can occur and the formation of some oligomers takes place, and as a result of corresponding peak intensities at 800 nm, 531 nm were increased. With the incorporated AAm units to the structure, the peak at 531 nm, which was assigned to the radical cation (polaron), produced during the oxidation of the film, disappeared. This data would indicate the reaction of AAm monomers with radicals formed from the radical cations of the oligomers with nucleophile in a fast step (Figure 5.3). In the presence of bromine substituents, the absorbance values were halved in accordance with the values of NECz. This is due to the reaction going through only –2 and/or 7 position of carbazole ring, since the –3 and/or 6 position of carbazole ring are brominated.

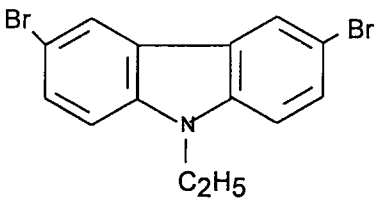

(5.1)

- The absorption intensities of this compound changes with and without acrylamide. With the incorporation of AAm to the structure, absorption values decreased and stayed constant at 800 nm for brominated NECz in comparison to the reaction between AAm and NECz, which corresponds to cation radical forms of dimer and/or oligomers. These results showed that acrylamide react with mostly 3,6'-positions of N-Carbazoles.

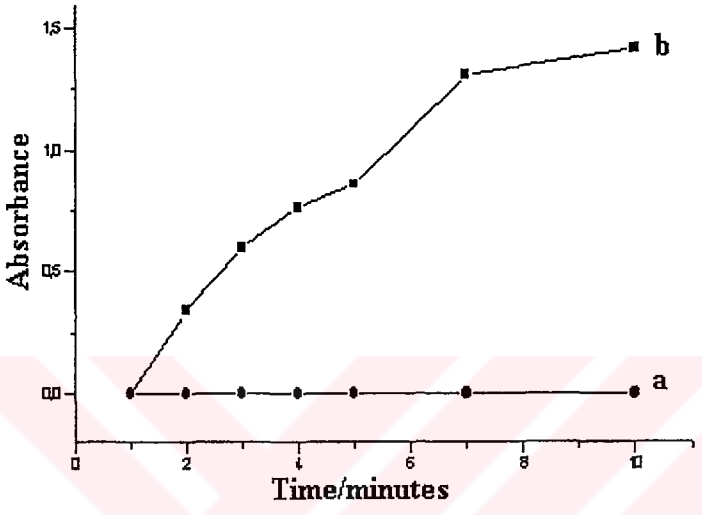

Figure 5.3 *In-situ* spectroelectrochemically obtained UV-visible absorption spectra values at 531 nm of a) AAm/NECz (20:1), b) NECz in ACN solution, supporting electrolyte: $1x10^{-1}$ mol dm^{-3} TEAP. Scan Rate: 0.05 V s^{-1}, Working and Counter Electrode: Pt, Reference Electrode: Ag/AgCI.

The electrochemical polymerization occurs via-3and/or-6 position of the carbazole ring, because this position is the most reactive. Polymerization via-2 and/or 7 position is also possible which results in a less conductive form of polymers. In the presence of AAm, radicals of carbazole formed after the subsequent step of nucleophilic attack on Cz radical cation reacting with AAm, resulting in a copolymer, in addition to having the possibility of AAm behaving as a dopant, and crosslinking to the growing chains of NCz (Scheme 4 and 5).

Probable polymer formation on the electrode surface may be as follows:

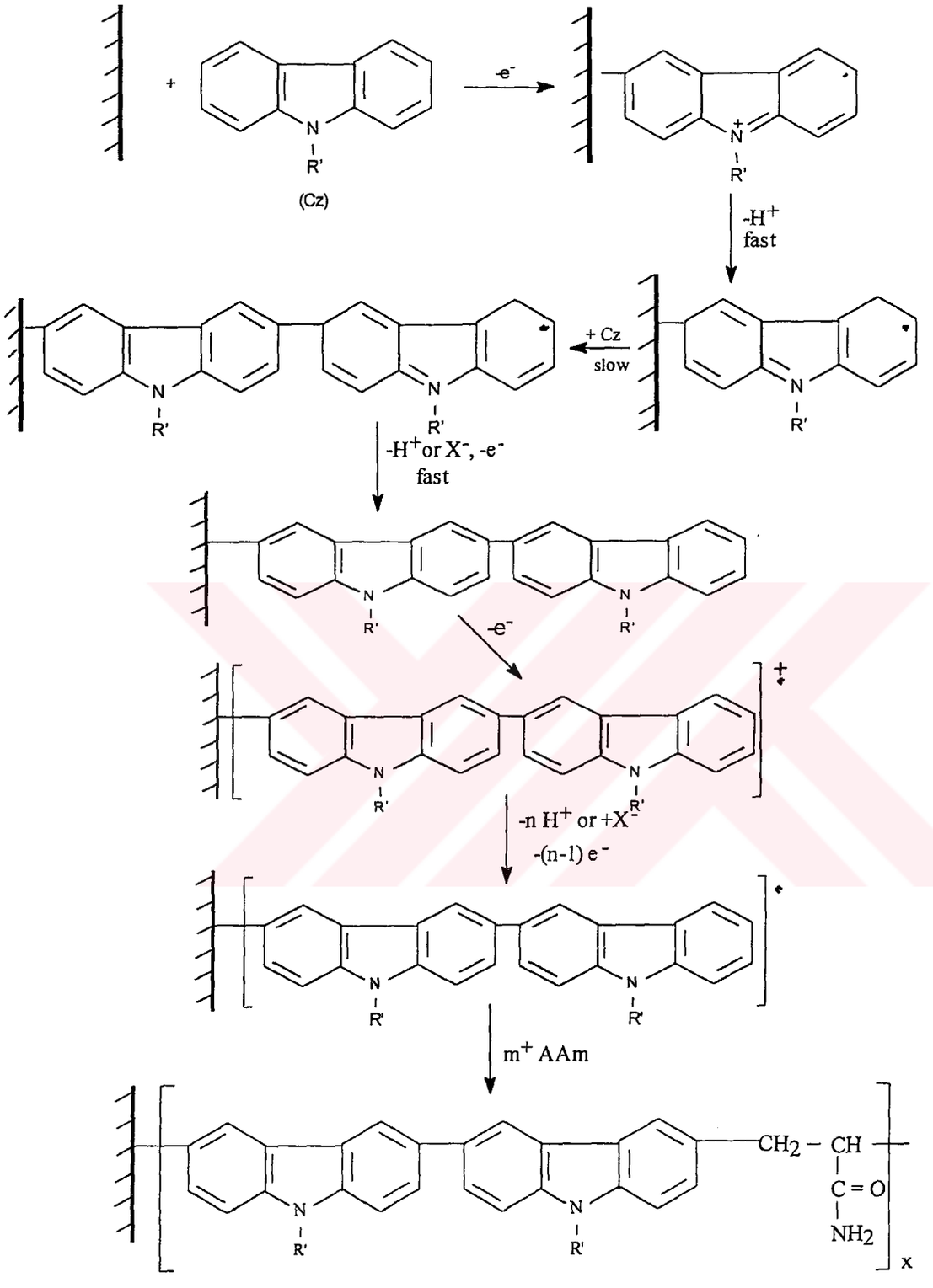

R'= H, CH_2=CH, C_2H_5, where **X**: ClO_4^- (Et_4ClO_4, $HClO_4$), OH^-, AAm

SCHEME 4

X: ClO_4^- (Et_4ClO_4, $HClO_4$), OH^-, AAm

R:

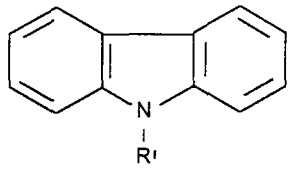

R' : H, $CH_2 = CH$, C_2H_5

Probable polymer formation can be summed up:

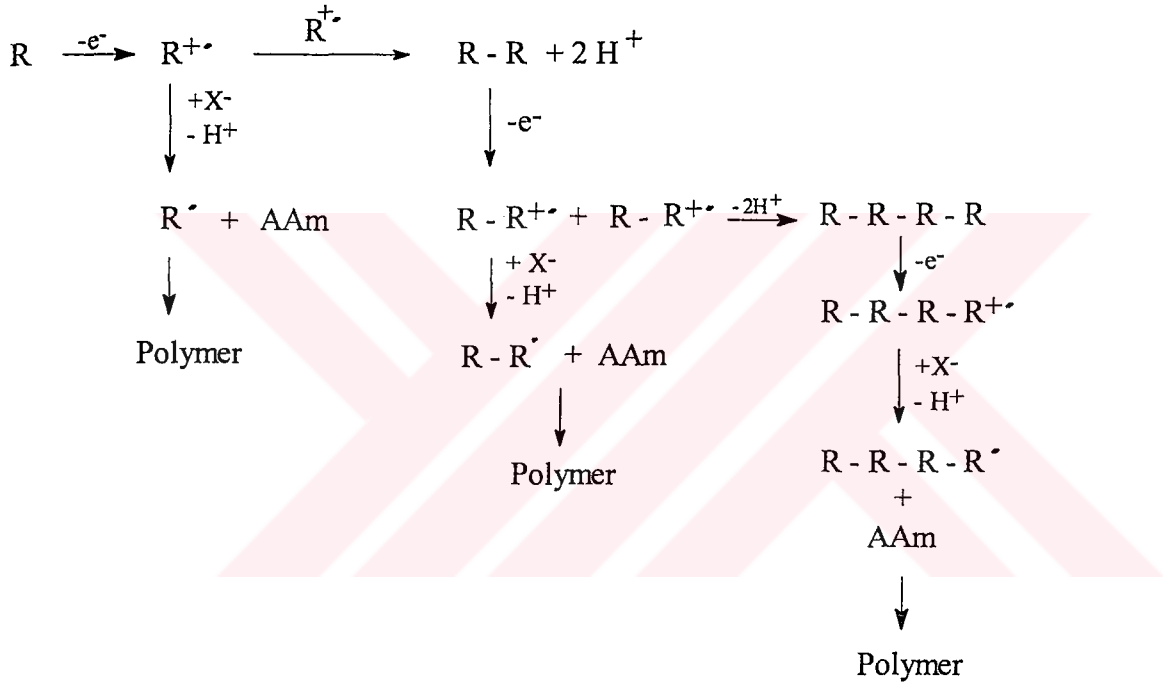

SCHEME 5

The electrochemical polymerization occurs via-3 and/or-6 and via-2 and/or 7 position of the carbazole ring. Polymerization via-2 and/or 7 position is less conductive. In the presence of AAm, polymerization might go each direction;

1)

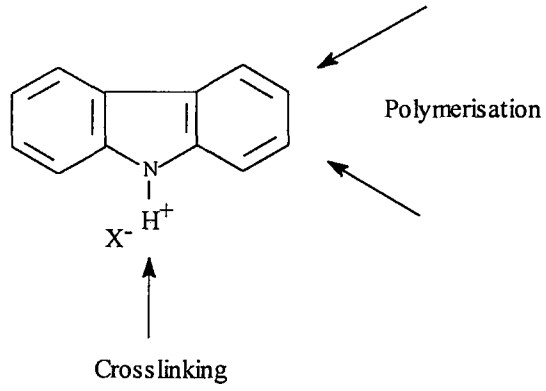

2)

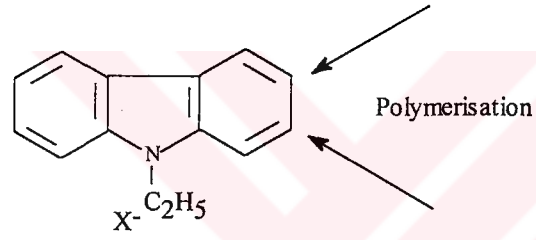

3)

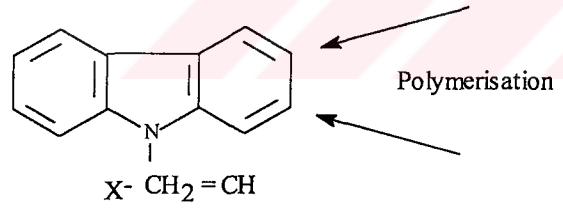

X⁻: Dopant

SCHEME 6

As a conclusion, the interaction of carbazole ring with acrylamide under forced conditions (200, 100, 20 times higher) is possible; polymers can be formed through carbazole ring or AAm or PAAm can behave as a dopant with less possibilty under certain conditions, or as a crosslinking agent between carbazole chains (including NCz, NECz, NVCz). Inclusion of AAm into the copolymeric and/or composite structure goes from the range of 5 % (n_{AAm}/n_{NCz}= 20) in ACN to 7 %

(n_{AAm}/n_{NCz}= 20) in ACN:H_2O (0.1 mol dm^{-3} $HClO_4$) for electrochemically synthesized NCz and 8 % (n_{AAm}/n_{NVCz}= 10), 99 % (n_{AAm}/n_{NVCz}= 100) in DMF for chemically synthesized copolymers. But even low amounts of AAm in the newly formed copolymer or composite structure changes the physical and chemical properties (i. e. solubility behaviour, thermal stability, flexibilty, conductivity etc.) in contrast to homopolymer (PCz, PECz, PVCz).

The resulting copolymer and/or composites due to these excellent properties would allow the use of carbazoles as potential polymers for several applications, i.e., as a biosensor electrode for protein determination or imprinting technologies due to their fluorescence properties. In addition to these, very careful controls of polymerization conditions allow us to produce several possible products, i.e. Vinylcopolymerization of NVCz with AAm gives a possiblity of having water-soluble (in certain solvents) copolymers with a fluorescing properties (application in ink, dye technologies, etc.).

A mechanistic approach in addition to the synthetic methods and a combination of several new techniques (DSC, TGA, SEM, *in-situ* spectroelectrochemistry) which were applied in a variety of conditions allowed us to define more exact structures and taylor new copolymer or composites which is not have been realized in literature.

REFERENCES

[1] **Nalwa** H. S., JohnWiley & Sons, *Handbook of Organic Conductive Molecules,* 1997, Vol. 2, p.774.

[2] **Biswas** M. and **Das** S. K., *Polymer*, !982, Vol. 23, 1713.

[3] **Bikales** N. J., Ed., *Water Soluble Polymers*, Plenum Press, New York, 1973.

[4] **Halverson** F. and **Panzer** H. P., **Grayson** M. Ed., Wiley, New York, *Encyclopedia of Chemical Technology*, 1985, Vol. 10.

[5] **Pearson** J. M., **Mark** H. F., **Bikales** N. M., **Overberger** C. G. and **Menges** G., Eds., 2nd ed., Wiley, New York, *Encyclopedia of Polymer Science and Engineering*, 1988, Vol 17, p.257.

[6] **Hallensleben** M. L., **Elvers** B., **Hawkins** S. and **Schulz** G., Eds., Verlag Chemie, Weinheim, *Ullmann's Encyclopedia of Industrial Chemistry*, 5th ed., 1992, A21, p.755.

[7] **Itaya** A., **Egawa** A., **Umehara** Y., **Sakai** H. and **Masuhara** H., *Polymer*, 1994, Vol 35, 15, 3149.

[8] **Rangaraj** A., **Vangani** V., **Rakshit** A. K., *J. Appl. Polym. Sci.*, 1997, Vol 66, 45-56. (deneysel kısımda floresans ile ayni referans)

[9] **Saraç** A. S., **Soydan** A. B., **Coka** V., *J. Appl. Polym. Sci.*, 1996, 62, 11.

[10] **Özeroğlu** C., **Güney** O., **Saraç** A. S., **Mustafaev** M. I., *J. Appl. Polym. Sci.*, 1996, 60, 759.

[11] **Saraç** A. S., *The Polym. Materials Encyc. Synth. Proper. and Appl.* (Ed. J. C. Salomone), review, 1996.

[12] **Erbil** C., **Cin** C., **Soydan** A. B. and **Saraç** A. S., *J. Appl. Polym. Sci.*, 1993, 47, 1643.

[13] **Akar** A., **Galioğlu** O., **Göçmen** A., **Saraç** A. S., *J. Appl. Polym. Sci.*, 1990, 39, 1657.

[14] **Saraç** A. S., **Başak** H., **Soydan** A. B. and **Akar** A., *Die Angewondte Macromoleculare Chemie,* 1992, 198, 191.

[15] **Saraç** A. S., **Erbil** C. and **Soydan** A. B., *J. Appl. Polym. Sci.*, 1992, 44, 877.

[16] **Saraç** A. S., **Şerife** Ö., **Ustamehmetoğlu** B., **Özgür** G., *J. Polym. Sci. Part A: Polym. Chem.*, 1999, in press.

[17] **Sezer** E., **Saraç** A. S., *Polym. for Adv. Tech.*, 1999, Vol. 10, 135-140.

[18] **Scolt** J. C., **Bredas** J. L., **Yakushi** K., **Pfluger** P. and **Street** G. B., *Synth. Met.*, 1984, 9, 165.

[19] **Kaufman** J. H., **Colameri** N., **Scott** J. C., **Kanazawa** K. K. and **Street** G. B., *Mol. Cryst. Liq. Cryst.*, 1985, 118, 171.

[20] **Baughman** R. H., **Murty** N. S. and **Miller** G. G., *J. Chem. Phys.*, 1983, 79, 515.

[21] **Nagatome** T., **Honma** T., **Yamamoto** C., **Negishi** K. and **Omoto** D., *J. Appl. Phys.*, 1983, 22, L275.

[22] **Bernier** P., **El-Khodary** A., **Maurice** F., *J. Phys. C*, 1983, 3, 583.

[23] **Kawde** R. B., **Santhanam** K. S. V., *Bioelectrochem. and Bioenerg.*,1994, 38, 405.

[24] **Kawde** R. B., **Laxmeshwar** N. B. and **Santhanam** K. S. V., *Bioelectrochem. and Bioenerg.*, 1994, 34, 83.

[25] *Brit. Pat.*, 1918, (130608).

[26] **Parravano** G., *J. Amer. Chem. Soc.*, 1951, 73, 628.

[27] **Yang** J. Y., **McEven** W. E. and **Kleinberg** J., *J. Amer. Chem. Soc.*, 1957, 79, 5833.

[28] **Desbene-Monvernay** A., **Lacaze** P. C. and **Dubois** J. B., J. *Electroanal. Chem.*, 1981, 129, 229.

[29] **Dubois** J. E., **Desbene-Monvernay** A., **Desbene** P. L., **Basselier** J. J. and **Richard** D., *J. Electroanal. Chem.*, 1985, 147, 107.

[30] **Lund** H. and **Baizer** M. M. (eds), *Organic Electrchemistry*, Marcel Dekker, New York, 1991.

[31] **Buu-Hoi** N. P. and **Do-Phuoc Hien**, *Biochem. Pharmacol.*, 1968, 17, 1227.

[32] **Nespurek** S., *Synth. Met.*, 1993, 61, 55.

[33] **Buu-Hoi** N. P., *Cancer Res.*, 1964, 24, 1511.

[34] **Tucker** S. H., *J. Chem. Soc.*,1926, 3033.

[35]**Ambrose** J. F. and **Nelson** R. F., *J. Electrochem. Soc.*, 1968, 115, 1159.

[36] **Bargon** J., **Mohmand** S. and **Waltman** R. J., *IBM J. Res. Dev.*, 1983, 27, 330.

[37] **O'Brien** R. N. and **Santhanam** K. S. V., *J. Electrochem. Soc.*, 1985, 132, 2613.

[38] **Waters** W. A. and **White** J. E., *J. Chem. Soc. C*, 1968, 740, and references to earlier work therein.

[39] **Ambrose** J. F., **Carpenter** L. L. and **Nelson** R. F., *J. Electrochem. Soc.*, 122, 876, 1975 and references therein.

[40] **Cattarin** S., **Mengoli** G., **Musiani** M. M. and **Schreck** B., *J. Electroanal. Chem.*, 1988, 246, 87-100.

[41] (a) **Breitenbach** J. W., *Makromol. Chem.*, 1960, 42, 171; (b) **Breitenbach** J. W. and **Srna** C., *Pure Appl. Chem.*, 1962, 4, 245; (c) **Sommer** F. and **Breitenbach** J. W., *Kinet. Mech. Polyreactions Int. Symp. Macromol. Chem. Prep.*, 1969, 1, 257.

[42] (a) **Phillips** D. C., **Davies** D. H. and **Smith** J. D. B., *Macromolecules*, 1972, 5(6), 674; (b) **Phillips** D. C. and **Davies** D. H. and **Smith** J. D. B., *Macromol. Chem.*, 1973, 169, 177; (c) **Davies** D. H., **Phillips** D. C. and **Smith** J. D. R., *J. Org. Chem.*, 1973, 38, 2562.

[43] **Dubois** J. E., **Desbene-Monvernay** A. and **Lacaze** P. C., *J. Electroanal. Chem.*, 1982, 132, 177.

[44] **Desbene-Monvernay** A., **Dubois** J. E. and **Lacaze** P. C., *J. Electroanal. Chem.*, 1985, 189, 51.

[45] **Papez** V. and **Josowicz** M., *J. Electroanal. Chem.*, 1994, 365, 139-150.

[46] **Crellin** R. A. and **Ledwith** A., *Macromolecules*, 1975, 8, 93.

[47] **Diaz** A. F. and **Bargon** J., in Skotheim T. A. (Ed.), Marcel Dekker, New York, *Handbook of Conducting Polymers*, 1986, Vol. 1, pp. 81-115.

[48] **Burgmayer** P. and **Murray** R. W., in T. A. Skotheim (Ed.), *Handbook of Conducting Polymers*, (Marcel Dekker, New York), 1986, Vol 1, p. 507-523.

[49] **Kaneto** K., **Kohno** Y., **Yoshino** K. and **Inuishi** Y., *J. Chem. Soc. Chem. Commun.*, 1983, 382.

[50] **Diaz** A. F. and **Hall** B., *J. Res. Dev.*, 1983, 27, 342.

[51] **Beck** F., **Braun** P. and **Oberst** M., *Phys. Chem.*, 1987, 91, 967.

[52] **Tsai** E. W., **Başak** S., **Ruiz** J. P., **Reynolds** J. R. and **Rajeshwar** K., *J. Electrochem. Soc.*, 1989, 136, 3683.

[53] **Yoshizowa** S., **Takehera** Z., **Ogumi** Z. and **Negai** C., *J. Appl. Electrochem.*, 1976, 6, 147.

[54] **George** L., **Thomas** C. W., **Thomas** N. W., *J. Polym. Sci. Polym. Chem. Ed.*, 1977, 15, 1819.

[55] **Bhadani** S. N., **Prasad** Y. K., *J. Polym. Sci., Polym. Letters Ed.*, 1977, 15, 721.

[56] **Pranab** K., **Chakraborty** S., *J. Macromol. Sci. Chem.*, 1984, A21, 701.

[57] **Hacıoğlu** B., **Akbulut** U., **Toppare** L., *J. Polym. Sci., Part A: Polym. Chem.*, 1989, 27, 3875.

[58] **Thomas** W. M., ' *Acrylamide Polymers'' in Encylopedia of Polymer Science and Technology* ', 1964, Vol 1, 177.

[59] **Ross** S. D., **Finkelstein** M. and **Petersen** R. C., *J. Am. Chem. Soc.*, 1966, 88, 4657.

[60] **Vollmert** B., *''Polymer Chemistry''*, Springer-Verlag, Berlin-Heidelberger, New York, 1973, 247.

[61] **Murakomi** Y., **Suzuki** T. and **Takegam** Y., *Polymer,* 1985, 855.

[62] **Samal** S. K. and **Nayak** B., *J. Polym. Sci. Part A: Polym. Chem.*, 1988, Vol 26, 1035-1049.

[63] **Bhadani** S. N., **Prasad** Y. K. and **Kundu** S., *J. Polym. Sci., Polym. Chem. Edt.*, 1980, Vol. 18, 1459.

[64] **Sengupta** P. K. and **Chakraborty** R., *J. Macromol. Sci.-Chem.*, 1984, A21, 701.

[65] **Biswas** M. and **Das** S. K., *Polym*er, 1982, Vol. 26, 1713-1726.

[66] **Geibler** U. and **Hallensleben** M. L., *Synth. Met.*, 1993, 55-57, 1483.

[67] **Gebler** D. D., **Wang** Y. Z., **Fu D.-K., Swager** T. M. and **Epstein** A. J., *J. Chem. Phys.*, 1998, 108, 18, 7842.

[68] **Geissler** U., **Hallensleben** M. L. and **Toppare** L., *Synth. Met.*, 1991, 40, 239.

[69] **Levin** K. L., **Zgonnik** N. V. and **Frolov** V. I., J. *Polym. Sci.*, 1993, 35, 1426.

[70] **Saraç** A. S., Sönmez G., **Ustamehmetoğlu** B., *Synth. Met.*, 1999, 98, 177-182.

[71] **Bevington** J. C., *J. Chem. Soc. Faraday Trans.*, 1975, 71, 2226,.

[72] **Tazuke** S., (a) *J. Chem. Soc. Chem. Commun.*, 1970, 20, 1277; (b) *J. Phys. Chem.*, 1970, 74, 2390.

[73] **Bowyer** P. M., **Ledwith** A. and **Sherrington** D. C., *Polymer*, 1971, 12, 509,.

[74] **Tazuke** S., **Nakagawa** K. and **Okamura** S., *J. Polym. Sci. Polym. Lettr. Ed.*, 1965, 3, 923.

[75] **Ledwith** A. and **Sherrington** D. C., *Macromol. Synth*, 1972, 4, 184,.

[76] **Penwell** R. C., **Ganguly** B. N. and **Smith** T. W., *J. Polym. Sci: Macromol. Rev.*, 1978, Vol.13, 63-160.

[77] (a) **Biswas** M.and **Kar** I., *Indian J. Chem.*, 1967, 5, 119; (b) **Miyama** H., **Tsuji** J., **Morikawa** M., **Kamachi** M. and **Nogi** T., *Japan pat.*, 1967, to Toyo Rayon Ltd., 16,049 ; (c) **Biswas** M. and **Kamannarayana** P., *J. Polym. Sci*, 1975, 13, 2035,.

[78] **Pielichowski** J., *J. Polym. Sci. Polym. Lett. Ed.*,1974, 12, 257,.

[79] (a) **Biswas** M. and **Chakravotory** D., **Bull.** *Chem. Soc. Jpn.*, 1970, 43, 1904; (b) **Biswas** M. and **Chakravotory** D., *J. Polym. Sci. Polym. Chem. Ed.*, 1973, 11, 7; (c) **Biswas** M. and **Chakravorty** D., *J. Polym. Sci. Polym. Chem. Ed.*, 1974, 12, 1337.

[80] **Tsuji** K., *Adv. Polym. Sci.*,1973,12, 131.

[81] **Stokla** M., *Pat. U. S., 1976, 3,994,994* to Xerox Corp..

[82] **Penwell** R. C. and **Prest** W., *Am. Chem. Soc. Polym. Prepr.*, 1976, 17, 931.

[83] **Biswas** M., **Roy** A., *Polymer,* 1993, Vol.34, 13, 2903.

[84] **Ryttel** A., J. M. S.-*Pure and Appl. Chem.*, 1997, 211.

[85] **Larringa** A., **Larrauri** E., **Rodriguez** M. and **Leon** L. M., J. M. S.-*Pure and Appl. Chem.*, 1994, A31(7), 883.

[86] **Pielichowski** J., **Lesiak** T. and **Daszkiewicz** Z., *Therm. Analy., Procee.* Fourth Icta Budapest, 1974, Vol.2.

[87] **Biswas** B., **Roy** A., *J. of Appl. Polym. Sci.,* 1996, Vol. 60.

[88] **Murray** R., ed., in *Techniques of Chemisry*, 1986, Vol.22, (A. Weissberger, ed.), Wiley, New York.

[89] **Skotheim** T. A. Ed., *Handbook of Conducting Polymers*, Marcel Dekker, New York, 1986.

[90] **Carlin** C. M., **Kepley** L. J. and **Bard** A. J., *J. Electrochem. Soc.*, 1985, 132, 353.

[91] **Higgins** S. J., **Christensen** P. A. and **Hamnett** A., *Electroactive Polymer Electrochemistry, Part 2: Methods and Applications*, edited by Michael E. G. Lyons Plenum Press, New York, 1996.

[92] **Higgins** S. J. and **Hamnett** A., *Electrochimica Acta* 1991, 36, 2123.

[93] **Christensen** P. A. and **Hamnett** A., *Electrochimica Acta,* 1991,36, 1263.

[94] Proceedings of ' *The 30th International Congres of Pure and Applied Chem.* ', Sept. 1985, *J. Chem. Soc. Faraday Trans.*, 1986, I, 82.

[95] **Pron** A., **Budrowski** C., **Przyluski** J., *Materials Science*, 1984, 10, 4.

[96] **Sundaresan** N. S. and **Santhanam** K. S. V., *Ind. J. Technol.*, 1986, 24, 417.

[97] **Madhavan** S. and **Santhanam** K. S. V., *Mol. Crystals Liq. Crystals*, 1988,160, 11,.

[98] **Mitcell** R. H., **Loi** Y. H., **Williams** R. V., *J. Org. Chem.*, 1979, 44, 4733.

[99] **Massel** L. H. and **Giang** R. (Eds. *Handbook of Thin Film Tech.*, Mc-Graw Hill New York, 1983, p.13.

[100] **Suen** T. J., **Schiller** A. M. and **Russel** W. H. *in Polymerization and Polycondensation Processes*, 1962, No: 34, (W. A. Platzer, Ed., Advances in Chemistry Series, American Chemical Society, Washington, D. C.).

[101] **Herman** B., **Mark** F., **Gaylord** N. M., **Bikales** I., Ed., *Encyclopedia of Polym. Sci. and Tech.*, 1987, Vol.1.

[102] **Bhadani** S. H., **Prasad** Y. K., *Makromol Chem.*, 1977, 178, 1841.

[103] **Guerrero** S. J., **Boldarino** P. and **Zurimendi** J. A., *J. Appl. Polym. Sci.*, 1985, 30, 956.

[104] **Minsk** L. M., **Chik** C. K, **Meyer** G. N. and **Kenyon** W. O., *J. Polym. Sci. Chem. Ed.*, 1974,12, 133.

[105] **Beaman** R. G., *J. Appl. Polym. Sci.*, 1965, 3949.

[106] **Tsvetkov** M. S. and **Koval'chuk** E. P., *Ukr. Khim. Zh.*, 1969, 35, 1217.

[107] **Bhadani** S. N. and **Kundu** S., *J. Polym. Mat.*, 1984, 1, 31.

[108] **Chiellini** E., **Solaro** R., **Collela** O. and **Ledwith** A., *Eur. Polym. J.*, 1978, 14, 489.

[109] **Pearson** J. M. and **Stolka** M., *Polym. Monographs, ' Polyvinylcarbazole '*, Gordon and Brech Sci. Pub. N. York, 1981, Vol. 2.

[110] **Tada** K., **Shiorata** Y. and **Mikawa** H., *Macromolecules*, 1973, 6, 9.

[111] **Chiellini** E., **Solaro** R., **Collela** O. and **Ledwith**, *Macromolecules*, 1980, 13, 1654.

[112] **Saraç** A. S., **Yavuz** Ö., **Güney** O., **Sezer** E., *Eur. Polym. J.*, 1999, (Submitted).

[113] **McCormick** C. L., **Chen** G. S. and **Hutchinson** B. H., *J. Appl. Polym. Sci,* 1982, 27, 3103.

[114] **Curteanu** S., **Simionescu** C. I. and **Talmaciu** V., *Acta Polymerica*, 1991, 7, 42, 298.

[115] **Majumdar** A. and **Biswas** B., *J. Appl. Polym. Sci.*, 1991, Vol. 42, 2489-2498.

[116] **Elias** H.-G., ' *Macromolecules* ', 2nd Edn., Plenum Press, New York, 1984, 383.

[117] **Bergfjord** J. A., **Penwell** R. C., **Stolka** M., *J. Polym. Phys. Ed.*, 1979, 17(4), 711.

[118] **Das** K., **Das** A. K. and **Kundu** K. K., *Electrochim. Acta*, 1981, 26, 471.

[119] **Nalwa** H. S. (edited by), *Handbook of Org. Cond. Mol. And Polym.*, 1996, Vol. 2, 436.

[120] **Mengoli** G, **Musuani** M. M., **Schreck** B. and **Zecchin** S., *J. Electroanal. Chem.*, 1984, 131, 2028.

[121] **Dong** S. and **Ding** J., *Synth. Metals*, 1987, 20, 119.

[122] **Wernet** W. and **Wernt** G., *Macromol. Chem.*, 1987, 188, 1465.

[123] **Qian** R., **Qiu** J. and **Shen** D., *Synth. Metals*, 1987, 18, 13.

[124] **Wernet** W., **Monkenbusch** M. and **Wegner** G., *Macromol. Chem. Rap. Commun.*, 1984, 5, 157.

[125] **Proft** A., **Kuchharaski** Z., **Budrowski** C., **Zagarska** M., **Krichene** S., **Suwalski** J., **Dene** G. and **Lefrant** S., *J. Chem. Phys.*, 1985, 83, 5923.

[126] **Kessel** R. and **Schultze** J. W., *Surf. Interf. Anal.*, 1990, 16, 403.

[127] **Verghese** M. M., **Basu** T., **Malhotra**, *Materials Sci. and Eng.: C3*, 1995, 215-218.

[128] **Mohilner** D. M., **Adams** R. N. and **Argersinger** W. J., *J. Am. Chem. Soc.*, 1962, 84, 3618.

[129] **LaCroix**, J-C. and **Diaz** A. F., *Macromol. Chem., Macromol Symp.*, 1987, 8, 17.

[130] **Zotti** G., **Cattarin** S. and **Comisso** N., *J. Electroanal. Chem.*, 1987, 235, 259.

[131] **Hayashi** S., **Kaneto** K. and **Yoshinu** K., *Solid State Commun.*, 1989, 61, 249,.

[132] **Azzam** R. M. A. and **Bashara** N. M., ' *Ellipsometry and Polarized Light* ', North-Holland: Amsterdam, 1979.

[133] **Higgins** S. J., **Christensen** P. A. and **Hamnett** A., *Electroactive Polymer Chemistry, Part 2: Methods and Applications*, edited by Lyons Michael E. G. Plenum Press, New York, 1996.

[134] **Abthagir** P. S., **Dhanalakshmi** K. and **Saraswathi** R., *Synth. Met.*, 1998, 93, 1.

[135] **Waters** W. A. and **White** J. E., *J. Chem. Soc. C*, 1968, 740 and references to earlier work there in.

[136] **Taoudi** H., **Bernede** J. C., **Bonnet** A., **Morsli** M., **Godoy** A., *Thin Solid Films*, 1997, 304, 48-55.

[137] **Sezer** E., **Saraç** A.S., and **Yavuz** Ö., *Corrosion* 1999, Vol. 55, No 7, 661.

[138] **Erdik** E., **Sarıkaya** Y., *Temel Üniversite Kimyası,* (Gazi Kitapevi, 11.baskı) 1997, 191.

[139] **Volke** J., **Liska** F., Springer-Verlag Berlin Heidelberg, *Electrochemistry in Organic Chem.*, 1994, 15.

[140] **Saçak** M., **Akbulut** U., **Cheng** C., **Batchelder** D. N., *Polymer*, 1994, Vol. 35, 12, 2495.

APPENDIX A: FT-IR MEASURMENTS OF POLYMERS

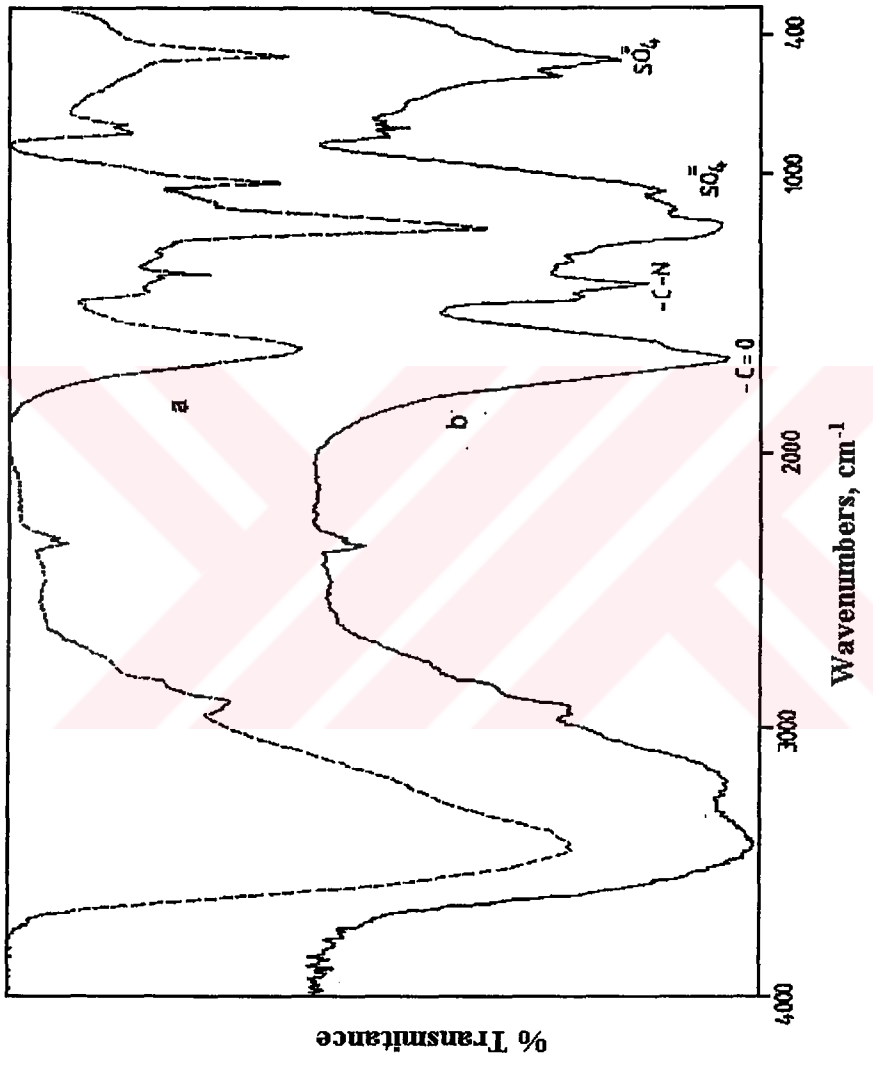

Figure A.1 The FT-IR spectra of PAAm obtained (a) in anode, (b) in cathode compartment, [AAm]= 0.5 mol dm^{-3}, [OA]= $2x10^{-2}$ mol dm^{-3} [H_2SO_4]= 0.1 mol dm^{-3}, [Ce(IV)]= $5x10^{-4}$ mol dm^{-3} .

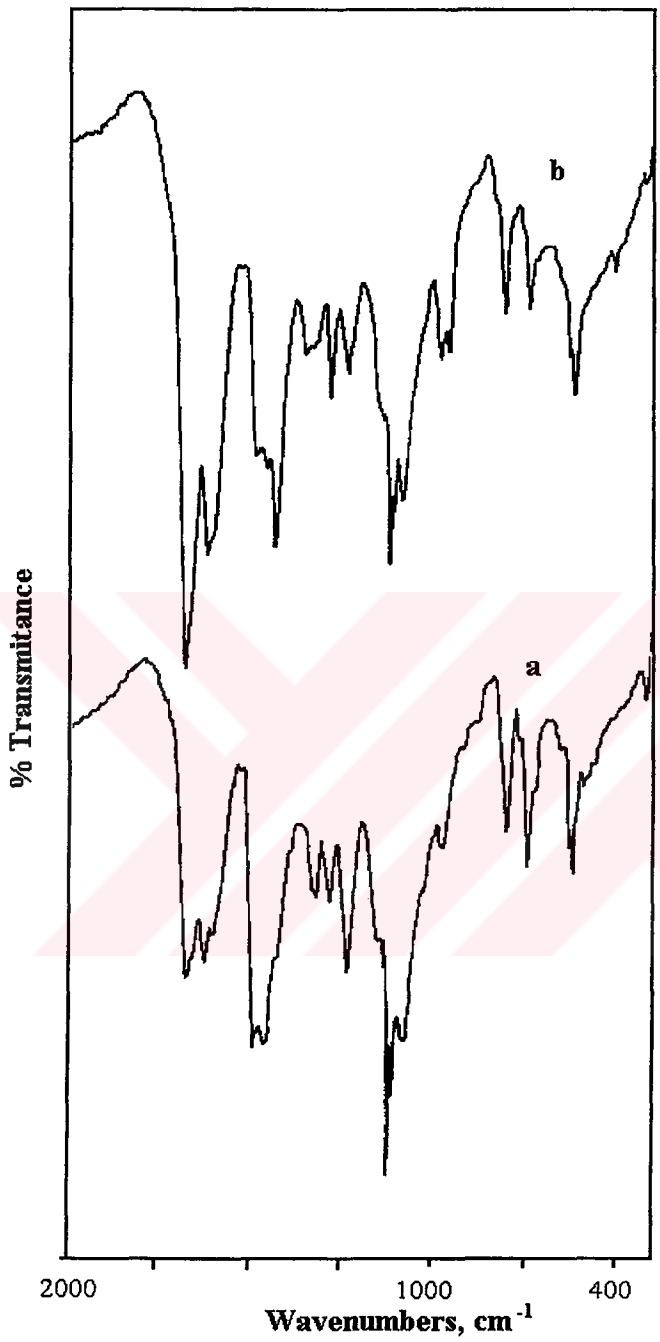

Figure A.2 The FT-IR spectra of copolymers (n_{AAm}/n_{NCz}= 50) obtaining in different voltages (a) 1.2 V, (b) 1.4 V.

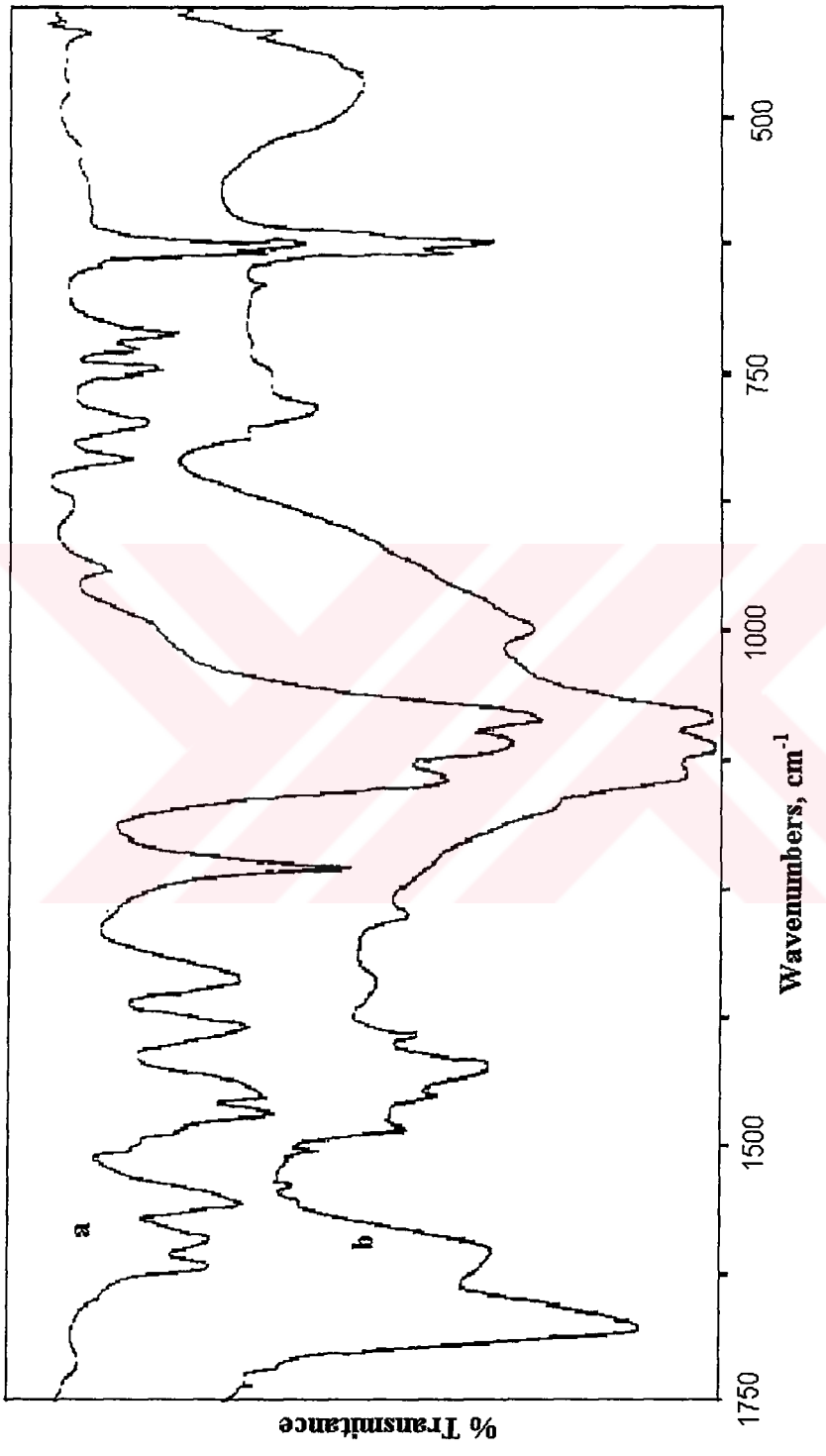

Figure A.3 The FT-IR spectra of PECz obtaining in protic acid media (ACN: $HClO_4$) (%50:%50) (1 mol dm^{-3}), (b) Copolymerized AAm:NECz in ACN solution ($1x10^{-1}$ mol dm^{-3} TEAP used as supporting electrolyte).

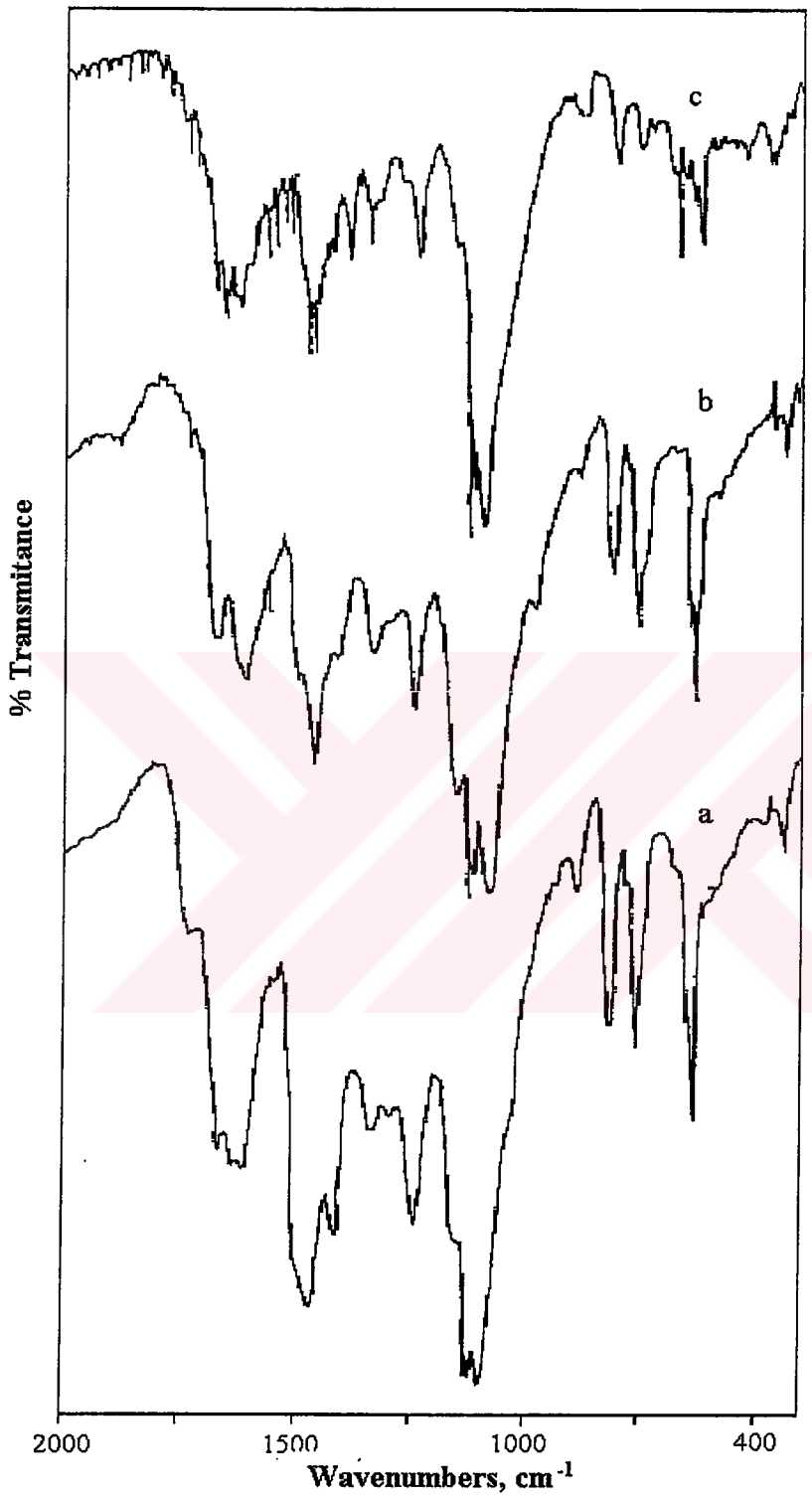

Figure A.4 The FT-IR spectra of a) n_{AAm}/n_{NCz}= 20, b) n_{AAm}/n_{NVCz}= 20, c) n_{AAm}/n_{NECz}= 20 electrochemically obtained in ACN media containing ($1x10^{-1}$ mol dm^{-3}).

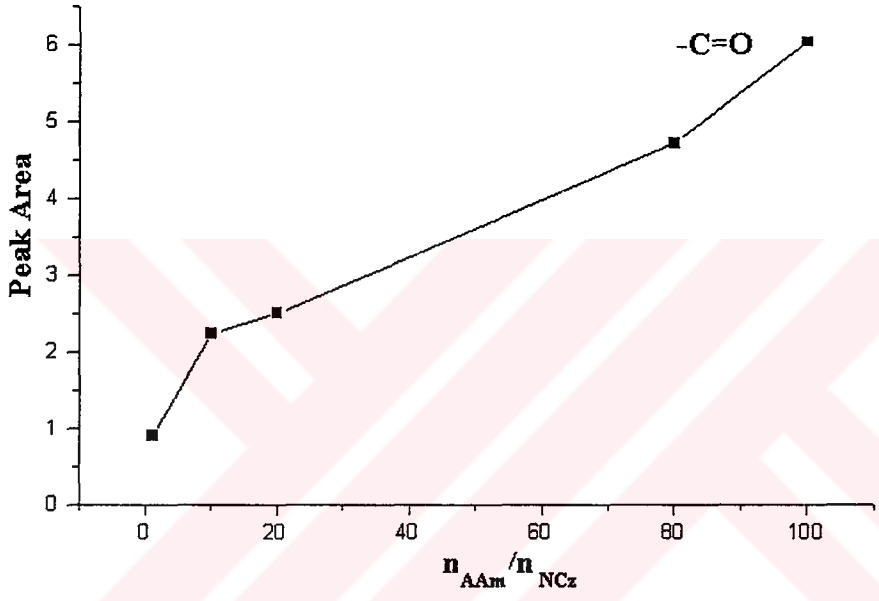

Figure A.5 The FT-IR peak area changes for –C=O at 1650 cm^{-1} for different AAm:NCz mole ratio.

APPENDIX B: UV-VISIBLE MEASUREMENTS OF POLYMERS

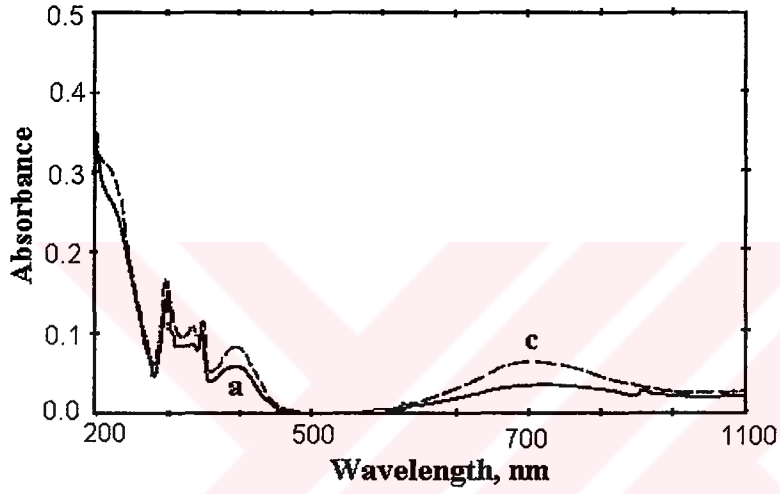

Figure B.1 UV-Visible spectra of electrochemically prepared AAm:NECz film (n_{AAm}/n_{NCz} =50) on ITO, and changes by increasing reaction time (a-c) at the 1.2 V applied potential in ACN.

APPENDIX C: THERMOGRAVIMETRIC MEASUREMENTS OF POLYMERS

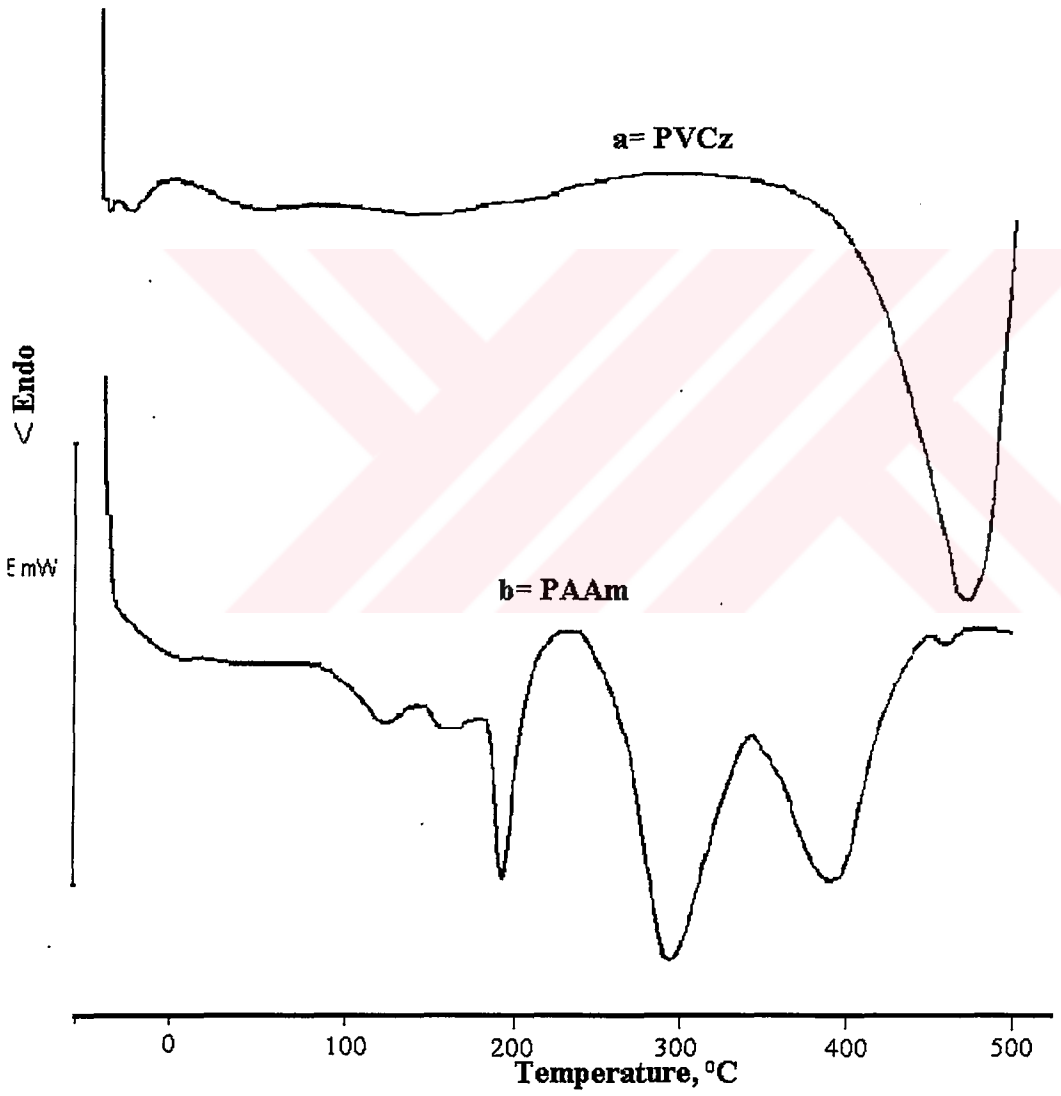

Figure C.1 The DSC curves for (a) PVCz, (b) PAAm.

APPENDIX D: ELECTROCHEMICAL PROPERTIES OF POLYMERS

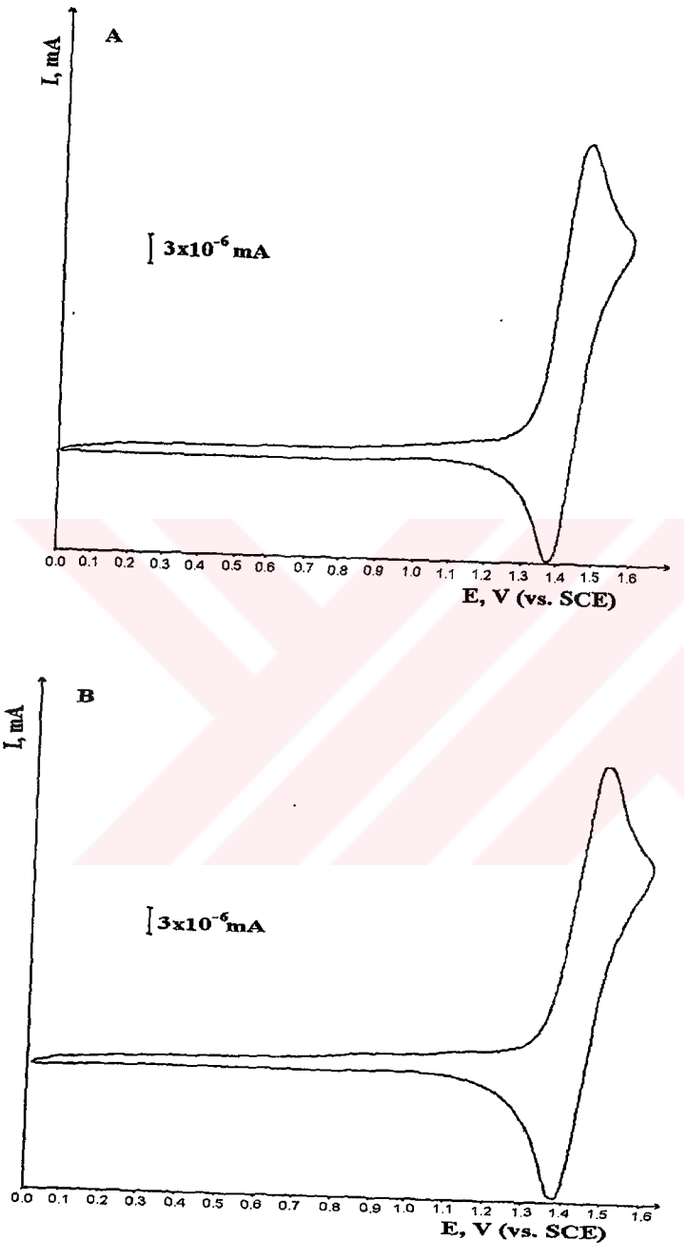

Figure D.1 Electrodepositing of A-) 3,6'-dibrECz, B-) AAm:3,6'-dibrECz (20:1) onto Pt in ACN solution, Scan Rate: 0.5 V s^{-1}, supporting electrolyte, $1x10^{-1}$ mol dm^{-3} TEAP.

APPENDIX E: ELLIPSOMETRIC MEASUREMENTS OF POLYMERS

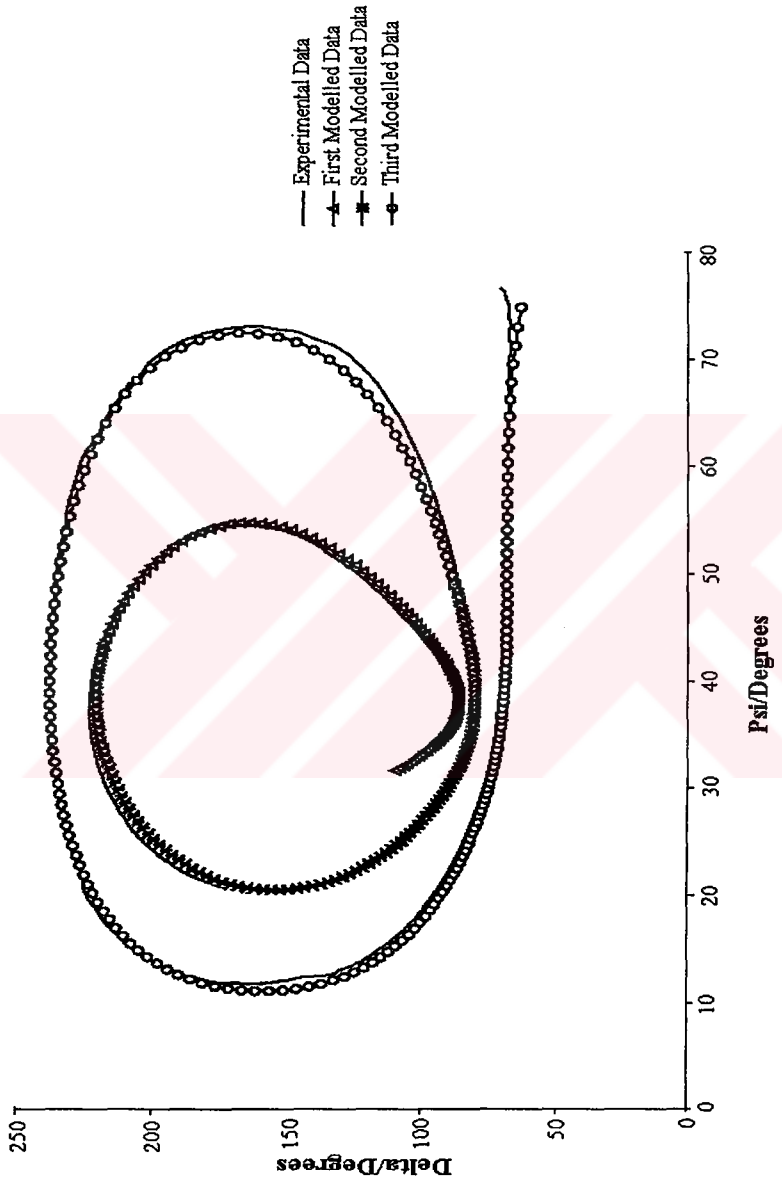

Figure E.1 Ellipsometric Δ-Ψ curves recorded during the growth of the copolymer films form a solution of AAm:NCz (10:1) in ACN. Scan Rate: 0.001 V s^{-1}

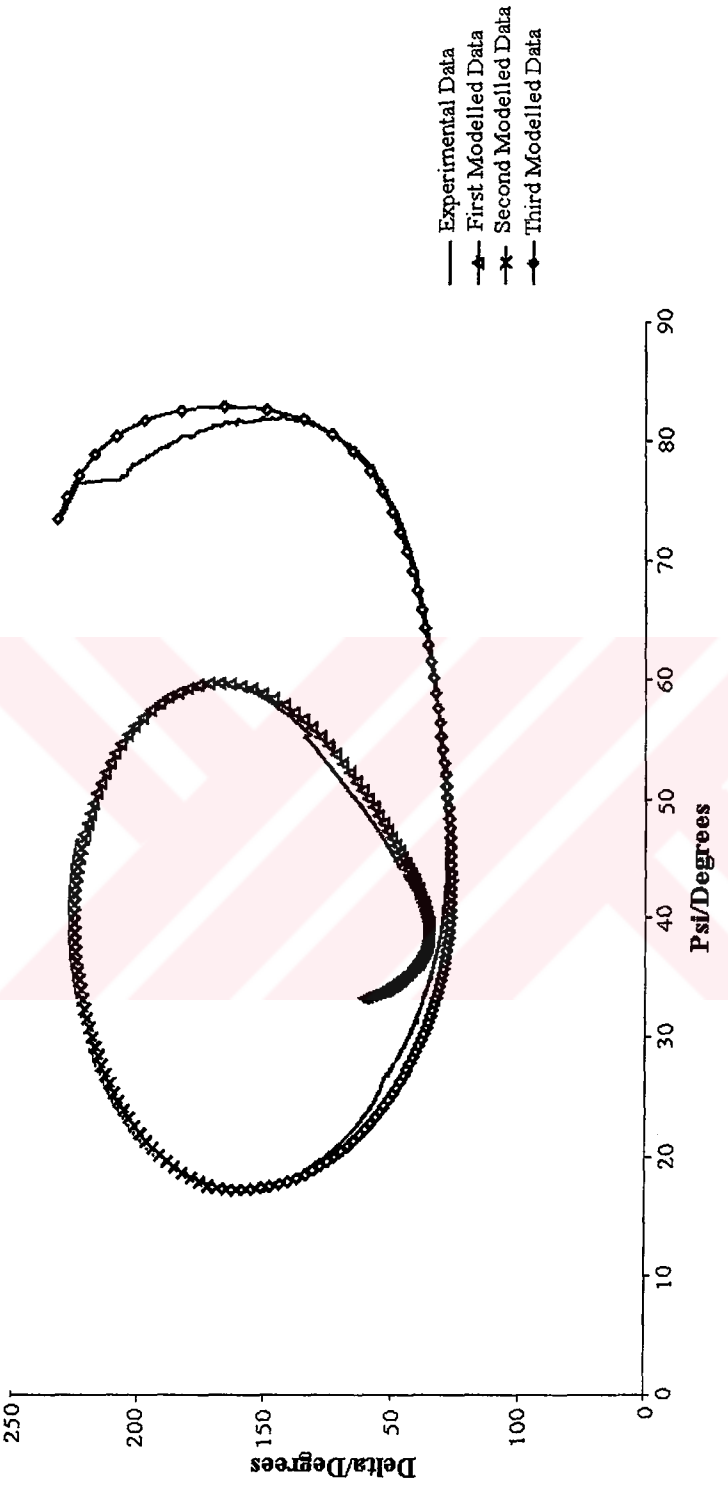

Figure E.2 Ellipsometric Δ-Ψ curves recorded during the growth of the copolymer films form a solution of AAm:NCz (1:1) in ACN. Scan Rate: 0.001 V s^{-1}.

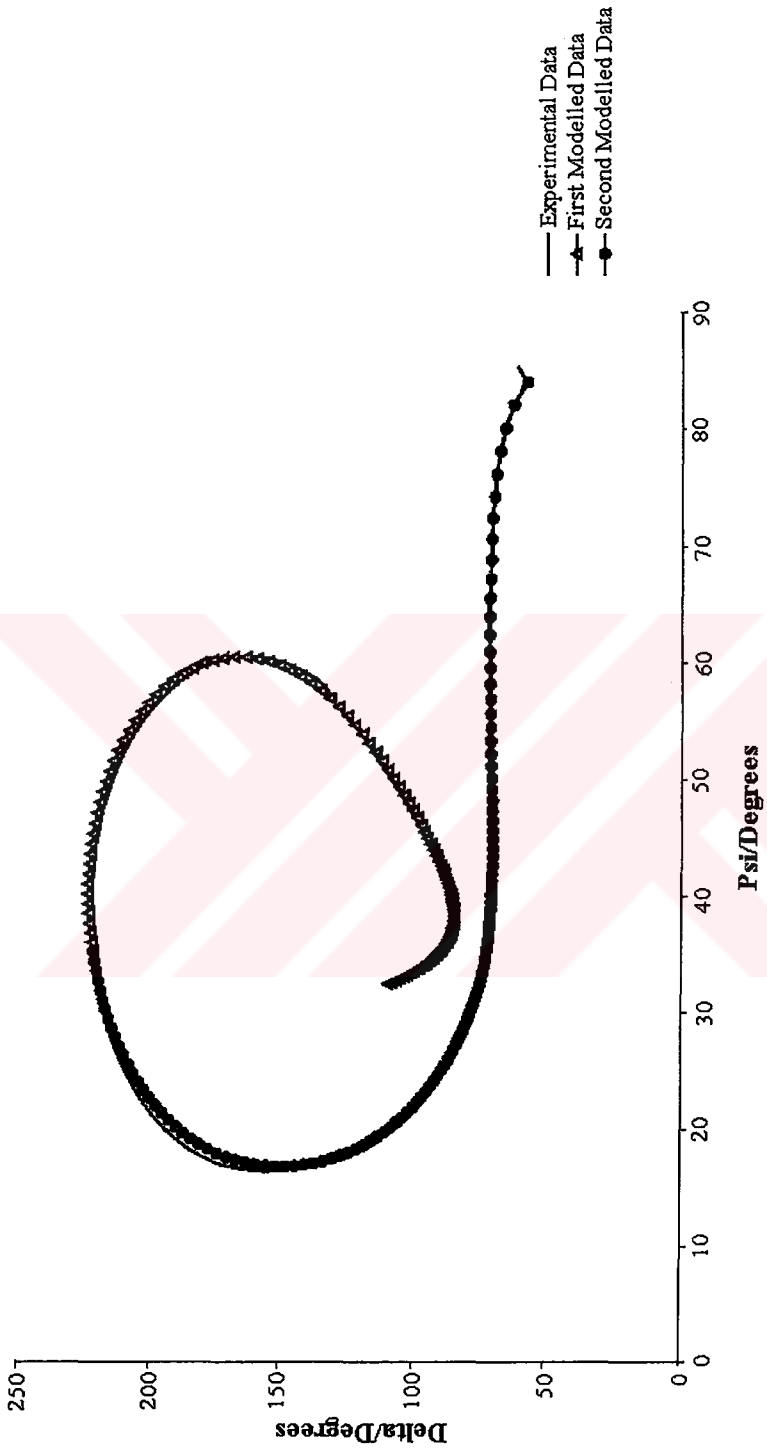

Figure E.3 Ellipsometric Δ-Ψ curves recorded during the growth of the copolymer films form a solution of AAm:NCz (10:1) in ACN. Scan Rate: 0.002 V s^{-1}.

BIOGRAPHY

Özlem Yavuz was born in İstanbul in 1969. She graduated from Yeşilköy 50. Yıl Lisesi in 1987, admitted to Istanbul Technical University and graduated as a Chemist in 1993.

She registered as an M.Sc. student in the Department Chemistry of Istanbul Technical University and graduated in 1995.

She started Ph.D. in the same department at the same university in 1995. During her Ph.D. studies, she visited to the University of Stratchlyde in Glasgow for various periods of times.

She has been working as a research assistant in the Physical Chemistry Department since 1994.

Published Papers

1. Electrochemically Induced Redox Polymerisation of Acrylamide, Saraç A. S., Yavuz Ö., Sezer E., *J. Appl. Polym. Sci.*, 1999, Vol. 72, 861-869.

2. Electrosynthesis and Study of Carbazole-Acrylamide Copolymer Electrodes, Saraç A. S., Yavuz Ö., Sezer E., *Polym*er, Vol. 1999, 41, 3, 839.

3. The Optical, Thermal and Electrochemical Properties of Co-Electropolymerised Films of Carbazole and Acrylamide, Yavuz Ö, Berlouis L. E. A., Hitchman M. L., Saraç A. S., *Synth. Met.*, 1999, (in press).

4. Electrochemical and Corrosion Behaviour of N-Vinylcarbazole-Acrylamide Copolymer Electrodes, *J. Electrochem. Soc.*, 1999, (in press).

Submitted Papers

1. Synthesis and Characterisation of Water Soluble Carbazole Containing Polymers, Saraç A. S., Yavuz Ö, Güney O., Sezer E., *Europ. Polym. J.*, 1999.

2. *In-Situ* Spectro-Electrochemical Investigation of N-Carbazole Derivatives in the Presence of Acrylamide, *J. Polym. Sci.*, 1999.